



UNIONE EUROPEA
Fondo Sociale Europeo



UNIVERSITA' DELLA CALABRIA

Dipartimento di Chimica e Tecnologie Chimiche

Dottorato di Ricerca in
Scienze e Tecnologie Fisiche Chimiche e dei Materiali

Con il contributo di
PON Ricerca e Innovazione 2014-2020

CICLO

XXXIII

**DESIGN AND DEVELOPMENT OF A FLEXIBLE AND LOW-COST ELECTROCHROMIC
DEVICE FOR SMART WINDOWS**

Settore Scientifico Disciplinare CHIM/03


Coordinatore: Ch.ma Prof.ssa Gabriella Cipparrone

Firma  Firma oscurata in base alle linee guida del Garante della privacy

Supervisore: Ch.mo Prof. Massimo La Deda

Firma  Firma oscurata in base alle linee guida del Garante della privacy

Dottorando: Dott. Francesco Parisi

Firma  Firma oscurata in base alle linee guida del Garante della privacy

PREMESSA

Con quasi 8 miliardi di abitanti nel mondo, il fabbisogno energetico per le attività umane sembra non essere mai sufficiente.

Il rapido aumento della domanda di energia è il risultato combinato di due fattori: in primo luogo il continuo desiderio di comfort da parte dei paesi ricchi ed in secondo luogo la corsa spasmodica per raggiungere le stesse condizioni da parte dei paesi in via di sviluppo.

La possibilità o meno di accedere alle fonti di energia traccia una profonda spaccatura tra le comunità umane, dove i più forti godono di tutti i comfort a prescindere dagli sprechi, mentre i più sfortunati sono condannati a non potersi permettere un tenore di vita accettabile.

Per mantenere un elevato tenore di vita e allo stesso tempo consentire lo sviluppo delle popolazioni meno avanzate in modo ecosostenibile, non basta affidarsi a fonti di energia rinnovabile ma è necessario altresì ridurre i consumi energetici attraverso l'utilizzo di dispositivi più efficienti.

Inoltre, negli ultimi vent'anni la questione ambientale ha assunto grande rilevanza, tanto che i governi dei Paesi e le organizzazioni sovranazionali stanno mettendo a punto strategie socio-economiche-culturali per limitare l'impatto delle attività umane sull'ecosistema terrestre.

In questa direzione si è mossa anche l'Unione Europea, proponendo un programma di crescita e sviluppo basato sulla transizione verde delle attività produttive, sulla riduzione delle emissioni di gas serra, sull'utilizzo di materiali riciclati o rinnovabili e sull'aumento dell'efficienza energetica degli edifici.

Questo piano è noto come Green Deal Europeo ed ha l'obiettivo di rendere l'UE ad impatto zero dal punto di vista climatico entro il 2050.

Un argomento chiave è riconsiderare gli edifici perché rappresentano il 40% del nostro consumo energetico totale.

Le finestre in particolare, sono il luogo dove avviene il maggiore scambio di luce e calore tra ambiente interno ed esterno, rendendo indispensabile il consumo di energia per avere un'abitazione più confortevole.

Il lavoro svolto per questa tesi di dottorato percorre questa strada, con lo sviluppo di un dispositivo elettrocromico economico, ecosostenibile ed efficiente dal punto di vista energetico, che può essere applicato a finestre preesistenti per modulare a piacimento i flussi radianti in ingresso, limitando il consumo di energia.

Utilizzare un dispositivo in grado di adattarsi ad infissi già esistenti, può convertire dei semplici vetri in finestre intelligenti, evitando la sostituzione integrale degli infissi e risparmiando notevolmente sui costi di installazione.

CONTENTS

1. INTRODUCTION	1
1.1. OUR PURPOSE	3
1.2. ELECTROCHROMIC DEVICES: TYPES AND CONFIGURATIONS	5
1.2.1. ECDs FOR OUR PURPOSE	8
1.3. ELECTRODES FOR OUR PURPOSE	11
1.4. ELECTROCHROMISM AND ELECTROCHROMES	15
1.4.1. ECs FOR OUR PURPOSE	17
1.4.1.1. VILOGENS AND POLYVILOGENS	19
1.4.1.2. COUNTER-SPECIES FOR OUR PURPOSE	23
1.5. ELECTROLYTE	25
1.5.1. ELECTROLYTES FOR OUR PURPOSE	26
1.5.1.1. CHITOSAN	29
1.6. METALLIC NANOPARTICLES FOR OUR PURPOSE	33
1.7. DEPOSITION TECHNIQUES	35
2. EXPERIMENTAL	40
2.1. POLYVILOGENS: SYNTHESIS AND CHARACTERIZATION	41
2.1.1. POLYVILOGENS: MATERIALS AND METHODS	45
2.2. ELECTROLYTE: SYNTHESIS	46
2.2.1. ELECTROLYTE: MATERIALS AND METHODS	50
2.3. CuNWs: SYNTHESIS	51
2.3.1. CuNWs: PURIFICATION AND CHARACTERIZATIONS	55
2.3.2. CuNWs: STORAGE AND AGING	59
2.3.3. CuNWs: MATERIALS AND METHODS	62
2.4. ALL-IN-ONE FILM-FORMING SOLUTION	64
2.5. OPTIMIZATION	69

2.5.1. FILM DEPOSITION	70
2.5.2. DEVICE ASSEMBLY	74
2.5.3. OPTIMIZE SPECIES	76
2.5.3.1. GLYCEROL AND LITHIUM BROMIDE	77
2.5.3.2. POLYVIOLOGEN	79
2.5.3.3. TMPD	80
2.5.3.4. COPPER NANOWIRES	82
2.5.4. SYNTHETIC PROTOCOL	85
3. RESULT AND DISCUSSIONS	87
3.1. MONITORING THE SWITCHING POTENTIAL	88
3.2. ELECTRONIC MEASUREMENTS	90
3.3. FILM THICKNESS AND MECHANICAL BEHAVIOUR	96
3.4. OPTICAL MEASUREMENTS	99
3.5. ELECTROCHEMICAL MEASUREMENTS	103
3.6. INVESTIGATIONS ON SOLUTION DEGRADATION	105
3.7. INSTRUMENTS	110
3.8. COST ANALYSIS	111
4. CONCLUSIONS	114
5. REFERENCES	118

1. INTRODUCTION

With nearly 8 billion inhabitants in the world, the energy needs for human activities never seems to be enough.

The rapid increase in energy demand is the combined result of two factors: primarily the continuous desire for comfort by rich countries and secondly the spasmodic race to achieve the same conditions by developing countries.

The possibility or not of accessing energy sources, traces a deep rift between human communities, where the strongest enjoy all the comforts regardless of waste, while the most luckless are condemned to being unable to afford an acceptable standard of living.

To maintain a high standard of living and at the same time allow the development of less advanced populations, in an eco-sustainable way, it is not enough to find renewable energy sources but it is also necessary to reduce energy consumption through the use of more efficient devices.

Furthermore, in the last twenty years the environmental issue has assumed great importance, so that even the governments of countries and supranational organizations are setting up socio-economic-cultural strategies to limit the impact of human activities on the terrestrial ecosystem.

The European Union has also moved in this direction, proposing a growth and development program based on the green transition of production activities, reducing greenhouse gas emissions, using recycled or renewable materials, and increasing energy-efficient buildings.

This plan is known as the European Green Deal and has the aim to make EU climate neutral in 2050.

A key topic is to reconsider buildings because they account for 40% of our total energy consumption.

Windows in particular, are the main place where the exchange of light and heat takes place between internal and external environment, making energy consumption indispensable for a more comfortable dwelling.

The work carried out for this doctoral thesis walks along this path, with the development of an inexpensive, eco-sustainable and energy-efficient electrochromic device, that can be applied to pre-existing windows in order to modulate the incoming radiant flows as desired, limiting energy consumption.

The use of an adaptable device would convert simple glasses into smart windows, without having to replace existing fixtures, thus greatly saving installation costs.

1.1. OUR PURPOSE

In the light of what has already been discussed, the final device will have very specific characteristics, listed below; some are purely technical, others are pursued in view of possible industrial production, latest ones aim to minimize the environmental impact.

- **Transparency** - the purpose of our device is to implement existing windows; therefore, it must be highly transparent and does not compromise the view of the outside.
- **Good optical contrast** - having the objective of modulating the incoming radiation, the greater the loss of transparency when switched on, the better the effectiveness of the device obtained.
- **Low working voltage** – in order to save energy, it is very important that the change from the bleached to the coloured state takes place with low power consumption.
- **Fast and reversible switching** – the change of state should be highly reversible and occur within a few seconds. Get this feature together with the previous one, make the device efficient.
- **Thinness** - a very small thickness, would allow an easier placement on pre-existing windows.
- **Flexibility** – to provide this property to the device, would make it less fragile, handier and more adaptable.
- **Scalability** -although the device will be developed in the laboratory, it will be designed for a possible future industrial production, therefore techniques and procedures re-proposable or convertible for industrial scale will be preferred.
- **Produced with safe solvents** - chemical synthesis of the components and assembly processes of the device should preferably use non-hazardous and non-toxic solvents to make the production phase as safe as possible.
- **Processed in a few steps** - if the production steps are few, the device is more attractive for the industry, because both the production cost and the chance of making mistakes decrease.
- **Low total production cost** - the lower the production cost of the device, the greater the profit margin that can derive from it.

- **Mild process conditions** - synthetic and process conditions of short duration, simple and occurring at low temperatures are preferable; this is appropriate for both industrial application and environmental impact.
- **Environmentally friendly** - following the perspective of green chemistry, it will be necessary to opt for the sparing use of low-polluting solvents; the reagents and the final product must be as eco-sustainable as possible. It will also be good that the device must be easily integrated with a green energy power system.

Confer these properties to the device, will constitute the guideline of the research path and will direct the choice of the various materials to be used.

The following chapter is an overview of the various components of electrochromic devices; although various types will be mentioned, we will focus on those most suitable for achieving our goal. The sections entitled "*... for our purpose*" will contain the evaluations for the choice of species, materials and techniques suitable for the realization of a final device with the characteristics listed above.

1.2. ELECTROCHROMIC DEVICES: TYPES AND CONFIGURATIONS

As mentioned in the previous sections, the purpose of this doctoral thesis is the realization of an electrochromic device (ECD), having predetermined characteristics. A brief description of the operating principle and the types of existing devices is certainly necessary to set the final objective more concretely.

Basically, there are three essential components to build an electrochromic device: the electrodes, the electrochromes and the electrolyte.

It is easy to deduce from its etymology that the device under construction must in some way allow the passage of current, therefore it must be crossed by electrons; this implies that the device is powered by an electric generator, which will be connected to the ends of the device, the *electrodes*, i.e. anode and cathode.

With respect to the IUPAC definitions, anodic currents are considered negative and cathodic currents positive; therefore the reduction reactions take place on the cathode while oxidations take place on the anode¹.

Since in electrochromic devices electrochemical reactions take place, the anode is associated with the positive pole, while the cathode is associated with the negative one.

The electrical potential difference between the electrodes is the driving force for the electrochemical process involving the electrochromic species. These *electrochromes* are responsible for the colour change and are therefore the core component of the device.

Lastly, the *electrolyte* supports the passage of current between the electrodes through the movement of the ions.

Although the description of a generic device is rather simple, its realization occurs with many different configurations.

First of all, there are the *liquid phase devices*. In solution there are both electrochromes and electrolytes, while the electrodes are immersed in the solution or confine it with the help of a sealant²; in the latter case, inert and insulating spacers

are necessary to avoid direct contact between the electrodes, which would cause a short circuit. A representative image of what has been said is shown in figure 1.

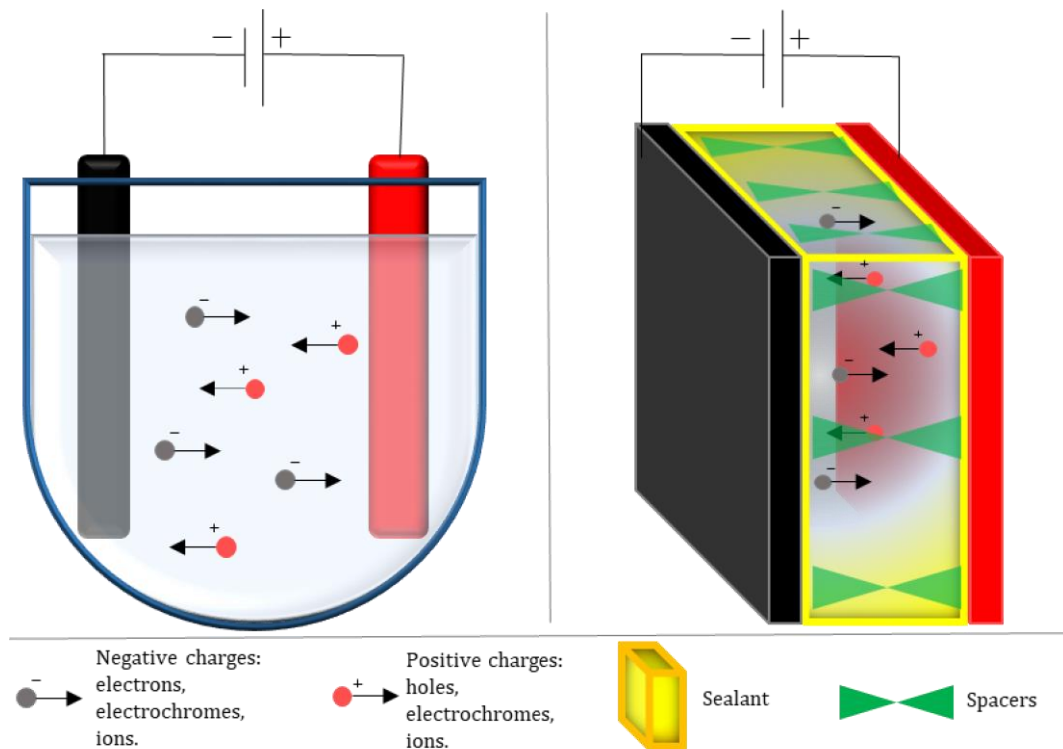


Figure 1 - Liquid phase devices: the whole electrochromic system is placed in an electrochemical-type cell (left); separated by spacers flat electrodes device, with internal electrochromic solution confined by sealant (right).

The main drawbacks that can occur using a liquid phase device, especially if it is flexible, are the solution leaking or drying, despite the meticulous application of the sealant.

To overcome these inconveniences, *solid-phase devices* have been developed. Solid-type ECDs exist in two configurations: multi-layer or single-layer.

Excluding electrode layering, the number of layers with which the device is built, are at least three: one electrochromic, often deposited on the surface of an electrode; a solid electrolyte, into which ions and electrons can migrate; and an ion storage layer, which can also be electrochromic, deposited on the counter electrode³.

Otherwise, single layer devices have a symmetrical architecture very similar to liquid phase devices; here too the electrochromes and the electrolyte are both dissolved in the same solid or semi-solid gel matrix, which will constitute the only layer between the electrodes⁴.

For this reason, a single-layer device is often called all-in-one device⁴; the generic representations of a multi-layer and a single-layer device are shown in figure 2.

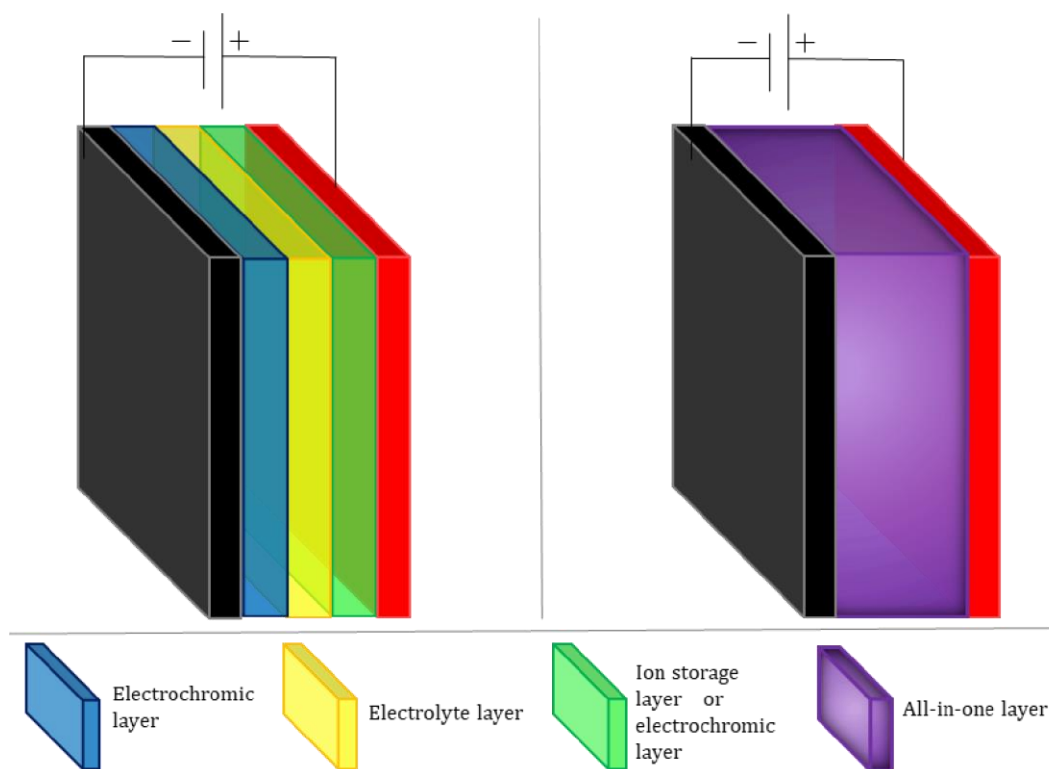


Figure 2 – A typical multi-layer (left) and single-layer (right) device. Note that the electrochromic layer and the ion storage layer can be one in place of the other.

It should be noted that using a gel matrix reduces but does not eliminate the risk of leaking or drying, therefore also in this case it is necessary to apply a sealant.

This brief description of the various electrochromic devices is already sufficient to start a decision analysis on what type our device will be. In the following section, we will focus exclusively on the architecture of our device, while the choice of each component will be subsequent and directly subordinate to this.

1.2.1. ECDs FOR OUR PURPOSE

As mentioned in the introductory section, the final device will have to possess different requirements. The ECD configurations will then be evaluated according to the achievement of these characteristics. Each architecture will be analysed and accepted until a relevant technical problem is found, which compromises the achievement of the intended targets. So if the problem is not considered solvable, the examination of that configuration is suspended and the others more suitable for our purpose are considered.

The electrolytic cell-type system shown in figure 1 obviously cannot find practical application. Although this architecture will not be considered for the realization of the device, it will be useful in the study of the properties and for the characterization of the final device (§ 3.5).

Otherwise, devices with flat electrodes and an electrochromic system placed between them, are perfectly suited to our purpose. A flat device recalls the geometry of a window, so it has a shape that lends itself to a good application.

The development of a liquid phase device has the advantage of having a single system solution, which is much appreciated in the industrial sector. However, at the same time it presents some technical difficulties which have already been partially seen previously.

First of all, the risk of leaking and drying is closely related to the sealing properties, so the sealant must not be permeable or interact with the electrochromic solution or its vapours. Furthermore, the sealant must adhere very well to the electrodes and must not shrink over time. To meet these needs, UV or thermo-cured epoxy resins or epoxy tape are often used as sealants^{2,5}.

Another problem lies in spacing the electrodes, not only to avoid the short circuit, but also to create an interspace to be filled with electrochromic solution. If epoxy tape is used, this is enough for spacing; alternatively, spacer beads are mixed with sealant resins. These procedures are not sufficient for big devices, because the larger size causes the device to bend in the central part. To remedy this, the spacer beads are scattered over the area of an electrode before assembling the device.

However, the greatest technical difficulty lies in filling the device with an electrochromic solution without trapping air bubbles during the process.

For small devices, a good filling method is based on the phenomenon of capillarity. Two openings left on opposite sides when sealing the device can be used to fill the interspace between the electrodes. The solution will enter from one hole and rise occupying the available space, favoured by the outflow of air from the opposite hole (Fig. 3). After this operation, a further sealant will be applied to plug the holes.

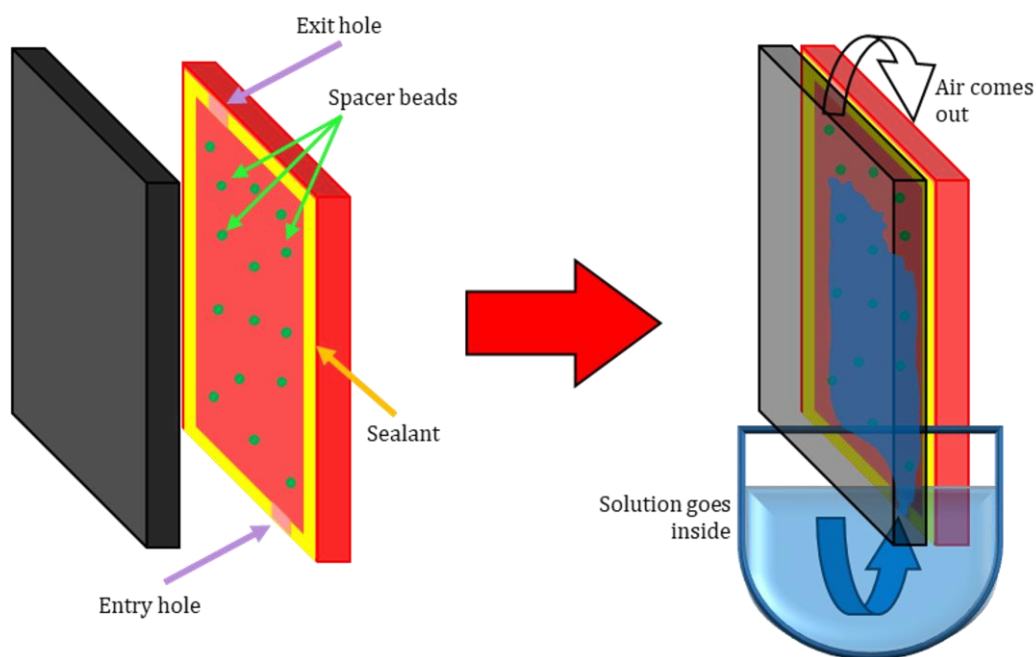


Figure 3 – Assembly and filling of a liquid phase device, using capillary action.

It is immediately evident that the main limitation of this method lies in the viscosity of the solution, mainly due to the physical properties of the solvent; as low viscous solvents are also very volatile, further care must be taken in the choice and application of the sealant.

Other difficulties arise on industrial scale processing, especially for large devices. Filling by capillarity would be more complicated and would require the use of low pressures; moreover, it would not allow having a continuous production process.

Finally, one of our goals is that the final device will have to be flexible, and the presence of a liquid phase inside it would make it really difficult to seal.

For all these reasons, it is advisable to set aside liquid phase devices and examine the opportunity to design an electrochromic device based on solid phases.

Unlike devices with liquid or semi-solid gel phases, the solid ones do not contain solvents, so they do not suffer from leaking or drying and do not need spacers or high-performance sealants. These features are a fundamental first step to obtaining a flexible device. Furthermore, the solid state approach may be more suitable for industrial development.

As mentioned in the previous section, solid phase electrochromic devices are made up of one or more layers. The technical difficulties in the realization of this type of device reside primarily in the formation of the thin layers or films; in fact, it is not sufficient for a substance to be soluble to also be filmable, that is, capable of forming a film.

Secondly, the formation of the film often takes place in not Standard Ambient Temperature and Pressure (SATP) and requires various steps.

Finally, the film is deposited through different techniques, which must be carefully chosen, considering both what you want to deposit and where. This will be widely discussed later (§1.7).

Considering only the procedural point of view, since these precautions must be taken every time for each layer to be deposited, it is much more convenient to develop a single layer device. On the other hand, from a synthetic point of view, this is the most tortuous road because it is necessary to find components that are stable in the same conditions, soluble and filmable in the same solvent and that do not react with each other.

Although the all-in-one configuration presents a high difficulty in the development phase, it makes the production phase much simpler, faster and cheaper, therefore industrially more interesting⁶.

After examining the different types and configurations of electrochromic devices, it was decided to develop a solid single-layer device, because it respects or will allow respecting all the established objectives.

Here the architecture of our device has been chosen, in the next sections we will examine the materials with which it will be built.

1.3. ELECTRODES FOR OUR PURPOSE

In the previous sections, the electrode was represented as a solid plate, coloured black or red depending on whether it represented the cathode or the anode. However, it is clear that for our purpose the electrodes must be as transparent as possible. So here we will concentrate on analysing only the transparent electrodes, excluding all other types from speculation, because they are not useful for achieving our goal.

Currently, the most common and used transparent electrodes are based on indium tin oxides (ITO) or fluorine tin oxides (FTO), deposited as a thin layer on a transparent glass substrate. Electrodes with FTO were developed after those of ITO with the intention of replacing Indium, an expensive and uncommon element, with Fluorine. Although the electrodes of FTO have a slight haze, the optical and electrical properties are comparable with those of ITO; in some respects, FTO is even better because it is more workable, chemically stable and cheaper than ITO. Despite this, the ITO has the advantage over the FTO about the smooth surface and the possibility of depositing it on flexible substrates⁷. It is precisely for this last property, which allows us to develop a flexible device, that we must discard the FTO.

Recently, alternatives to ITO-based flexible substrates are being researched, for example depositing zinc oxide layers⁸, producing a thin film of zinc oxide doped with aluminium (AZO) and metal nanoparticles⁹, rather than involving silver¹⁰ or copper^{11,12} nanowires in composite films. Another line of research focuses on the use of carbon derivatives such as nanotubes^{13,14} or graphene¹⁵ or conductive polymers¹⁶.

While these alternatives have bright prospects, ITO-based technology is the most mature and established technology today and on it falls the choice to build our device.

ITO is a mixture of indium(III) oxide (In_2O_3) and tin(IV) oxide (SnO_2), in usual ratio (90:10) wt%. It can be deposited both on glass and polyethylene terephthalate (PET), making the surfaces conductive while preserving their transparency (Fig. 4). Although our final electrochromic device will be flexible, it may be useful in the initial step to use a more rigid equivalent electrode, to limit technical assembly

problems that may occur in the development phase. Therefore, both ITO/glass and ITO/PET electrodes will be investigated.

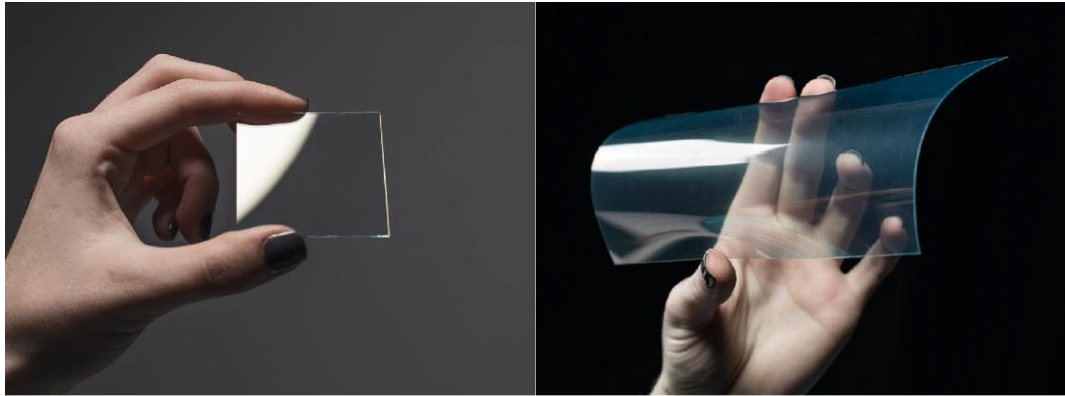


Figure 4 – ITO/glass (left) and ITO/PET (right) electrodes both have excellent transparency; by retaining the properties of the substrates, the former is rigid and brittle while the latter is very light and flexible.

As can be seen from the photos above, the high transparency allows their use in electro-optical devices such as electrochromic ones. To be precise, of these two electrodes, the most transparent is the one with the glass substrate, as confirmed by the manufacturer's technical sheets. Spectroscopic measurements in percentage of transmittance (T%) were carried out for the two electrodes with particular attention to the wavelengths in the visible range (390-760 nm) (Fig. 5).

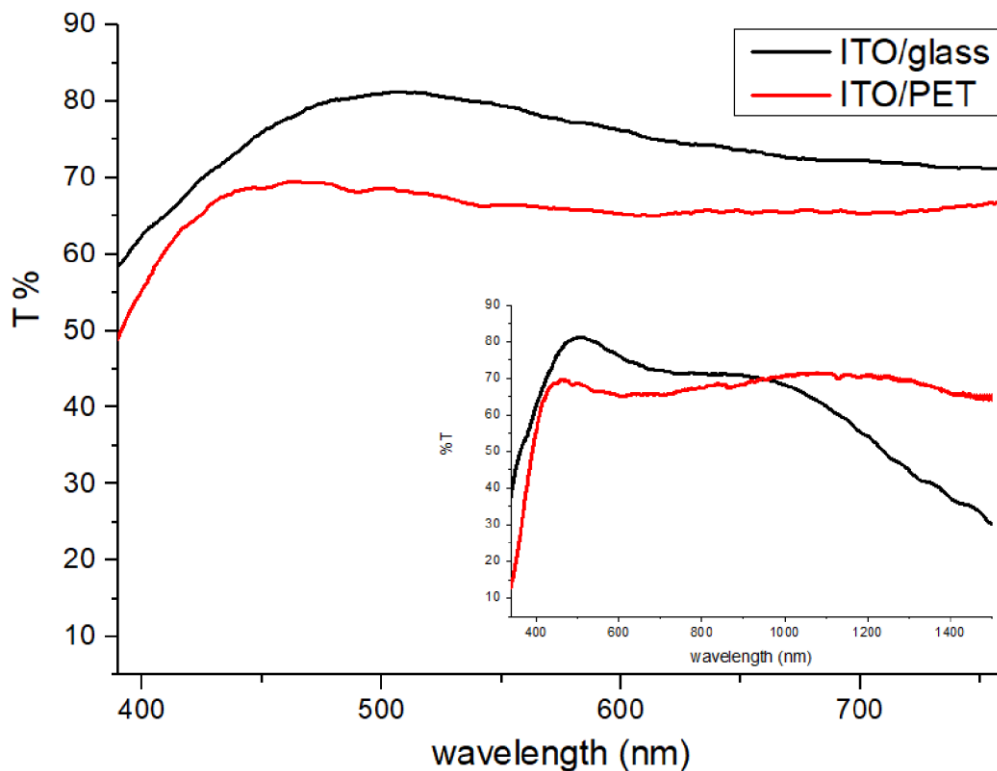


Figure 5 – Comparison between the spectra of ITO/glass (black lines) and ITO/PET (red lines). Transparency in the visible range is higher for ITO/glass although ITO/PET is not much lower. In inset: wider spectra with UV and NIR segments.

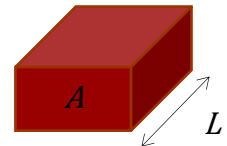
Rather than recording only the higher values, it is thought more useful to report both averages of T% in the aforementioned range.

According to our measurements, ITO/glass has an average transmittance in the visible range of 75% with a maximum of 81% at 509 nm; instead ITO/PET has an average T=66% with a maximum of 70% at 464 nm.

From the comparison between the technical sheets, it is clear that the ITO/glass electrode is also more conductive than the ITO/PET one, having a lower surface resistance (15-25 Ω/sq vs 60 Ω/sq). To avoid any misunderstanding, the meaning of surface resistivity is specified below.

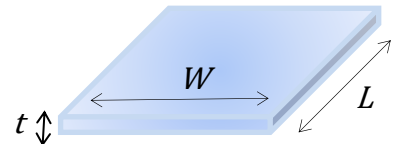
Surface resistance (R_s), (also known as *surface resistivity* or *sheet resistance*) is an electrical property used to characterise conductor or semiconductor thin films. As is known, the resistance (R) of a generic parallelepiped conductor can be calculated using the formula:

$$R = \rho \cdot \frac{L}{A} \quad \text{where} \quad \begin{array}{l} \rho = \text{resistivity} \\ L = \text{length} \\ A = \text{area} \end{array}$$



Similarly, the resistance of a conductor thin film is calculated by:

$$R = \rho \cdot \frac{L}{A} = \rho \cdot \frac{L}{t \cdot W} \quad \text{where} \quad \begin{array}{l} L = \text{length} \\ t = \text{thickness} \\ W = \text{width} \end{array}$$



Taking a square surface, thus having the same dimension for L and W, we have that:

$$R = \frac{\rho}{t} \Rightarrow R = R_s$$

Hence the resistance of a square thin film, regardless of its size, is equal to the surface resistance (R_s). Although the unit of the surface resistance is the ohm [Ω], this will be expressed as Ω/sq (or Ω/\square) in order not to confuse it with the bulk resistance (R). For non-square films, the resistance value can be calculated by multiplying R_s by the aspect ratio.

The greater transparency and conductivity of the ITO/glass electrode can be explained by the greater affinity of the conductive layer with the substrate. This

allows for a more uniform and smoother deposition on the glass in comparison to the PET, as visible from the SEM images⁸ in figure 6.

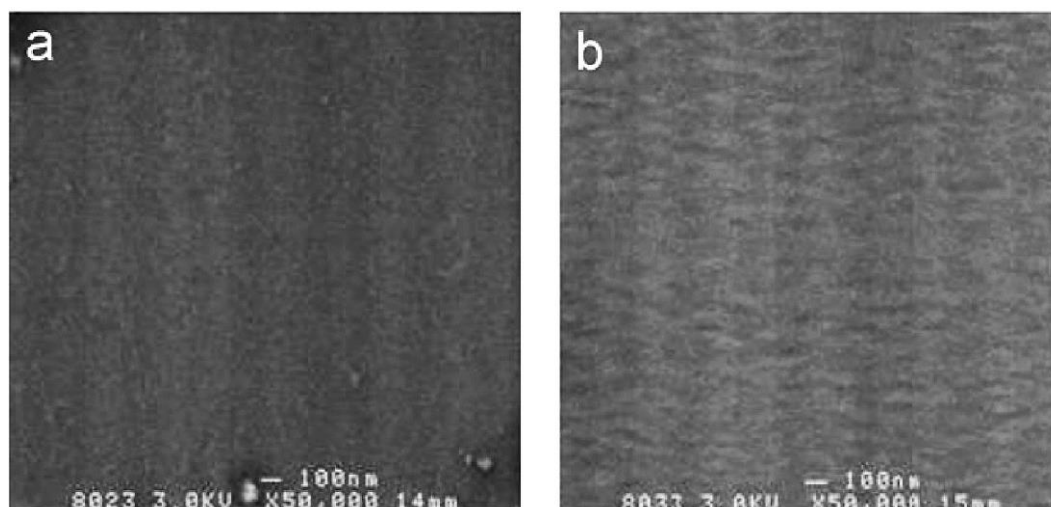


Figure 6 – SEM images of ITO depositions on glass (a) and PET (b) substrates. The surface of the ITO/glass appears smoother while the ITO/PET has a greater roughness. From ref. 8.

Although the conductive layer deposited is ITO for both glass and PET, the different affinity towards the two substrates causes a different surface morphology. This could cause a slightly different wettability of electrodes and will be considered in the development phase of the all-in-one film-forming electrochromic solution.

Therefore, the next sections will focus on the choice of electrochromic species, of electrolytes and, last but not least, of solvents; each one must necessarily be compatible with each other; moreover, the resulting film-forming solution must, in turn, be compatible with the chosen electrodes and generate a device with the properties established in the introductory section.

1.4. ELECTROCHROMISM AND ELECTROCHROMES

Exactly 60 years ago a scientific article was published in which the term "*electrochromism*" was mentioned for the first time¹⁷. Similarly, to photochromism and thermochromism, also in this phenomenon there is a reversible colour change, but here due to the application of an electric field. Materials that display electrochromic behaviour are called *electrochromes* (ECs).

The ability to change colour can occur with the reaction of electron uptake or release by the electrochrome; for this reason, we can refer to a reduction in the first case and oxidation in the second.

Since this electron transfer takes place on the electrode surfaces, required for the application of the potential, we can use extensively the definition *cathodically colouring* for species that are reduced by the cathode (negative electrode); vice versa we define *anodically colouring* species those that are oxidized by the anode (positive electrode)¹. For many years, although each redox reaction causes a change in the absorption spectrum, the only materials in which these changes are appreciable and fall at wavelengths in the visible range and not in the ultraviolet (UV) or near-infrared range (NIR), can be considered electrochromic¹⁸. In more recent times it is considered more appropriate to include previously discarded materials in the large family of electrochromics.

Since 1975, the main classification of electrochromes has not been much based on their inorganic or organic class, but on their phase in the initial state and in the reduced or oxidized state¹⁹.

According to this convention, electrochromes are classified into three types:

- **Type I** - Electrochromes are soluble both in the initial state and after electron transfer reaction.
- **Type II** - Electrochromes are soluble in the initial state and become insoluble after the electron transfer reaction
- **Type III** - Electrochromes are always in the solid phase, before and after the electron transfer reaction.

Many have tabulated the electrochromes, more or less in detail, either by type or by class^{18,20,21}; For greater immediacy, here we propose a summary scheme (Table 1) containing both characteristics.

TYPE	CLASS		
	INORGANIC	ORGANIC	ORGANOMETALLIC
I	<p>Hexacyanoferrates(III) Fe(III)thiocyanate</p>	<p>Short alkyl viologens*: e.g. Methyl viologen Ethyl viologen</p> <p>Carbazoles Fluorenones Quinones Phenylene diamines</p> <p>Tetracyanoquinodimethane (TCNQ) Tetrathiafulvalene (TTF) Triphenylamine (TPA)</p>	<p>Metal coordination complexes: e.g.</p> <p>Mo (or V) Nitrosyl complexes, [M^{II}(bipy)₃]²⁺ complexes (with M=Fe, Ru, Os)</p>
II	<p>Solid products of electrodeposited metals such as Bi, Pb, Ag</p>	<p>Polymethoxyfluorenes</p> <p>Heptyl viologen, Benzyl viologen, Cyanophenyl paraquat</p>	
III	<p>Metal oxides/hydroxides: e.g. WO₃, MoO₃, NiO, V₂O₅, Nb₂O₅, TiO₂, Ir(OH)₃</p> <p>Metal hexacyanomethylates: e.g. Fe^{III}₄[Fe^{II}(CN)₆]₃ Fe^{III}₄[Ru^{II}(CN)₆]₃ Ni^{II}₂[Fe^{II}(CN)₆]</p>	<p>Polyviologens</p> <p>Conjugated polymers: e.g. Polyaniline (PANI) Polypyrroles Polythiophenes</p>	<p>Metal phthalocyanines: e.g. Lu(Pc)₂ Co(Pc)</p> <p>Metallopolymers: e.g. Poly[Ru^{II}(vbpy)₂(py)₂]Cl₂</p>
* Viologens: (1,1'-Disubstituted-4,4'-bipyridinium salts)			

Table 1 - Types and classes of the most common electrochromes. The main groups are shown in bold.

The variety of the physical states of the electrochromes predetermines the different requirements needed for the operation of the final device. For example, a device that uses type I and type II electrochromes will have to contain a liquid phase inside it, so it will require a suitable seal to prevent the system from drying out and from leaking; otherwise, type III electrochromes do not suffer from the aforementioned problems, but often need higher voltages due to the lower mobility of the charges.

Similarly, the choice of electrochromes class not only determines the technical characteristics, but imposes materials and methods for process and assembly of the final device.

1.4.1. ECs FOR OUR PURPOSE

The reasons for avoiding a liquid phase inside the device have been previously discussed; therefore, we can exclude the use of type I and type II electrochromes, because they work through a solution. Based on the choices already made, the most suitable electrochromes are those of the third type, able to operate in solid phase.

Now it is necessary to decide which class of materials to use and within this the most adaptable species to achieve our goals

According to a comparative analysis from the literature²² and as re-proposed in table 2, the use of polymeric electrochromes has several advantages compared to inorganic species.

Property	EC Inorganic materials	EC Polymers
Method of preparation	Needs sophisticated techniques such as vacuum evaporation, spray pyrolysis, sputtering, etc.	The material can be easily prepared by simple chemical, electrochemical polymerization and the films can be obtained by simple techniques such as dip-coating, spin coating, etc.
Processibility of the materials	The materials are poor in processibility	The materials can be processed very easily
Cost for making the final device	High as compared to the polymer based devices	Low cost as compared to the inorganic materials
Colours obtainable	A limited number of colours are available from a given material	Colours depend on the doping percentage, choice of the monomer, operating potential, etc. Hence, a large number of colours are available with the polymeric materials
Contrast	Contrast is moderate	Very high contrast can be obtained
Switching time (ms)	10-750	10-120
Lifetime (cycles)	10 ³ -10 ⁵	10 ⁴ -10 ⁶

Table 2 – Comparison between inorganic and polymeric electrochromes. From ref. 22.

The table above shows several critical issues for inorganic electrochromes, both in the preparation phase and in the final properties. Not insignificant is the poor adaptability of the deposition methods on flexible polymer-based substrates and the difficult industrial scalability.

Regarding the organometallic electrochromes, the main incompatibilities with the device we want to create are mainly the absence of a transparent redox state²³ or the efficiency in the NIR ^{24,25}; furthermore, they all have rather long and difficult syntheses.

In light of what has been considered, the best choice is to use polymeric electrochromes; therefore, the behaviours and characteristics of electrochromic polymers will be evaluated for achieving our aim.

Conjugated polymers are very interesting because they have the potential to be adequately functionalized to acquire tailor-made properties such as a specific solubility or certain multi-chromaticity. This is possible through the modification of the starting monomers or through subsequent addition of functional groups. Moreover, by selecting specific building blocks, it is possible to synthesize polymers that are at the same time donors and acceptors of electrons, significantly increasing the performance of the devices^{26,27}. Despite this great adaptability, which makes them interesting not only in the electrochromic field, the synthesis and processibility of conjugated polymers often involves organic or halogenated solvents, such as toluene, dimethylformamide (DMF) and chloroform.

Considering that, in recent years, greater attention has been paid to reducing the use of solvents that are dangerous for handling and are harmful to health or the environment²⁸, it is preferable to choose electrochromic polymers soluble in so-called green solvents.

It would be even better if the polymers were processable by water, the green solvent par excellence. Although this trend is commonly accepted and encouraged, the synthesis of water soluble electrochromic polymers is rare²⁰.

A very recent study has reviewed water soluble electrochromic organic materials; only some of these have a transparent state, while others vary in colour²⁹. As noted by this work, most of the water-soluble polymers are based on viologens which, despite having potential toxicity, remain the most used. This is probably due to the faster and easier synthesis which makes them less expensive than many conjugated polymers, for which further development needs to be achieved.

Precisely the characteristics listed above, namely polymeric nature, one colourless oxidation state, easy and fast synthesis, solubility in water and low cost, make polyviologens the ideal electrochromic materials for our device, making it scalable at the industrial level.

1.4.1.1. VILOGENS AND POLYVILOGENS

The *Viologens* constitute a large family of electrochromic species, so called because they become intensely violet after reduction³⁰. They are synthesized by diquaternising 4,4'-bipyridine to form substituted bipyridinium salts (Fig. 7).

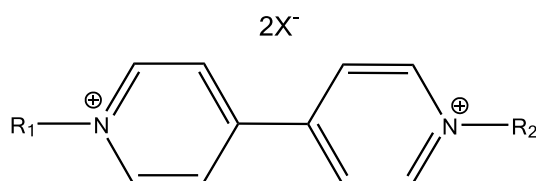


Figure 7– Structural formula of a generic viologen.

Although the compounds have formal IUPAC name *1,1'-di-substituent-4,4'-bipyridinium* if the two substituents on the nitrogens are the same ($R_1=R_2$) and *1-substituent-1'-substituent'-4,4'-bipyridinium* when they differ ($R_1\neq R_2$), the nomenclature of symmetrical and asymmetrical viologens is widely used today.

The positive charges shown on nitrogens is better viewed as being delocalised over the respective rings. There is little delocalization between the two rings due to the lack of π -overlap, which is a consequence of the large dihedral angle between them³¹.

The colourless bipyridinium dication (commonly abbreviated "*bipm*²⁺" or "*V*²⁺"), is the species obtained through synthesis and is the most stable redox state among the three possible shown in figure 8.

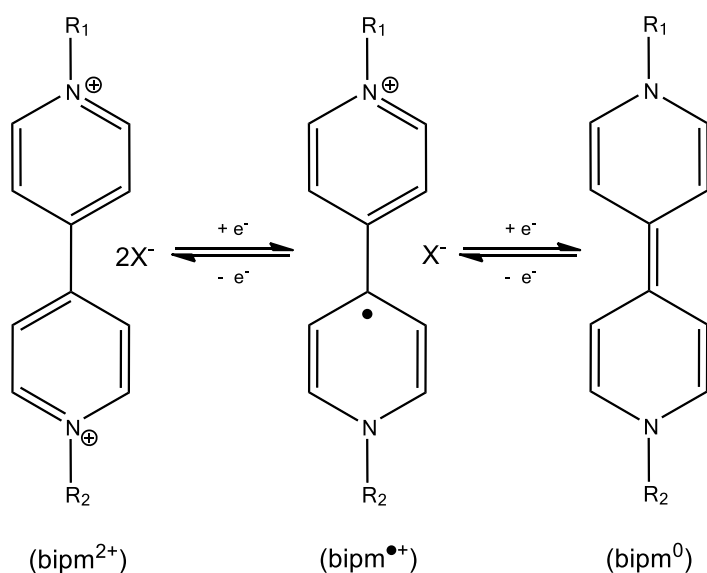


Figure 8– Structural formulas of the three redox states of the bipyridinium: from the dicationic to the neutral form from left to right.

The other two are obtained by successive reductions and are respectively the strongly coloured radical cation ($bipm^{\bullet+}$) and the weakly coloured neutral compound ($bipm^0$).

The radical cationic viologens ($bipm^{\bullet+}$) are among the most stable organic radicals and form salts stable in the air³². This high stability is due to the delocalization of the radical on both pyridine rings; in fact, the molecule becomes planar when reduced and, contrary to the dicationic form, allows the conjugation of the rings through π -overlap. This large delocalization is also responsible for the strong colouration as it leads to intramolecular photo-effected electronic excitation³¹.

Instead, the neutral form ($bipm^0$) is not very colourful because no optical charge transfer or internal transition occurs within the visible range; these compounds act trivially as reactive amines³³.

Explained the electrochemical action of the bipyridinium heart, which is responsible for the electrochromic properties of the viologens, the roles of counterions and substituents need to be investigated.

The anionic counterpart ($2X^-$) often results from the synthetic process; it generally consists of two monovalent anions, but it is also possible that it is a bivalent one. The anionic species is significant for the solubility in different solvents^{34,35} and also for stability^{35,36} of the viologens. The negative charges for electronic balancing of the dication can also be grafted as a substituent functionality, making viologen a zwitterionic molecule^{37,38}.

Following what has been said, the key role of the substituents in conferring different properties to the viologen appears evident. For example, the filmability of a viologen is obtained only when the effective length of the substituent chains exceeds the four CH_2 units, but a sufficiently stable film is obtained starting from the six methylene bridges³⁴.

From this arises the type of electrochrome of the given viologen: those having short substituents are type I, the intermediate ones are type II, the longest are type III electrochromes.

Also polymeric viologens are electrochromes of the third type and some can be obtained very easily by reacting the 4,4' bipyridine with the substituent in equimolar concentration.

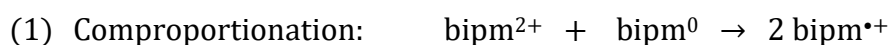
Polyviologens have electronic properties similar to those of their respective monomers, inherit the possibility of being easily functionalized, carry electrons in the solid state³⁹ and form very robust films with good mechanical stability due to their high molecular weight⁴⁰.

Since the great weight of the polymer gives better strength to the film, the crosslinking of the polymer chains should generate film with even greater mechanical properties; the main drawback of the crosslinking is the loss of solubility. The copolymerization of a polyviologen with an anionic polymer also causes insolubility⁴¹.

The lack of solubility would require film formation techniques which often involve high temperatures, at which the polymer is melted and can be deposited; despite these techniques, the cross-linked polyviologens do not form films, because they are infusible and decompose starting from 250 Celsius degrees⁴¹.

Although the development of devices with water-soluble polyviologens can reduce the environmental impact and risks to human health during film deposition operations, attention should be paid to adverse reactions that may occur.

In aqueous environment, side reactions of comproportionation (1) and dimerization (2) have been observed; viologenes form aggregates that are difficult to reoxidize^{42,43} and cause yellow-brown stains on the electrodes⁴⁴.



This aging effect can be avoided by using organic solvents such as propylene carbonate^{43,45} or acetonitrile⁴³, or by incorporating the polyviologen into a matrix to distance the polymer chains⁴⁶; dimerization is reduced in both cases and reversibility is increased¹⁸.

Since it has been decided to use a viologen as the main cathodically colouring electrochromic species, it is of great importance to choose a suitable anodically colouring counter-species, in order to facilitate the electrochemistry of the device.

1.4.1.2. COUNTER-SPECIES FOR OUR PURPOSE

In the previous description of the various types of ECD, the concept of ion-storage layer or counter-layer was mentioned. This layer is essential for efficiency and charge balance purposes of the whole ECDs based on a non-zwitterionic electrochrome such as a simple viologen. Counter-layer can be constituted either by a colourless redox-active material or by an electrochrome with behaviour opposite to the main one⁴⁷. In our case, since the viologen is coloured by reduction, a counter-species is required which is transparent in the initial state and is coloured after oxidation; in this way both electrochromes will respond coherently to the potential and will be simultaneously in the transmissive or coloured state²⁰. Moreover, the introduction of an anodic electrochrome that acts as electron donor, improves the ECD performance in terms of increasing optical contrast and cycle stability, lowering the operating voltage and shortening colouring/bleaching times⁴⁸.

Many electrochromic molecules that can be used as counter-species are based on carbazoles⁴⁹, quinones⁵⁰, fluorenones⁵¹ and various aromatic amines^{52,53}. For our purpose, taking advantage of the experience gained by others^{42,46,54}, it seems appropriate to use the *N, N, N', N'*-Tetramethyl-1,4-phenylenediamine (TMPD). This anodic electrochrome is colourless in the neutral state and acquires an intense navy blue colour when oxidized. Further loss of electron results in a light blue hue⁵⁵. The various redox states of TMPD are shown in figure 9.

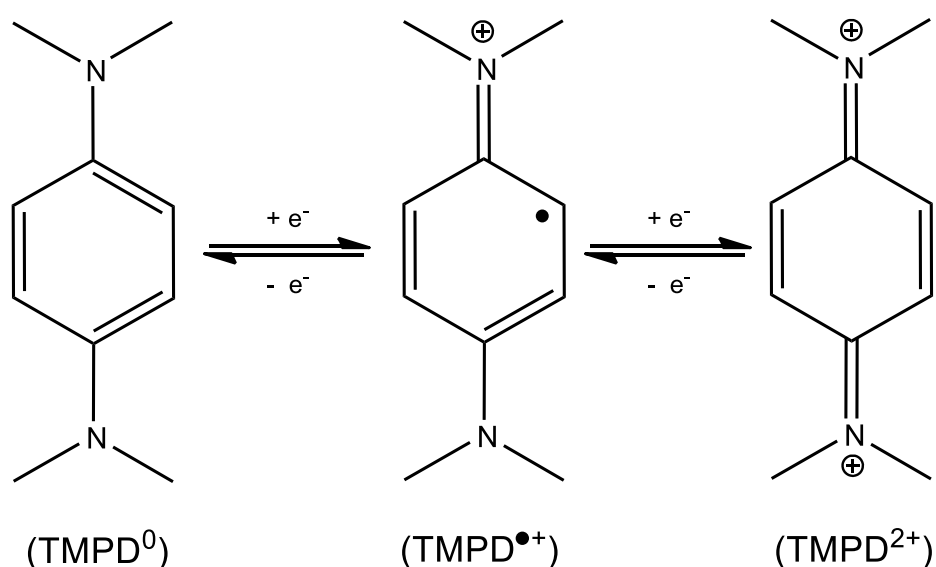


Figure 9 – Structural formulas of the three redox states of the TMPD: from the neutral to the dicationic form from left to right.

In aqueous environment TMPD is mainly in its radical form, which for this reason is often called Wurster's blue; the dicationic form is very labile and often returns easily to the radical one⁵⁶.

In the exact opposite way to what occurs to viologens, TMPD can undergo two oxidations; operating in overlapping potential windows⁵⁵, it happens that when the viologen is reduced, the TMPD is oxidized and vice versa.

Moreover, since the electrochromes are both soluble in water, they are compatible with the development of the all-in-one solution.

As the solubility of electrochromes in aqueous phase is in line with our goal, it seemed a good solution to disperse these in an electrolytic matrix not only to obtain a future solid system, but also to isolate them and reduce possible side reactions. Therefore, the characteristics of the aforementioned matrix will be established in the following section, from which the choice of materials will arise.

1.5. ELECTROLYTES

The electrolyte has a very important function not only in ECDs but in all electrochemical systems, because it allows the electronic charge to flow through the movement of the ions between the electrodes^{57,58}. Classically the electrolyte consists of the dissociation in a solvent of an ionic salt⁵⁹.

Among others, lithium salts are the most used for the constitution of electrochemical devices, because the resulting cations Li^+ are very small and they have excellent solubility both in organic solvents⁶⁰ and in aqueous environment, depending on the anion forming the salt. Moreover, lithium ions move easily through membranes and polymer chains, making them usable even in solid state technologies, such as batteries and electrochromic cells⁶¹. Whatever the application, the electrolyte does not get involved in electrochemical reactions and just acts as Li ion-conductive media.

Nowadays, different classes of electrolytes are used such as liquids, gel, ceramics, inorganic solids or polymers⁶²⁻⁶⁷.

The arguments previously discussed in the electrochromes section (§1.4.1) also apply to the choice of the electrolyte; therefore, for our purpose, liquid and gel electrolytes are excluded to avoid leakage, while the use of solid, flexible and transparent electrolytes is preferable.

The advantage of ceramic and inorganic solid electrolytes lies in their non-flammability, but they have poor flexibility and low ion conductivity due to their high grain boundary resistance⁶⁸. Furthermore, the deposition and aging phases often involve highly acidic solutions and high temperatures, which results in a reduced affinity with the plastic substrate of the electrodes.

On the contrary, polymeric electrolytes possess excellent flexibility, relatively wide electrochemical window⁶⁶ and can also easily acquire other properties through various functionalization; their deposition takes place in mild chemical-physical conditions and the filmability is great.

1.5.1. ELECTROLYTES FOR OUR PURPOSE

Electrolyte polymers were first synthesized in 1973⁶⁹ and consist of a polymer with salts dissolved in it⁷⁰. These materials allow the passage of ions inside them avoiding the use of solvents.

Although the final material is solvent-free, it must not be forgotten that the use of solvents is unavoidable in the production phase; therefore, the choice of the electrolyte polymer for our purpose will be taken also considering the dangerousness and toxicity of the solvents used for the synthesis.

It is obvious that the electrolyte salt and the polymer must both be soluble in the same solvent; from this observation arises a first subdivision of electrolyte polymers: those soluble in organic solvents and those soluble in aqueous environment. Although the use of organic solvents in the process allows a greater range of available polymers, at the same time it could cause fire hazard and health safety issues, especially on an industrial scale where the amount of solvent required is considerable.

Another major subdivision within the electrolyte polymers can be based on their nature: synthetic ones derive from chemical processes, while natural ones derive from biological processes that occur in plants or animals and are therefore eco-sustainable, cheap and abundant.

There are many synthetic electrolyte polymers used in the field of electrochromism, such as PMMA⁴⁶, PVC⁷¹, PEO⁷² and PVA^{73,74}, while among the polymers of natural origin we can mention ethyl cellulose⁷⁵, chitosan⁷⁶, corn starch⁷⁷ and rice starch⁷⁸.

Whether they are synthetic or natural, electrolyte polymers must possess certain requisites, as reported by others^{48,68,79-81} and re-proposed below:

- **High optical transparency.** Since our application requires the device to be transparent, the electrolyte polymer must have a good transmittance.
- **High ionic conductivity.** Good mobility of the ions inside the electrolyte polymer, allows the current to flow in the device preventing the charges from collecting on the electrode surfaces.

- **Electrical insulation.** In the device we want to make, the electrolyte polymeric matrix will constitute the predominant part of the layer interposed between the two electrodes, therefore it will also electrically isolate the anode and the cathode to prevent a short circuit.
- **Thermal and chemical stability.** The electrolyte must be thermally and chemically inert in the operating conditions of the device, to avoid degradation or side reactions during use.
- **Wide potential window.** This indicates the potential range within which the electrolyte polymer retains its integrity, without undergoing oxidation or reduction. The larger the potential window, the more the electrolyte lends itself to integration with different electrochromes.
- **Solubility.** For our purpose, electrolyte polymer must be able to act as a host matrix for electrochromic species, so it must be soluble in the same solvents.
- **Filmability.** Since the desired device will be placed on already existing windows, it is preferable that it has a very small thickness; therefore, obtaining the electrolyte polymer as a thin layer or film is functional to our goal.
- **Easy processing.** The considerable advantages deriving from the use of polymers is their extensive workability and adaptability to different process techniques, facilitating industrial scalability.
- **Mechanical strength.** Polymers are generally tolerant to shock, vibration, and mechanical deformation. Using an electrolyte with these properties makes the whole device more robust.
- **Flexibility.** Using a flexible electrolyte polymer is essential for making a non-rigid device. Furthermore, having fewer interactions between the polymer chains favours the passage of ions between them.
- **Adherence.** The electrolyte polymers can act as a binder of the whole device and through a good adhesion with the electrodes ensures good electrical contacts.
- **Cheapness and environmental friendliness.** In view of a future industrial application, it is preferable to use economic materials and eco-sustainable processes.

Taking into account the characteristics listed above and remembering what has been said in the previous sections, the most coherent choice regarding the electrolyte to be used in the realization of our ECD can only concern the use of natural polymers which can be processed in an aqueous environment. Chitosan in particular seems to fit perfectly with the electrochromic system under development, so the next section will be dedicated to the deepening of this material.

1.5.1.1. CHITOSAN

As mentioned in the previous section, using solid electrolytes based on natural polymers allows avoiding polymers deriving from non-renewable fossil sources, whose synthesis and processing often generates dangerous chemical agents and takes place in toxic solvents. Synthetic polymers with very slow natural decomposition contribute to the increase of environmental waste.

Conversely, using a natural, abundant, renewable, biodegradable and low-cost polymer, such as chitosan, can be the breakthrough for large-scale, inexpensive and eco-friendly production of ECDs⁸².

Chitosan is a natural polymer derived from chitin, one of the most naturally occurring organic compounds after cellulose. Unlike the latter which derives from plants, chitin has animal origin. Most chitin is extracted from crustacean shells or insect cuticles, but is also present in mushrooms, green algae, cell walls, and yeasts⁸³. The waste produced by the marine food industries, is the major commercial source of chitin.

Chemically speaking, chitin is a linear aminopolysaccharide consisting mainly of (β -(1-4)-N-acetyl-D-glucosamine) units^{84,85} (Fig. 10).

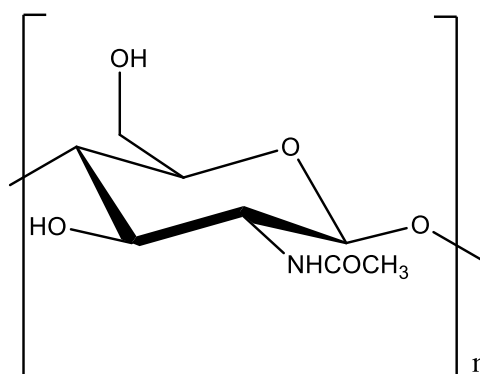


Figure 10 – Structural formula of chitin monomer.

Because of its high crystalline structure and intra- and intermolecular hydrogen bonding network between carbonyl, hydroxyl, and acetamide groups, this natural polymer is insoluble in common organic and inorganic solvents⁸⁶ but, it is soluble in concentrated inorganic acids, such as hydrochloric acid, sulfuric acid, and phosphoric acid⁸⁵.

The removal of the acetyl group from chitin leads to the synthesis of chitosan, whose structural formula is shown in figure 11.

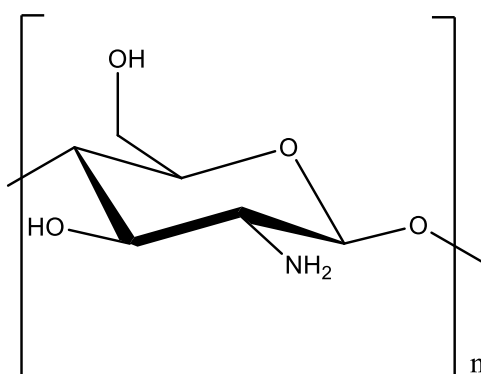


Figure 11 – Structural formula of chitosan monomer.

The amino group, with pKa from 6.2 to 7.0, located in the repeating unit of chitosan, allows the natural polymer to be soluble in a slightly acidic environment ($\text{pH} < 6$); the amine quaternizes and assumes a positive charge, making the chitosan soluble in aqueous solutions. On the contrary, in conditions of $\text{pH} > 6$, chitosan has only tertiary amines, the polymer has no positive charges and does not possess water solubility⁸⁷.

Since in the chitin to the chitosan conversion process, not all acetyl groups are removed, the percentage of deacetylation of commercial chitosan can vary from 50% to 98%, and this is crucial for its solubility⁸⁸.

Another very important parameter used to classify chitosan is the molecular mass. Generally, it refers to low molecular weight for 50-190 kDa, medium molecular weight for 100-300 kDa, or high molecular weight for 310-375 kDa; as the molecular weight increases, the viscosity of the chitosan solution increases, which must be taken into consideration during the processing phase.

From the chitosan solution a transparent film can be easily obtained, which will be the starting point for the constitution of the solid electrolyte to be used in the electrochromic device under construction.

The chitosan film will act as a matrix, inside which a lithium salt will be dissolved for ionic conduction. Similar to what happens in PEO-based electrolytes⁸⁹, lithium ions can interact with oxygen and nitrogen lone pairs⁹⁰, allowing cationic transport through the segmental motion of chitosan chains^{91,92}. It follows that the ionic

conductivity is closely related to the mobility of the chains, therefore to the flexibility of the film.

Since hydrogen bonds and ionic forces are established between chitosan polymeric chains, through amine, acetyl amine and hydroxyl groups⁹³, the resulting film is rather rigid and brittle.

As reported in the literature ^{94,95}, the dissolved salt ions act as charge modifying agents towards the chitosan chains, screening their charges and generating electrostatic repulsion between them; this leads to an increase in inter-chain distances and consequently to an increase in free volume of the whole polymer matrix, which makes the electrolyte film more flexible.

Although the presence of ions improves the flexibility of the film, the introduction of plasticizer molecules that intercalate between the chitosan chains, gives them greater mobility and therefore greater flexibility to the film⁸⁸, also allowing a smaller amount of electrolyte salt to be used⁹⁶.

Among the various plasticizers suitable for chitosan⁹⁷⁻⁹⁹, the best seems to be glycerol¹⁰⁰⁻¹⁰³, because it has three hydroxyl groups capable of forming hydrogen bonds¹⁰⁴ so that it can replace the network of inter-molecular hydrogen bonds between the chitosan chains, spacing them without forming new cross-linking¹⁰⁵.

Another very positive aspect that makes us inclined towards the use of glycerol lies in the fact that it fits very well with the guideline of our purpose regarding environmental friendliness.

By combining the action of the electrolyte salt ions and the plasticizer, the amorphous phase of the chitosan increases, implying greater mobility of the polymer chains and thus supporting the ionic conductivity¹⁰⁶⁻¹⁰⁸. Using a natural polymer, preferably plasticized, with a lithium salt dissolved therein constitutes the suitable choice for the constitution of the solid electrolyte constituting the electrochromic device in our purpose.

Furthermore, the electrolyte matrix and therefore the resulting film can be improved by inserting metal nanoparticles inside it, with the aim of increasing the electrical conductivity and consequently the electrochromic activity. For this reason,

the possibility of using metal nanoparticles will be analysed in the next section, choosing their nature and shape, remaining faithful to the guidelines outlined at the beginning.

1.6. METAL NANOPARTICLES FOR OUR PURPOSE

Over the last few decades, the combination of metal nanoparticles and electrochromes has increased as many advantages have been highlighted. First of all, it is easy to understand that the presence of metal particles facilitates the electrical conduction inside the device. This is possible because the characteristics of the metal are preserved even on a very small scale¹⁰⁹. Indeed, it has been verified that the metallic nanoparticles close to the electrode increase the charge transfer ability¹¹⁰. This aspect is very important as the polymer matrix must be insulating to avoid short circuits during operation; therefore, increasing the presence of electrons in the matrix allows a greater number of electrochromic molecules to be reduced, increasing the colouring efficiency of the device¹¹¹. Furthermore, the slow relaxation of the charges around the nanoparticles generates a greater optical memory, thus allowing the device to remain coloured for longer after turning off the power supply¹¹².

Therefore, believing that the insertion of nanoparticles inside the device can improve it, we need to establish the nature and the most suitable form for our purpose.

Unlike the cited articles, in which gold or silver nanoparticles are used, in our work we will try to introduce copper nanoparticles, a less expensive metal but with excellent properties.

Copper is a good electrical conductor with a conductance ($\sigma = 5.96 \cdot 10^7$ S/m) comparable to silver ($\sigma = 6.3 \cdot 10^7$ S/m), the best ever; on the other hand, compared to the latter it is about a thousand times more abundant and a hundred times less expensive¹¹³. These features make it the ideal metal to implement our low-cost device.

Like other metals, copper can be synthesized into nanoparticles of various shapes and sizes^{114–118}. For our purpose, it could be advantageous to use elongated nanoparticles, able to introduce themselves along the whole bulk of the film. Therefore, we opt for the use of long non-enveloped nanowires, which can position themselves through different sections of the film and interconnect them, enhancing electrical conduction.

Although nanowires have a lower surface-to-volume ratio than other nanoparticles, they exhibit greater durability because, thanks to their unique surface structure, they resist better Ostwald ripening and other dissolution phenomena^{119,120}. Furthermore, metal nanowires have been shown to enhance electrochemical processes as they can act as catalysts¹²¹.

In conclusion, due to their catalytic function and cheapness, it was decided to use copper nanowires as agents facilitating the electrochromic activity of the device under construction.

Since the electrochromic layer must be like a film to be interposed between the electrodes, the next section will deal with the various techniques commonly used to obtain films and subsequently the choice of the most suitable one for the intended purpose.

1.7. DEPOSITION TECHNIQUES

In the previous sections, the materials considered most suitable for the realization of the electrochromic device with the desired characteristics have been analysed and consequently chosen. Both electrochromic and electrolytic species were voluntarily selected as having film-forming abilities, good optical transparency and green solvents solubility.

In this section we will evaluate which is the best deposition technique to obtain the electrochromic film, taking into account several factors: the nature of the materials, the characteristics of the solvents that can be used, the wettability of the electrode substrates and the adaptability on a larger scale.

The intent is to mix in a single solution the viologen, the chitosan matrix and the lithium salt, from which the film will be obtained. Due to the organic nature of the main species composing the electrochromic system, it is preferable to use deposition methods that operate in mild physical conditions to avoid degradation of the electrochrome and polymeric matrix molecules. Among the various deposition techniques¹²², those involving high temperatures will be discarded, while those that exploit the sol-gel method will be analysed and compared.

The *sol-gel method*¹²³ consists in depositing a layer of the film-forming solution on the substrate to be coated; during the evaporation of the solvent, self-assembly of the solute molecules will take place, from which the formation of the film will arise.

The method just described is the basis of dip-coating, spin-coating, spray-coating and solvent-casting. The main common advantage of all these techniques lies in the low cost, low temperature conditions and easy scalability.

The difference between the four techniques lies in the first step, precisely in the way in which the solution is deposited, after which the chemical-physical processes that follow are the same.

*Dip-coating*¹²⁴ involves the immersion of the substrate in the film-forming solution and the subsequent rising from it. In this way, a thin liquid layer will remain adhered to the substrate and will generate the film after solvent drying (Fig. 12). The

parameters through which this technique allows to adjust the thickness of the final film are the immersion time, the rising speed and the drying conditions.

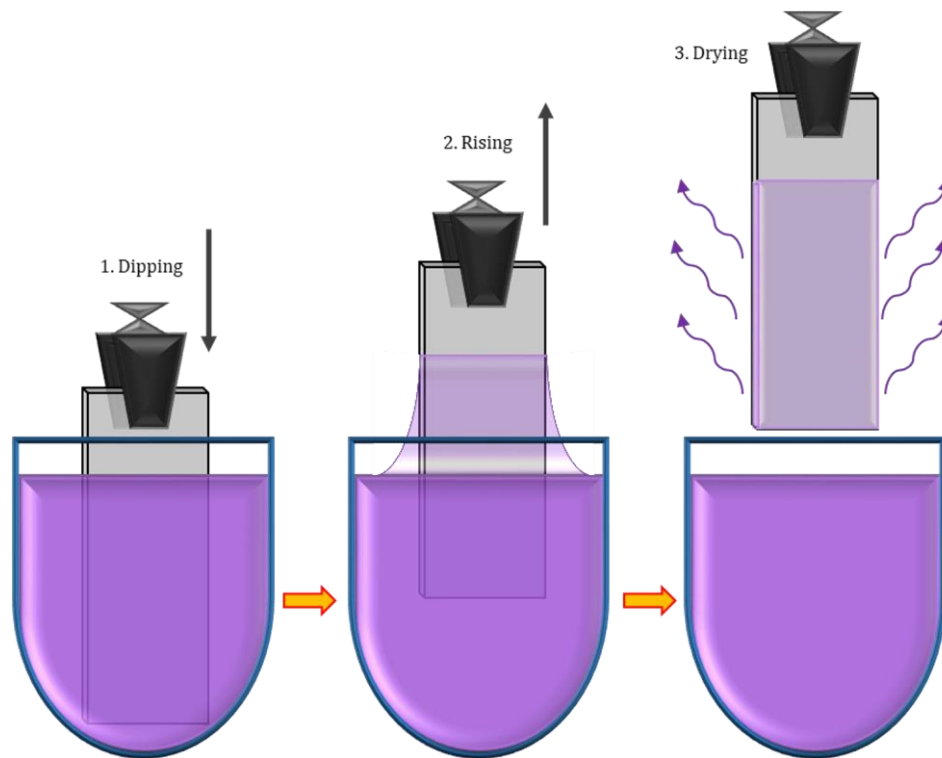


Figure 12 - The three steps of dip-coating method.

A notable advantage of the dip-coating lies in its versatility which makes it suitable also for very viscous solutions, which can be deposited by greatly reducing the rising speed. Furthermore, if desired, it allows coating both faces of the substrate at the same time.

A limiting factor for the dip-coating is the need to have a vessel large enough to contain the substrate and to fill it with a consistent amount of film-forming solution. This causes many difficulties in adapting the technique to an industrial level, as well as the need to work with considerable quantities of solution in line with the size of the substrate to be coated.

*Spin-coating*¹²⁵ method could be a good alternative to save the solution; in effect, this technique consists in employing the minimum quantity of film-forming solution on the substrate, which is placed on a rotating base. Due to rotation, the excess solution is eliminated by centrifugal forces, leaving a thin wet layer on the substrate, which forms a film after drying (Fig. 13). For this technique, the parameters on which the thickness of the film will depend are the rotation speed, the spin time and the drying conditions. what makes this technique unsuitable for industrial

application is the need to have rotating support dimensionally adequate for the substrate, therefore impractical to cover a large area. Furthermore, it does not allow continuous processing, thus making production difficult to automate.

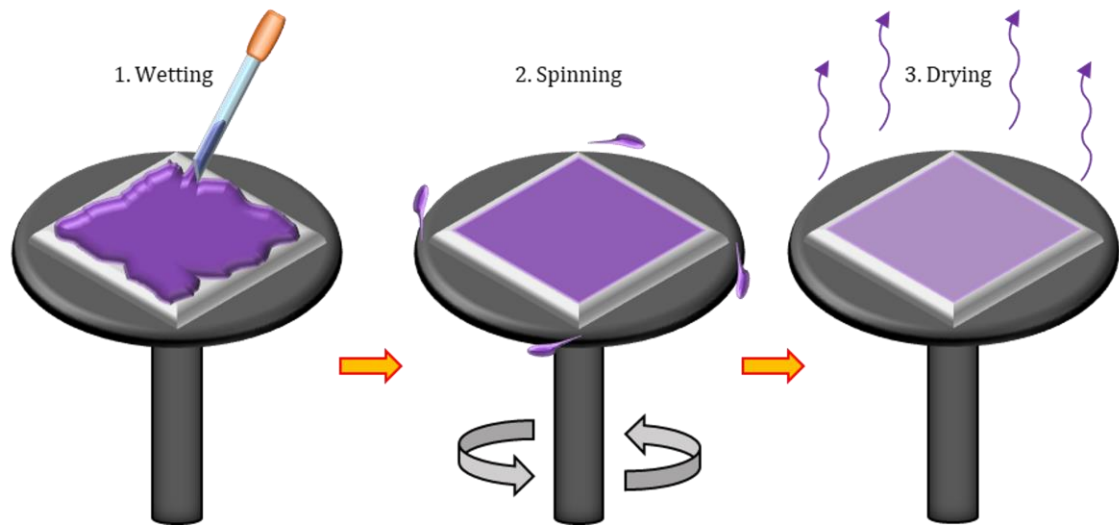


Figure 13 – The three steps of spin-coating method.

The *spray-coating*¹²⁶ method represents a further step forward in choosing the most suitable technique for our purpose; it consists in spraying the right amount of film-forming solution on the substrate followed by the drying step (Fig. 14).

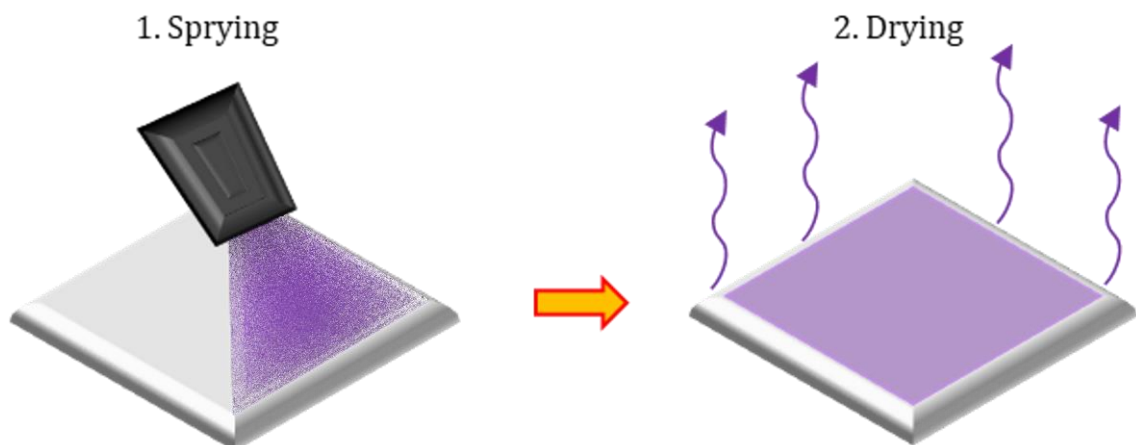


Figure 14 – The two steps of spray-coating method.

The thickness of the film can be varied by changing the operating pressure and the number of sprays. Although not very suitable for viscous solutions, spray-coating is interesting because it avoids the waste of solution and provides the possibility of working in a continuous process. On the other hand, as for the other two techniques seen previously, the indispensable condition for deposition is the remarkable affinity between solution and substrate. This is called *wettability* and is the biggest

limitation of the three techniques just described. When there is poor wettability, most of the film-forming solution tends to go away from the substrate, while the remaining part is organized in drops, thus avoiding the formation of the thin wet layer, which is the starting point for obtaining the film.

*Solvent-casting*¹²⁷ is an excellent method for obtaining films in case of poor wettability. This technique consists in casting a fair amount of solution directly on the substrate, preferably confined by removable walls; the solution cannot slip away and slowly loses the solvent by evaporation, which causes the progressive precipitation of the solute and the formation of the film (Fig. 15).

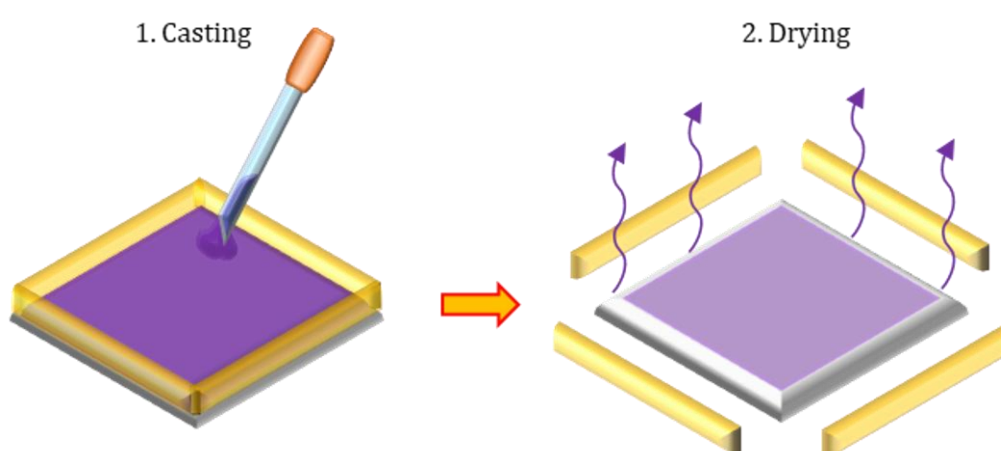


Figure 15 –The two steps of solvent-casting method.

It is not always necessary to use walls in the casting step but it depends on the cohesion forces of the film-forming solution, on its viscosity and the wettability evaluation.

This technique controls the thickness of the final film by adjusting the quantity and concentration of the poured solution. In order to have a good homogeneity of the film produced it is necessary to work on a level surface, perfectly parallel to the ground.

Since for our purpose it is expected to deposit a film from an aqueous solution on a substrate having poor wettability towards water, solvent-casting seems to be the most suitable.

Although difficult to use on an industrial level, in reality, the solvent-casting method is quite approximate to the *Doctor blade* or *knife-coating*¹²⁸ technique. This deposition method is widely used in various industrial sectors where it is necessary

to spread a solution on support and allows to work in a continuous process if the substrates are flexible enough to be roll-up.

The action of the winding roller causes the unrolling of the substrate along a path in which the film-forming solution is poured over it and subsequently levelled using a blade. The wet layer thus deposited undergoes drying later in the path and the film will be formed (Fig. 16). The height of the cut can be varied as needed and will determine the amount of solution deposited.

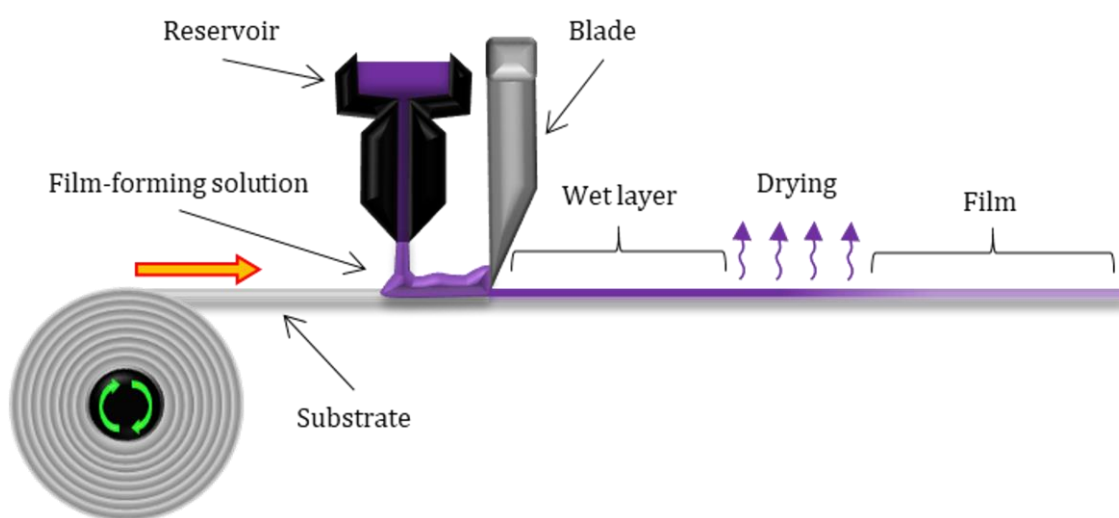


Figure 16 –Scheme of the knife-coating method.

The knife-coating technique works best if the depositing solution is at least somewhat viscous and the substrate is partially wettable by it.

Since the solvent-casting will be used in the laboratory for the development of the film-forming solution, which is fundamental to generating the core film of our electrochromic device, the right attention must be paid to ensure that everything can be transposed into the knife-coating technique.

Having made this last decision, it is important to find the most suitable synthetic protocols for each species and the way to convey all the products in a single solution. After this, we proceed with the assembly of the device and the appropriate characterizations.

The synthesis of the components, the technical problems and the relative solutions as well as the measurements of the electrochromic properties, will be the topics of the next chapter.

2. EXPERIMENTAL

In the previous chapter, some goals were set to be pursued to develop an electrochromic device with the desired characteristics. Each material that will constitute the device has been carefully chosen to be introduced in a single solution made with green solvents.

The synthesis and technical processes that will be used in the preparation of the materials and the assembly of the final device will be chosen with a spirit of economic and energy-saving, as well as with the prospect of scaling up production in the industrial sector. Furthermore, great attention will be paid to ensure that everything is respectful of the environment and safe for human health.

The materials will be obtained starting from synthetic protocols known in the literature, therefore the validation of the products can be ascertained through the simple verification of the properties that will be compared to the results presented in the reference articles.

As already mentioned, the choice of materials was made taking care that all of them are soluble in the same solvent. If despite everything, there is precipitation or aggregation during the preparation of the film-forming solution, appropriate measures must be taken to remedy this, either by changing the order of the additions or, in the most extreme cases, by replacing the material used with another more compatible.

It is important that the film-forming solution maintain always characteristics such as clarity and homogeneity to ensure optimal deposition and consequently the formation of a good film.

The amount of materials used and the operating procedures will be optimized starting from the verification of the macroscopic characteristics of the film, primarily the transparency and the absence of visual defects.

Secondly, it will check whether the device is working and, if so, the operational potential will be recorded; if the latter is high, priority will be given to lowering it and only afterwards will be evaluated the electrochromic parameters such as optical contrast, colouring/bleaching times and cyclic repeatability.

2.1. POLYVIOLOGENS: SYNTHESIS AND CHARACTERIZATION

Unlike many electrochromic polymers which are produced through multi-step synthesis, polyviologens have the great advantage of growing from low-cost precursors via simple one-step synthesis⁴⁰. In fact, many polyviologens having halides as counter-ions are synthesized through the *Menšutkin reaction*⁴¹.

The reaction mechanism involves the conversion of a tertiary amine into a quaternary ammonium salt, through the reaction with a terminal halide of an aliphatic chain or even of an aromatic compound. In our case there is a molecule with two tertiary amines, due to 4,4'-bipyridine; consequently, the corresponding reagents will be symmetric dibromides to allow the polymerization to start from each side of the bipyridine¹²⁹. In simple S_N2 Menšutkin reactions, bromides are good leaving groups upon the nucleophilic attack by nitrogen centres of 4,4'-bipyridine¹³⁰; the nitrogens involve one electron of their lone pair to form a new bond, generating quaternary ammonium salts having bromides as counterions. In this way, four polyviologens have been synthesized, as shown in figure 17.

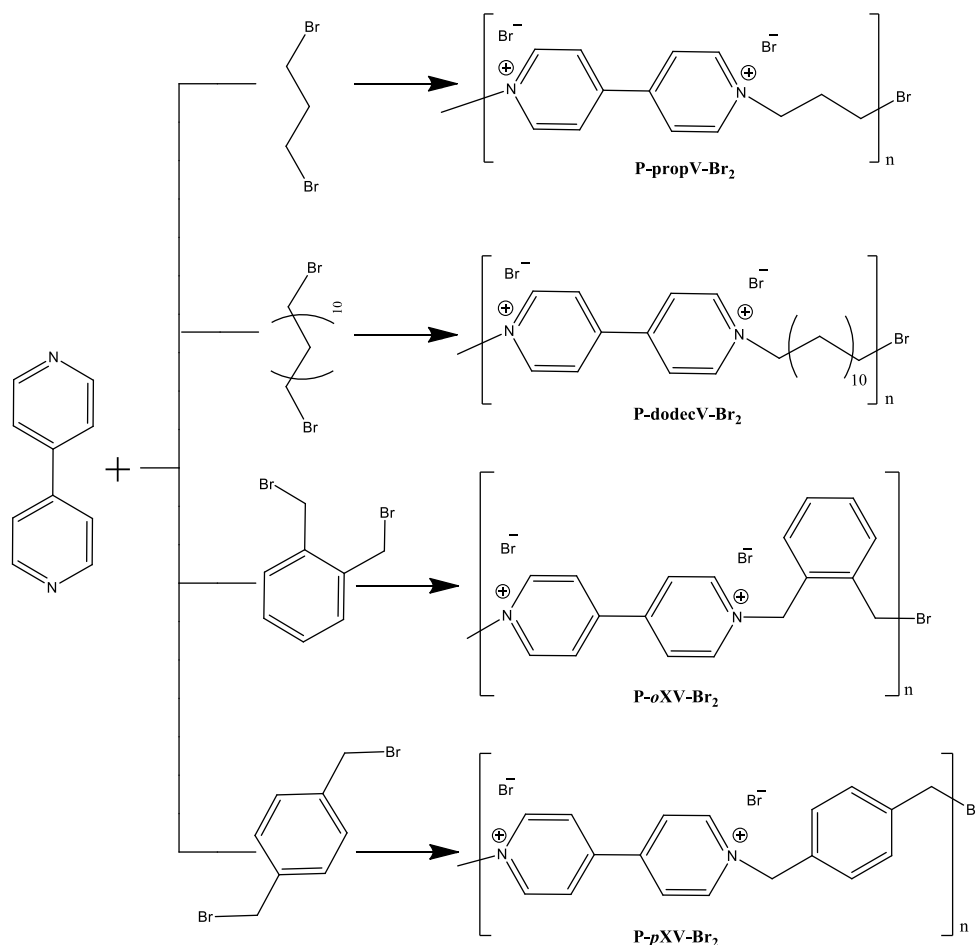


Figure 17 – Menšutkin reaction scheme. All reactions occur under acetonitrile reflux, 80 °C, for 24 hours.

Through this synthetic route, similar to polyadditions, two monomers form a repeating unit and no small molecules are released, contrary to what happens in polycondensation reactions. Therefore, the reaction yields are good and higher than 75%, as already reported by the literature⁴¹.

Two polyviologens have aliphatic chains of different lengths in the repeating unit (P-propV-Br₂ and P-dodecV-Br₂), while the other two have an additional aromatic group (P-*o*XV-Br₂ and P-*p*XV-Br₂).

In polyviologens, the substituent groups not only act as linkers of the viologen groups¹³¹, but also determine their mobility; in fact, the greater the degree of unsaturation of the linkers, the more the polymer has rigid conformation.

Since the synthesized polyviologens have very similar characteristics both from the electrochromic and chemical-physical point of view, a greater rigidity of the chains directs the choice of the most suitable polymer for the device under construction.

In fact, while the aliphatic chains predispose the polymer to self-winding, the presence of aromatic groups makes the polymer chains more rod-like and, as already hypothesized for nanowires, they can position themselves through different sections of the film and interconnect them.

Among P-*o*XV-Br₂ and P-*p*XV-Br₂ we opt for the use of the latter since the growth in extension of the polymer chain is favoured by the substituents occupying the opposite ends of the aromatic ring.

The synthetic protocol that leads to the synthesis of P-*p*XV-Br₂ has been consolidated and widely reposed for several decades by a multitude of scientific works. Consequently, the verification of the product obtained was validated by comparing our results with those reported in the literature.

From a colourless solution, following the reaction, a yellow solid precipitates, in accordance with the reference articles^{40,132}. The solid has been verified to be soluble in water, infusible but degradable starting from the temperature of 250 °C⁴¹, as shown by the thermogravimetric analysis(Fig. 18).

In the first part of the thermogram, in the range 25 - 100 ° C there is a weight loss equal to 7.5%, easily attributable to the moisture content incorporated by the

hygroscopic polymer.

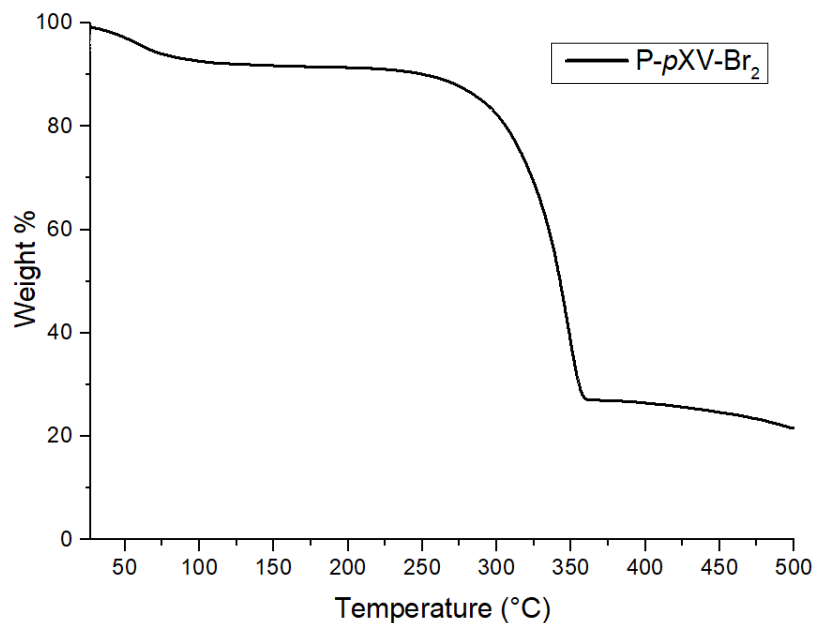


Figure 18 – Thermogravimetric analysis of P-pXV-Br₂ powder from 25 to 500 °C.

From 100 to 250 °C there is practically no weight loss, meaning that the polyviologen is thermally stable. Starting from 250 and up to 360 °C there is a sudden and significant weight loss of 62.9% indicating polymer degradation. Beyond, further degradation occurs which continues even above 500 °C.

The aqueous solution of polyviologen P-pXV-Br₂ is colourless as it absorbs in the UV region. As shown by the UV-visible spectrum (Fig. 19), there is only one absorption band centred at 262 nm, assignable to the π - π^* intramolecular transitions of the viologen units^{41,133}.

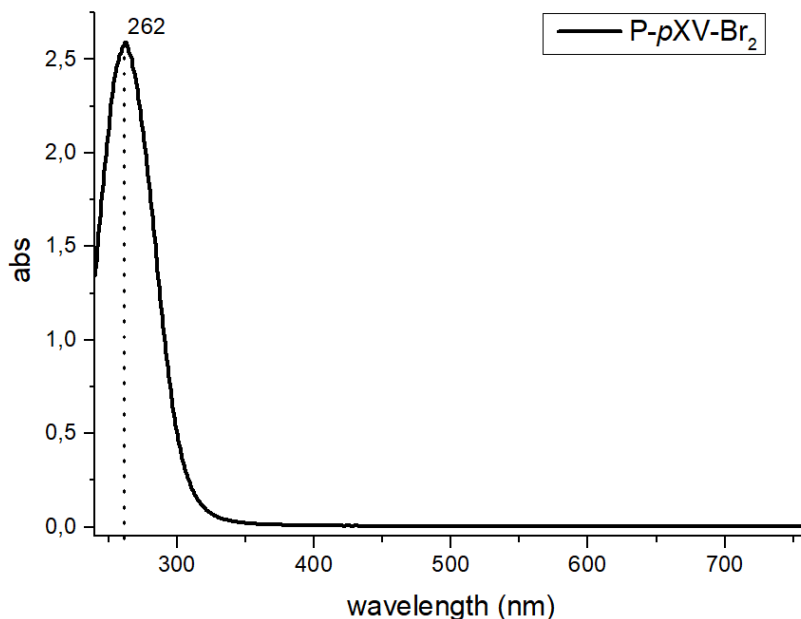


Figure 19 – UV-visible spectrum of P-pXV-Br₂ in H₂O.

Filmability was verified by electrodepositing on an ITO/glass electrode and electrochromic functionality by testing in an electrolytic solution; the initially slightly light yellow film has turned violet¹³⁴ due to the application of the electric potential.

2.1.1. POLYVILOGENS: MATERIALS AND METHODS

*4,4'-Bipyridine, 1,3-Dibromopropane, 1,12-Dibromododecane, α,α' -Dibromo-*o*-xylene, α,α' -Dibromo-*p*-xylene* and *Acetonitrile* were purchased from *Merck*[®] and used as received without further purification.

All polyviologens have been synthesized according to the literature^{41,135} with minor modifications.

In a flask of suitable size (e.g. 50 ml), under magnetic stirring, put acetonitrile (e.g. 20 ml) and equimolar quantities of 4, 4' bipyridine (e.g. 300 mg) and the desired dibromide (e.g. 507 mg of α, α' - Dibromo-*p*-xylene). Leave to reflux ($\sim 80^\circ \text{C}$) for 24h. The solution slowly changes colour from clear to yellowish, until a yellow precipitate forms. After the solution cools, filter and wash the precipitate copiously with acetonitrile. Dissolve the powder obtained in the minimum quantity of H_2O , and recrystallize with acetonitrile. Filter the yellow powder, let it dry well and put it in the oven overnight at 100°C .

The yield of the synthesis is about 77%, perfectly in agreement with the data reported in the literature¹³². The polyviologen synthesized through this protocol has a large polydispersion index; although the different fractions can be separated through the chromatographic column, in this work this is not done because it is considered superfluous.

2.2. ELECTROLYTE: SYNTHESIS

As seen in the previous chapter, the employability of chitosan involves its acidification. Very widely in the literature, we can read that chitosan is solubilized in a 1%_(v/v) aqueous solution of acetic acid^{98,100,102,108}; equally common are the papers in which chitosan is plasticised with various percentages of glycerol^{96,99,101,103,105,136}. The plasticization process increases the mobility of the chitosan chains, significantly reducing the lithium salt amount necessary for the operation of the device and therefore reducing its overall cost. As well understood by others, it is the chitosan content that determines both the rheological behaviour of the film-forming solution and the thickness of the final film⁹⁶, while the glycerol and to a lesser extent the electrolyte salt¹⁰⁸ act as plasticizers.

Consequently, the synthesis of the electrolyte matrix involves a continuous adjustment of the quantities of chitosan, glycerol and lithium salt, so that the film retains transparency, increases elasticity and preserves ionic conductivity.

From an initial weight ratio of chitosan and glycerol, the quantity of the latter was progressively increased, until the deposition produced a film with evident elastic ability.

After reaching a sufficient degree of elasticity, the amount of lithium salt was gradually lowered, until the electrochromic activity of the device remained unchanged. Beyond the economic aspect, this is advantageous because the use of a lower concentration of salt prevents the formation of aggregates that would decrease the ionic conductivity^{93,137}.

The water solubility of the lithium salt is a necessary but not sufficient condition to be suitable for our purpose. For example, lithium perchlorate (LiClO₄) is widely used in many electrochromic systems but reacts with polyviologen and exchanges anions through metathesis; the amount of polymer that acquires perchlorate anions loses its water solubility and precipitates, making the solution opaque and the resulting film less transparent. To overcome this problem, it was decided to avoid introducing different anions into solution, and therefore to use lithium bromide (LiBr) as electrolyte salt. This hypothesis proved to be justified and thus avoided the partial precipitation of the polyviologen, as visible from the photo in figure 20.

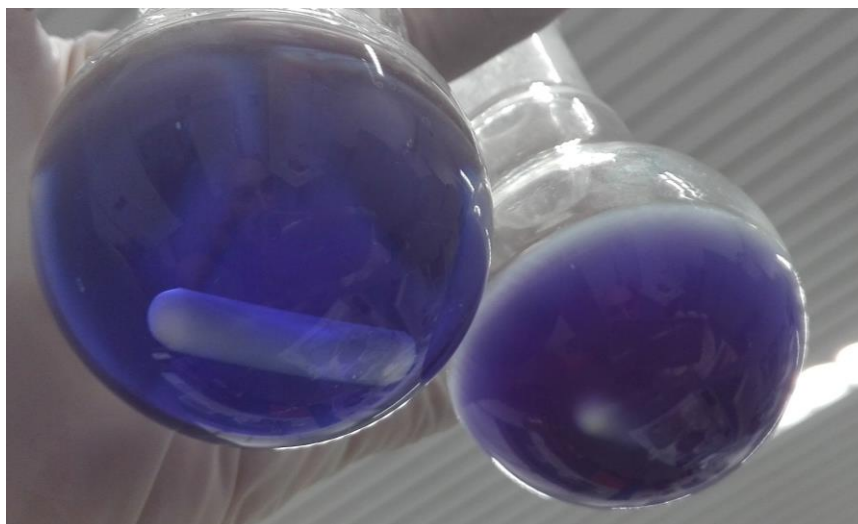


Figure 20 - On the left, the solution containing LiBr is clear; otherwise on the right the solution containing LiClO₄ is opaque. The presence of TMPD, responsible for the colouring, makes the differences more visible.

Although this electrolyte matrix shows encouraging characteristics, first experimental evidences indicate that the high water content of the film-forming solution causes poor wettability towards the support electrode; this makes the film inhomogeneous, due to shrinkage of the solution during the deposition step. Also in this case a trick was necessary to solve the problem and increase wettability. It was successfully verified that by adding ethanol to the solution, the latter increases affinity towards the substrate and covers its whole area (Fig. 21).

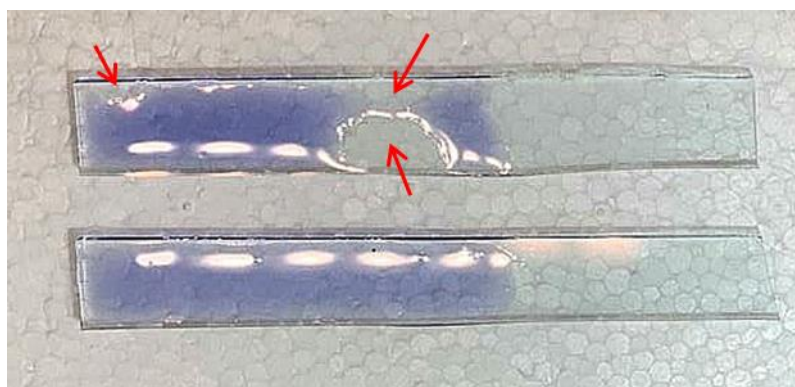


Figure 21 - The difference in wettability of the solution without (above) and with (below) ethanol on ITO/glass substrates. Again TMPD with its colour facilitates observation.

In addition to improving wettability, the use of increasing amounts of ethanol was found to speed up the drying process. At this point, there are many species in solution which contribute in one way or another to making the chitosan chains more distant and less interacting, thus the resulting electrolyte film more plastic.

Figure 22 shows the inter-chain space of chitosan in the absence of any other molecule and with the typical hydrogen interactions responsible for the mechanical characteristics of the resulting film.

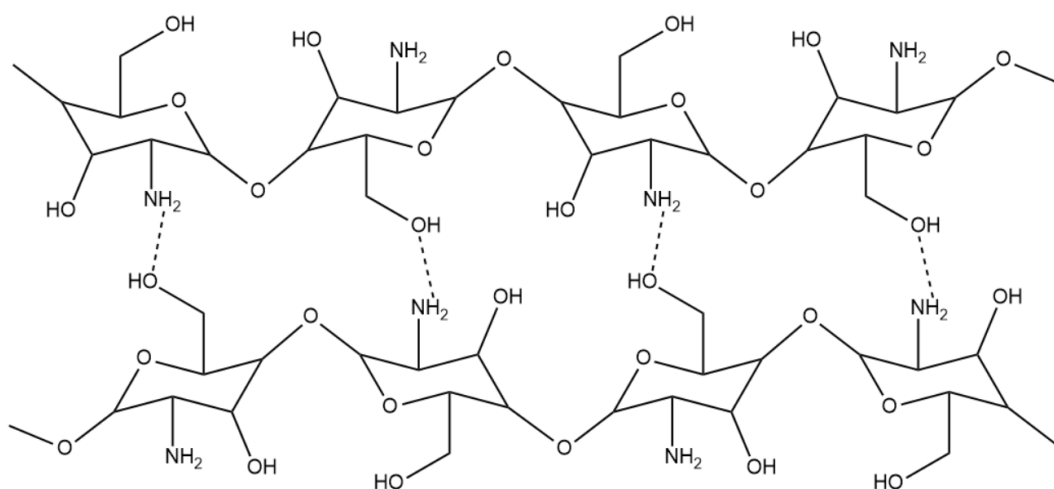


Figure 22 - Representation of H-bonds between chitosan chains.

The introduction of molecules and ions capable of intercalating between the chains causes the breaking of previous hydrogen bonds and the increase of distance between the chains (Fig. 23) through several actions listed below.

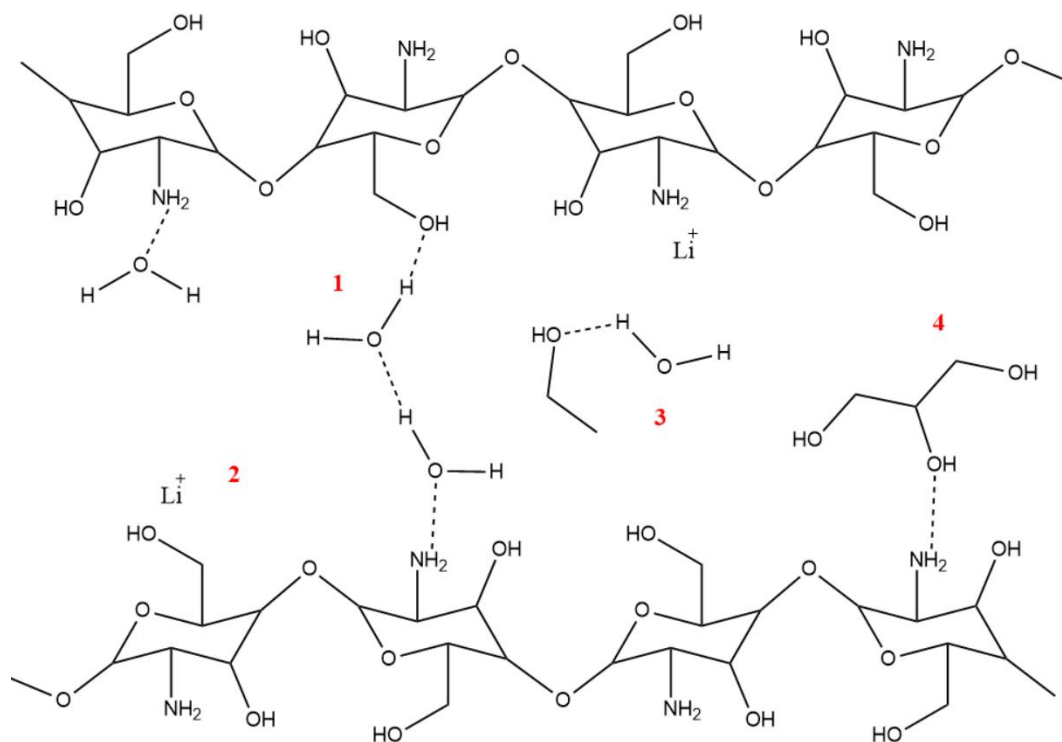


Figure 23 - Representation of inter-chain space of chitosan after addition of other species. The red numbers indicate the different roles of additive species and are discussed in the text.

1. When water molecules entered inter-chain space, they destroy hydrogen bonds between chitosan molecules and form new ones^{105,138}. These molecules can be classified as bound water, while those that do not interact with chitosan will evaporate in the drying step and are defined as free water¹³⁶.
2. The cations interacting with the unpaired electrons of the amino nitrogens and hydroxyl oxygens, lead to electrostatic repulsion among the chains and hinder the formation of H-bonds⁹⁴.
3. Water molecules having hydrogen bonds with ethanol molecules cannot interact with chitosan chains¹³⁶. Furthermore, ethanol molecules have only one site for hydrogen bonding and when bound to chitosan they inhibit the formation of the hydrogen network.
4. The glycerol molecules form H-bonds with those of chitosan, leaving the hydrophobic aliphatic parts as terminal groups¹⁰⁵. Since glycerol is not volatile, it remains in the inter-chain space even after the drying step, therefore it is the main responsible for plasticization. The amount of glycerol must be carefully dosed as it must not cause phase separation¹³⁹ in solution, nor after drying of the film.

2.2.1. ELECTROLYTE: MATERIALS AND METHODS

Chitosan (medium molecular weight 100-300 kDa, degree of deacetylation $\geq 75\%$) were purchased from *Acros Organics*[®] and used as received without further purification. *Lithium bromide*, *glycerol*, *glacial acetic acid* and *ethanol* were purchased from *Merck*[®] and used as received without further purification.

The synthetic protocol developed for the production of the film-forming electrolyte solution is rather simple and consists of a few steps.

In a flask of suitable size (e.g. 100 ml), under magnetic stirring, put 1% aqueous solution of acetic acid (e.g. 23 ml), lithium bromide (e.g. 50 mg) and chitosan (300 mg). Leave under stirring until all the chitosan is perfectly solubilized and when the solution appears completely transparent and homogeneous add glycerol (e.g. 0.44 ml) and ethanol (e.g. 23 ml). Leave under stirring until complete homogenization after which you can proceed with the deposition.

The film obtained by pouring the entire solution into a Petri dish is transparent, free of macroscopic defects and exhibits a good elasticity, which makes it much more flexible than the ITO/PET support electrode.

2.3. CuNWs: SYNTHESIS

Although viologens are low cost and easy to process, they lack electrical conductivity, long-term cyclic stability and fast response times¹⁴⁰. Therefore, to limit these shortages and improve the performance of a polyviologens-based electrochromic device, it could be advantageous to insert copper nanowires (CuNWs) as transport promoters for electrons that trigger the redox processes, which are the basis of the electrochromic behaviour.

As in the previous materials, also in this one synthesis with few steps and the use of green solvents is preferred. Among the various synthetic protocols published in the literature¹⁴¹⁻¹⁴⁶, those with safe procedures and with an aqueous reaction environment seemed to be very suitable for our purpose^{147,148}. In particular, a synthesis based on the hydrothermal reduction of the copper salt $\text{CuCl}_2 \cdot 2\text{H}_2\text{O}$ was performed, using glucose as a mild reducing agent and hexadecylamine (HDA) as a coating agent¹⁴⁹. A further reason for choosing the hydrothermal method lies in its easy scalability, to obtain a large production of CuNW¹⁵⁰.

The synthetic procedure consists in dissolving copper salt, glucose and HDA in H_2O ; good stirring is necessary to obtain an emulsion, due to the poor water solubility of the HDA. The salt dissociates completely in water, the Cu^{2+} ions are complexed by HDA molecules and the emulsion acquires the typical blue color¹⁵¹ (Fig. 24). The Cu(II) complexes are generated via nitrogen lone pair of the amine and this is a fundamental process for initiating seeding¹⁵².

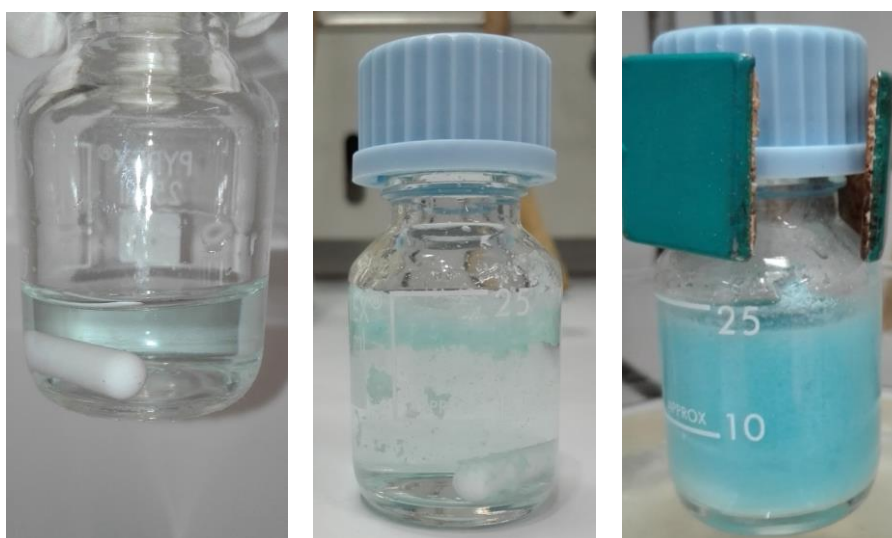


Figure 24 - Emulsion preparation: dissolving Cu salt, adding glucose and HDA, prolonged stirring (from left to right).

The emulsion is then placed at 100 °C for about 12 hours, during which the process of seeding and growth of the nanowires takes place; the colour of the emulsion varies gradually until it has the characteristic copper-red colour (fig. 25).

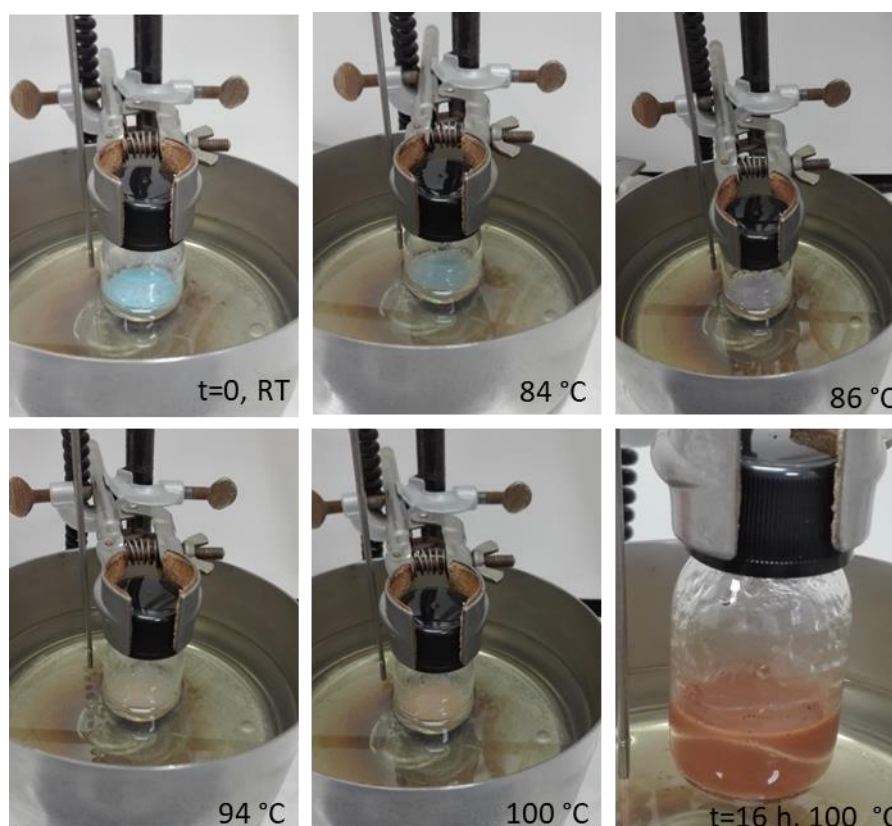


Figure 25 - Colour change of the emulsion leading to the formation of nanowires during heating.

Glucose, a mild reducing agent, determines a lower reaction temperature, therefore it is useful in terms of energy-saving and safety¹⁵².

During the heating of the solution, the slow reduction of the complexes takes place in favour of the formation of penta-twinned seeds with different sizes¹⁵². The smaller seeds have greater surface energy than the large ones, therefore they gradually dissolve over time, generating copper atoms that recrystallize on the large seeds¹⁵³; this phenomenon is known as Ostwald ripening.

Metals such as copper, silver and gold have highly symmetrical face-centred cubic (fcc) structure so an external force is required to promote anisotropic growth¹⁵³; consequently, if growth were driven only by these phenomena, we would simply have the round enlargement of the seeds. Instead, as the seeds grow, the function of the HDA changes; indeed, after an initial role in the complexation of Cu^{2+} ions, HDA becomes important as a directing agent for the anisotropic growth of nanowires¹⁵².

Alkylamines, including HDA, are known to preferentially bind to some of the crystal facets of nanoparticles^{154,155}. During the growth step, HDA selectively adsorbs on the $\{100\}$ side facets, because these planes offer more open sites for interaction. HDA capping stabilizes the $\{100\}$ facets of the seeds and reduces their lateral growth by acting as external confinement¹⁵².

On the contrary, on the crystalline planes $\{111\}$ there is a poor capping of HDA, allowing the Cu atoms, generated both by Cu(II)-HDA complexes and by Ostwald ripening, to deposit and recrystallize. These processes lead to the formation of pentagonal nanowires that grow along the $\langle 110 \rangle$ direction¹⁵³(Fig. 26).

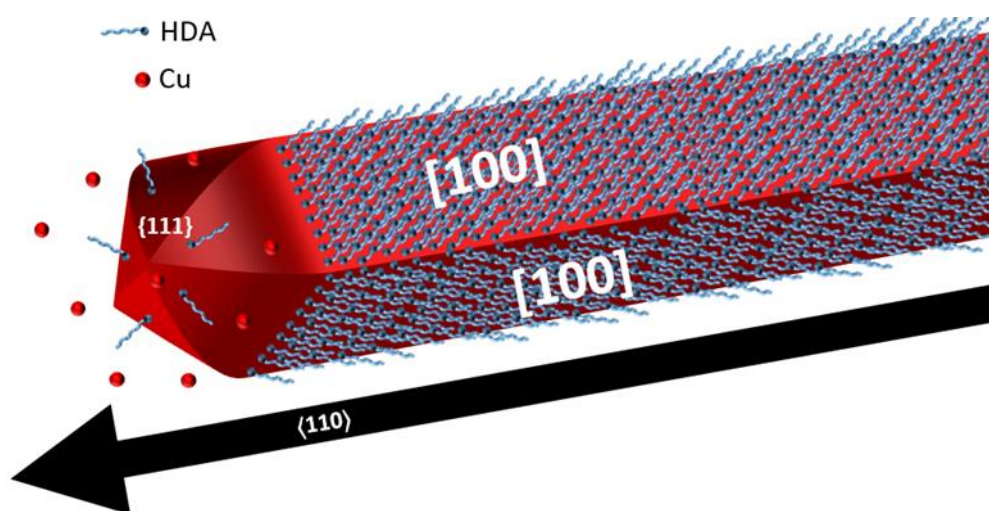


Figure 26 - Representation of the five-fold twinned structure of copper nanowire bounded by five $\{100\}$ planes and capped by ten $\{111\}$ planes.

Summing up we can identify some key conditions for the formation of CuNWs:

- I. The complexation of Cu^{2+} ions by HDA is fundamental for the formation of penta-twinned seeds.
- II. The five-fold twinned structure of the seeds, acting as internal confinement, is critical for the unidirectional growth of the nanowires.
- III. HDA, with its preferential adsorption on the $\{100\}$ planes, acts as an external boundary and contributes to direct the growth along the $\langle 110 \rangle$ direction.
- IV. It is necessary to work with a slight excess of HDA so that the facets $\{100\}$ are undoubtedly stabilized and do not allow the growth of stockier nanoparticles.
- V. A large excess of HDA still generates nanowires but with a larger diameter.

- VI. HDA is a good capping agent, which prevents CuNWs oxidation for a long time.
- VII. Finally, it is absolutely necessary that the reaction of seeding and growth of CuNWs takes place in a closed vessel with a screw cap. If this were not the case, the copper hydroxide present in the solution would react with the carbon dioxide, generating the typical green-coloured cupric hydroxide carbonate (Fig. 27); this phenomenon is called passivation and is described by the following reaction.

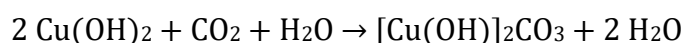


Figure 27 -If the same reaction is not closed and is carried out under reflux conditions through a condenser, it does not lead to the formation of CuNWs.

After the synthesis, the delicate purification step follows, which aims to isolate the CuNWs both from the unreacted species and from the nanoparticles of different morphology.

Finally, the correct procedure for storing CuNWs will be adopted, to preserve the latter from oxidation which would alter their chemical-physical properties.

These two topics will be dealt carefully and with a wealth of figures in the following section.

2.3.1. CuNWs: PURIFICATION AND CHARACTERIZATIONS

In the previous section, the synthesis of CuNWs and the mechanisms leading to their formation were illustrated; it is clear, however, that in the reaction environment there are not only the desired products, but also unreacted reagents and by-products such as non-filiform copper nanoparticles. Therefore, a suitable purification procedure is necessary to isolate the nanowires useful for our purpose.

The literature at this point is divided: on the one hand those who operate a purely morphological separation, through cross-flow purification using a hollow fiber filter¹⁵⁶; on the other hand, those who take advantage of the different solubility of the coating agent through the cross-phase method using a biphasic solution¹⁵⁷.

The second technique was chosen based on the instruments available to us; moreover, this separation method is simple, fast, and can be easily scaled up to yield high-purity nanowires¹⁵⁷.

First of all, the post-reaction emulsion is transferred into conical tubes and centrifuged to eliminate the excess reactants, especially the HDA. Once the supernatant is removed and the precipitate is redispersed in distilled water, an aqueous phase dispersion of copper nanoparticles of various sizes and shapes remains.

The next step involves the formation of the biphasic system through the introduction of a water-immiscible organic solvent, specifically chloroform.

As described in the previous section, the CuNWs sides are well coated with HDA while the ends are very lightly coated; this induces the nanowires to enter the organic phase, within which there is further desorption of the HDA molecules and relative destruction of the multilayer responsible for the stability of the dispersion in water¹⁵⁷.

On the contrary, the other copper nanoparticles having a total surface area smaller than the nanowires and {100} surface facets, are better stabilized in water by the HDA multilayer and scarcely migrate into the chloroform¹⁵⁸.

Thanks to these phenomena, within a few minutes, a biphasic system is obtained in which the upper aqueous phase contains the dispersed nanoparticles, while the

flocculation of the nanowires takes place in the underlying organic phase. The action of this separation is visible to the naked eye and is shown in figure 28.



Figure 28 -The addition of CHCl_3 (left); the biphasic system with nanoparticles in water above and nanowires in chloroform below (right).

After purification, the two phases can be easily separated with a Pasteur pipette; the organic phase containing the CuNWs is centrifuged to eliminate the chloroform and the precipitate is transferred to a glass jar of suitable size, then dried and redispersed in ethanol through a mild sonication (Fig. 29).

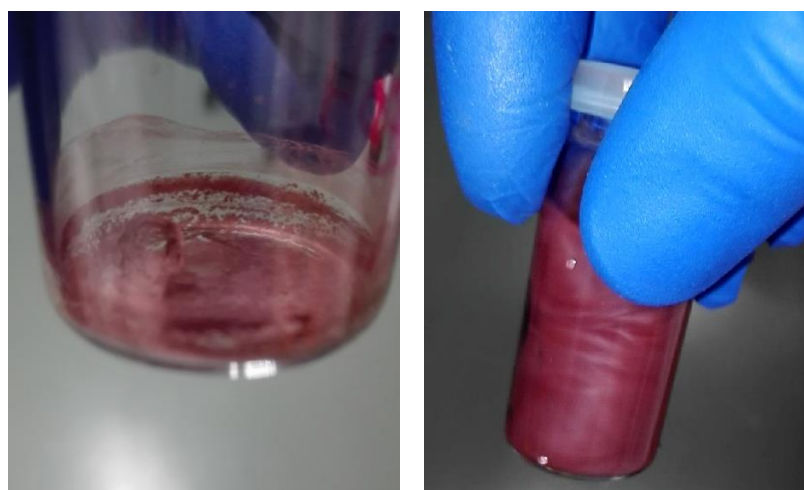


Figure 29 -Copper nanowires precipitated after centrifugation and dried (left); the same CuNWs redispersed in ethanol (right).

The effectiveness of the separation method is evident by observing the sample with an optical microscope during the various steps (Fig. 30), and even better through transmission electron microscopy (TEM) as shown in figure 31.

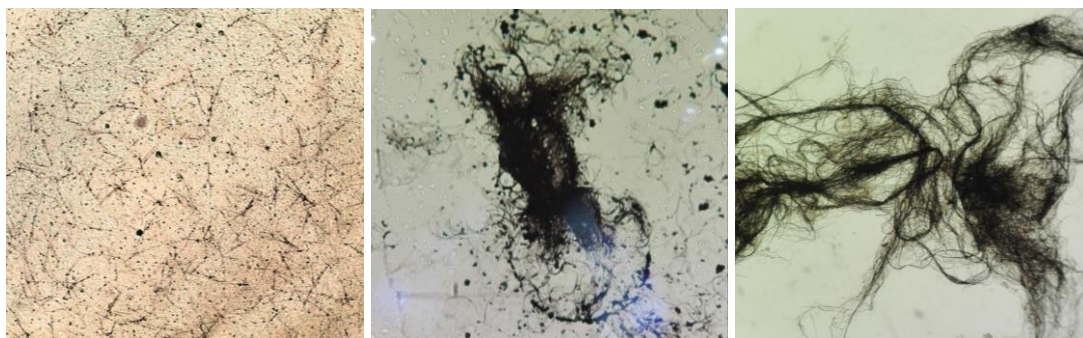


Figure 30 –From left to right: sample as synthesized, with excess HDA; sample purified with CuNWs and CuNPs; sample after cross-phase separation method largely composed of CuNWs.

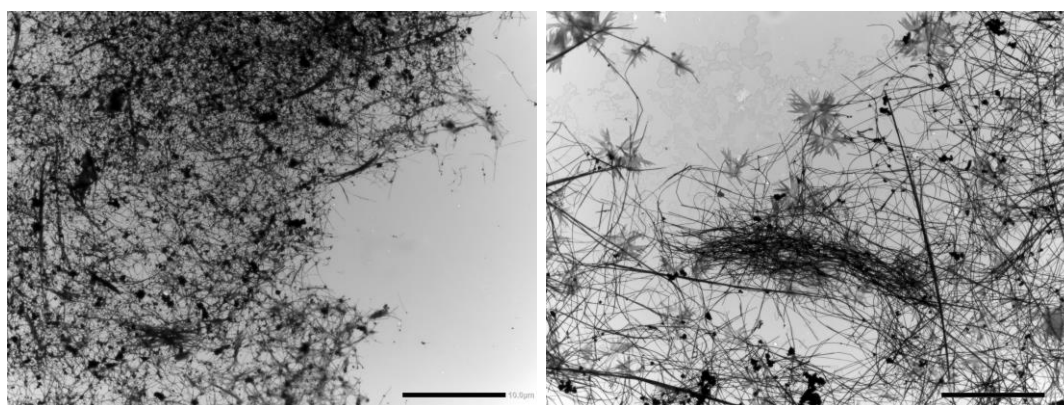


Figure 31 –TEM images of sample before the biphasic solution shows a large number of nanoparticles (left); after separation, long nanowires prevail (right). Scale bar is 10 μ m for both.

According to reference paper¹⁴⁹, the nanowires obtained have penta-twinned ends with an average diameter of 25 ± 5 nm and a length ranging from tens to hundreds of μ m. These data were obtained by carrying out graphic measurements on some TEM images (Fig. 32); the reference length is the scale bar of the scanned images.

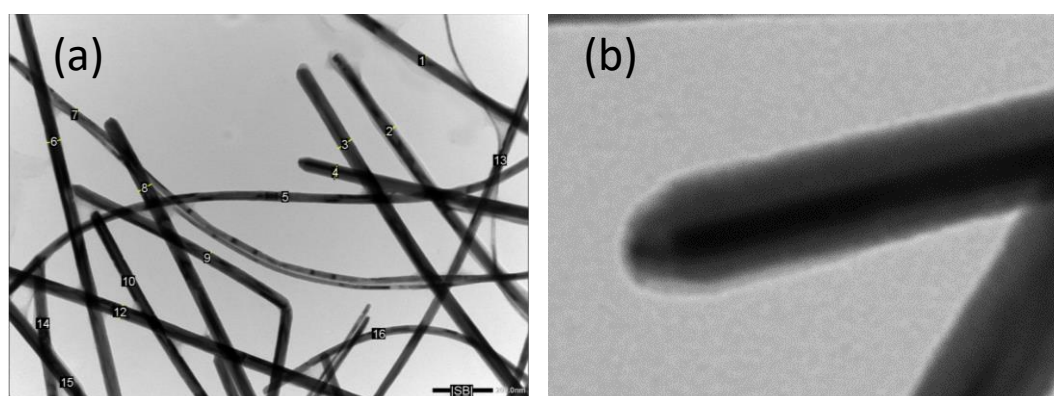


Figure 32 –(a) Yellow lines along the diameter of each nanowire is a relative sampling, from which the data was derived. (b) Magnification of the CuNW penta-twinned end.

Furthermore, as copper exhibits localized surface plasmon resonance (LSPR) peaks in the visible region when it is prepared as nanostructures¹⁵⁹, UV-vis spectra were recorded to further confirm the morphological separation. The data obtained match

those present in the literature and show an absorption band centred at 590nm^{115,116,149} for the nanoparticles and a characteristic shoulder absorption at 560nm^{147,149,152,160,161} for the nanowires, as shown in figure 33.

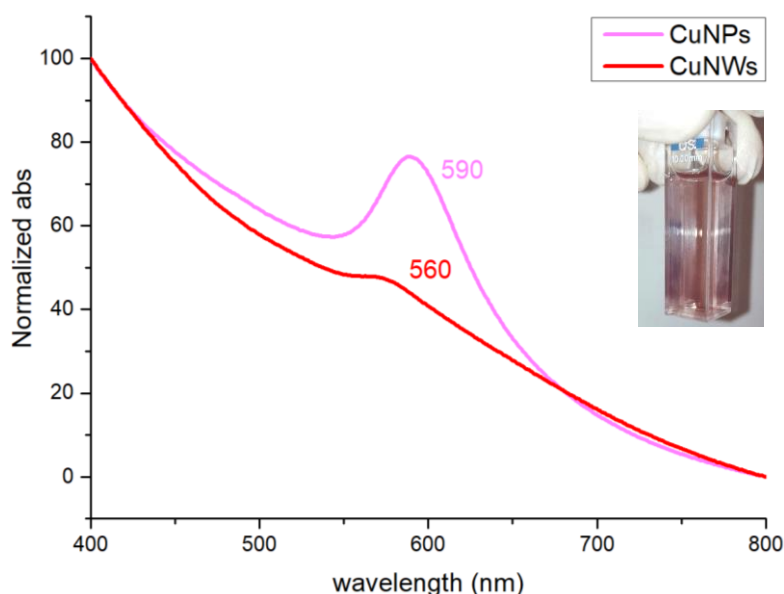


Figure 33 –Absorption spectra of CuNPs in H₂O (pink line) and of CuNWs in ethanol (brown line). In insert: cuvette containing the alcoholic dispersion of CuNWs.

As you can guess from the spectra and can be seen in the photos, the absorption in the visible range gives colour to the nanowires dispersion. Therefore, the amount to be used in our purpose device must be well dosed to take advantage of the benefits due to the insertion of CuNWs, while maintaining a neutral colour. This topic will be dealt with in the descriptive section on the preparation of the single film-forming solution (§2.4).

In conclusion, this purification method allows the good separation of nanowires from other nanoparticles. Particular attention is required in the steps following the addition of chloroform, as the prolonged permanence overtime of the nanowires in halogenated solvents causes their complete denudation from the HDA coating agent, thus initiating degradation phenomena, as shown in figure 34.



Figure 34 – CuNWs must be quickly extracted from CHCl₃ in order to avoid copper reoxidation phenomena, highlighted by the change in colour of the organic phase.

2.3.2. CuNWs: STORAGE AND AGING

Unlike noble metals such as gold, copper is known to easily suffer from oxidation and the same is true of its nanostructures. In a specially conducted study, it was found that CuNWs coated with aliphatic amines have better stability in polar organic solvents, while in non-polar solvents and water they easily undergo aggregation and oxidation¹⁶². Similarly, we have found that the best solvent to store CuNWs is ethanol, as oxidation occurs more slowly than dimethyl sulfoxide or water. The oxidation stability has been verified in these three solvents because they are the most compatible for the development of our device; copper nanowires were dispersed in the previously mentioned solvents and TEM images were acquired after one week of storage (Fig. 35).

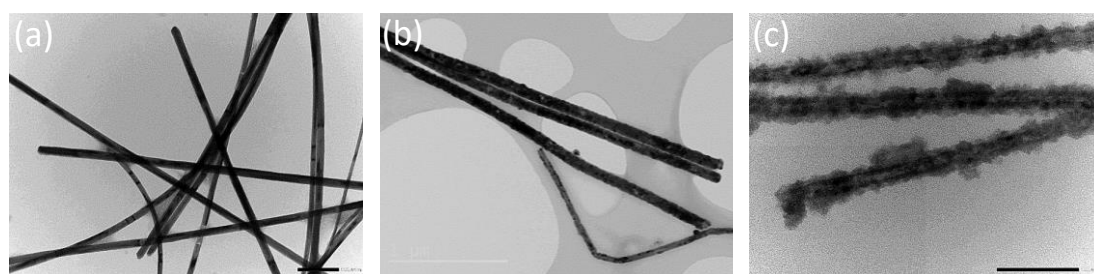


Figure 35 – TEM images of the nanowires oxidation process in (a) EtOH, (b) DMSO and (c) H₂O, after one week of storage.

As can easily be seen from the TEM images, after a week the CuNWs in dimethyl sulfoxide show a superficial oxide patina and much more is the oxidation in water. On the contrary, nanowires dispersed in ethanol have the same morphological characteristics as just synthesized. The storing validity of ethanol is much beyond a week and even four months later the CuNWs maintain almost the same characteristics, as demonstrated by spectroscopy and TEM in figure 36. Comparing the absorption spectrum of the just synthesized nanowires with the spectrum of the same CuNWs after four months of storage in ethanol, no major variations in the plasmon band are evident. Similarly, the TEM images of the two samples demonstrate that the nanowires maintain the same morphological characteristics and have no signs of surface oxidation.

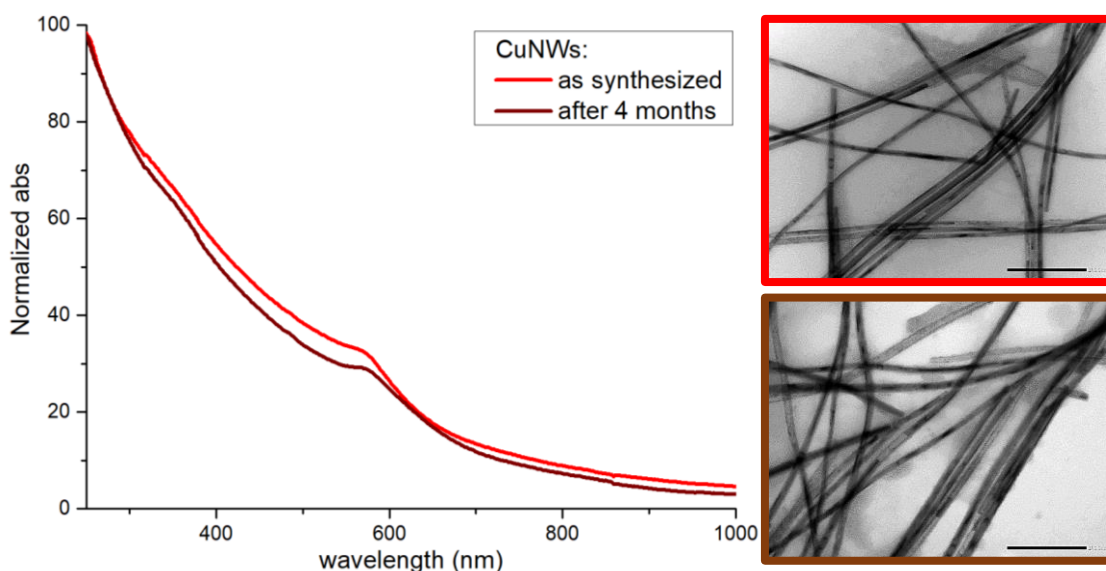


Figure 36 – On the left: comparison of the absorption spectra of the just synthesized CuNWs (red line) and the same after 4 months (brown line). On the right: TEM images of the just synthesized nanowires (red box) and the same after 4 months (brown box).

However, for longer storage times, copper nanowires undergo aging, slowly coating their surface with oxide. This phenomenon is also macroscopically evident by the browner colour of the aged alcoholic dispersion than the fresh one. The three highly demonstrative photos in figure 37 show that even the decanted, which occurred by flocculation of the nanowires due to their high length, appears very different and easily distinguishable.



Figure 37 – In each photo: fresh nanowires on the left, aged ones on the right. (a) Comparison of the decanted. (b) Slightly shaken samples. (c) Samples redispersed by mild sonication.

By depositing a small quantity of the two suspensions on a microscope slide and observing them with optical microscopy, it is evident that the filiform structure of the fresh nanowires disappears in the aged ones (Fig. 38). This is probably due to the progressive oxidation of the CuNWs which causes them to break up into shorter structures, converting the long nanowires into lower aspect ratio nanoparticles.

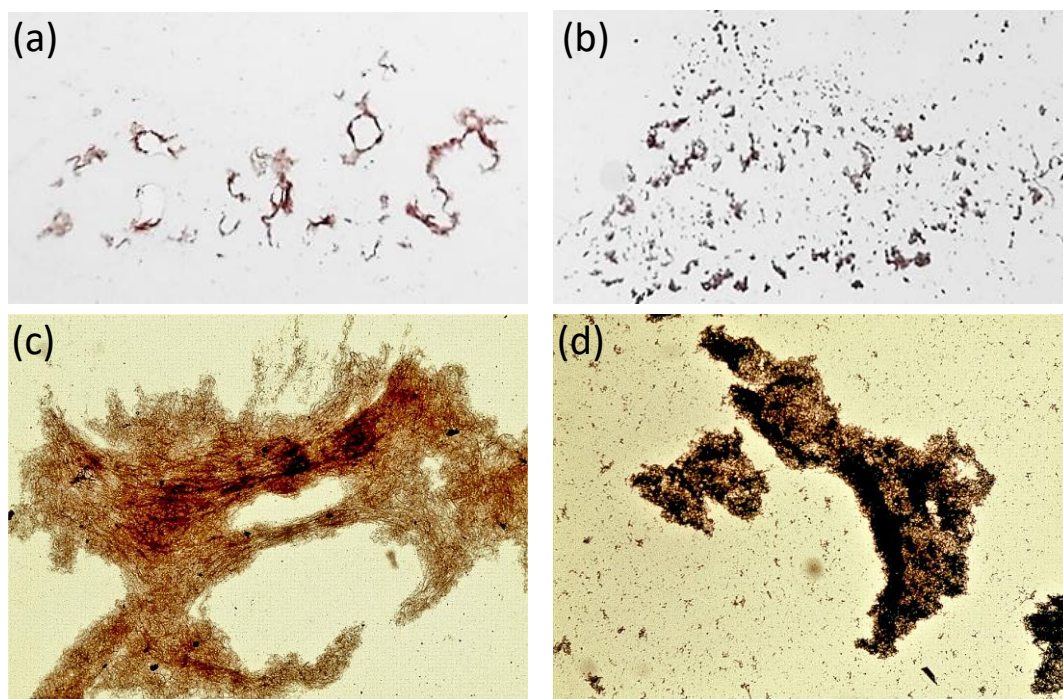


Figure 38 – Depositions on a microscope slide of the fresh (a) and aged (b) nanowires. Magnification of fresh CuNWs (c) shows filiform morphology, while in aged ones (d) it is not observed.

In summary, the storage of copper nanowires in ethanol allows them to be preserved from oxidation for at least four months. The storage vessel should be closed as much as possible to decrease oxygen permeation. The CuNWs must be used for our purpose before their surface oxidation and rupture, which is easily evidenced by the browner colour of the dispersion.

2.3.3. CuNWs: MATERIALS AND METHODS

Copper(II) chloride dehydrate (CuCl₂ · 2H₂O), D-(+)-Glucose, Hexadecylamine (HDA), Chloroform and Ethanol were purchased from Merck® and used as received without further purification.

Copper nanowires have been synthesized according to the literature¹⁴⁹ with minor modifications.

CuCl₂ · 2H₂O (e.g. 63 mg), glucose (e.g. 150 mg) and hexadecylamine (e.g. 540 mg) are placed together in a screw-top vessel of suitable size (e.g. 50 ml), filled with distilled H₂O (30 ml) and stirred at RT overnight. After this time, a blue-coloured emulsion is formed which is transferred to the oil bath, keeping the vessel closed, under moderate stirring and setting the temperature at 100 °C. During the 16 hours of reaction, the emulsion gradually changes hue, until it reaches the red-brown colour which indicates the reduction of copper (II) to metallic copper. The emulsion obtained contains CuNWs which must be purified from excess reagents and by-products consisting of non-filiform copper nanoparticles.

First, the post-reaction emulsion is transferred to a conical tube and centrifuged at 4000 rpm for 30 minutes. The supernatant is removed with a Pasteur pipette and the conical tube is refilled with H₂O without shaking; new centrifugation at 4000 rpm for 10 minutes follows. If after the second centrifugation the supernatant still has a yellowish colour, the procedure is repeated until the washing water is transparent.

The supernatant from the last wash is removed and replaced with H₂O (e.g. 25 ml); the red precipitate is redispersed through a short but vigorous manual stirring or mild sonication. When a good dispersion is obtained, chloroform (e.g. 5 ml) is added, for about 1/5_(v/v) of H₂O and shaken vigorously but briefly by hand. A few minutes are enough to obtain the formation of a biphasic system, having CuNPs dispersed in H₂O at the top and CuNWs flocculated in CHCl₃ below. Separate the two phases using a Pasteur pipette and centrifuge the one in chloroform at 4000 rpm for 15 minutes.

Discard the supernatant and transfer the wet precipitate to a glass jar of suitable size (e.g. 10 ml). Dry the sample for a few minutes with the help of a low vacuum pump, making sure there is no more chloroform. Weigh the dry precipitate (e.g. 10

mg) and refill the jar with a suitable quantity of ethanol (e.g. 10 ml) to reach a concentration of 1 mg/ml. Properly close the jar and redisperse the nanowires through a mild sonication; the dispersion thus obtained will tend flocculation due to the length of the CuNWs, but will be easily recoverable with a short and mild sonication.

According to what has been observed, the nanowires resist oxidation for at least four months of storage, and probably even more if the dispersion is treated with inert gas and hermetically sealed.

With this section ends the preparation of all materials necessary for the constitution of our device. The next sections will be dedicated to the preparation of the all-in-one film-forming solution, to the optimization of the amounts to be used, to the assembly of the electrochromic device, and its characterizations.

2.4. ALL-IN-ONE FILM-FORMING SOLUTION

Previously, the syntheses of each material that will be used in the preparation of the all-in-one film-forming solution have been described in detail. Mixing all these species is not a simple procedure because, in addition to each material's right dosage, the order in which they are added is of fundamental importance for obtaining a homogeneous and stable solution capable of generating a film with electrochromic activity.

To decide how to start the preparation of the film-forming solution, it is useful to make a summary of all materials to be used and their solubility (Table 3), taking into account that they have been chosen to be soluble in water or ethanol and that these solvents are miscible with each other.

Material	Role	Solubility
P- <i>p</i> XV-Br ₂	Cathodic electrochrome	Water
TMPD	Anodic electrochrome	Water and Ethanol
Chitosan	Biopolymer matrix	1% Acetic acid aqueous solution
Glycerol	Plasticizer for biopolymer matrix	Water and Ethanol
LiBr	Electrolyte salt	Water and Ethanol
CuNWs	Coadjutor of electrochemical activities	Ethanol

Table 3 – List of materials, their role and their solubility.

Unlike other materials which are easily soluble, chitosan is the one that needs particular attention as it requires an aqueous solution of acetic acid. It is very important that the pH of the solution is sufficiently acidic to solubilize the chitosan, otherwise, there is a risk of not obtaining complete solubilisation of the biopolymer, which would make the solution non-homogeneous.

Starting with the formation of a chitosan solution and then adding the other materials, at first it seemed the most obvious method. In reality, although the

addition of lithium bromide was successfully carried out leading to its complete solubilisation, it was not the same with the addition of polyviologen which appeared as inhomogeneous particulate generated by agglomerates of different sizes. It was not possible to break these agglomerations neither by prolonged agitation nor by ultrasonic sonication, probably due to the viscosity of the chitosan solution.

At this point it was inevitable to start all over again, first solubilizing the polyviologen and the lithium bromide in water and then acidifying the environment with acetic acid and adding chitosan powder. Unlike what was previously obtained, a perfectly transparent and homogeneous solution was reached through magnetic stirring, a sign that all the introduced species were completely solubilized.

The timing and method for adding the CuNWs are very delicate and finding the right conditions took a long time.

The first attempt was to introduce the dispersion of nanowires just before the addition of the chitosan; the expected bad result was the rapid precipitation of the CuNWs, due to their non-friendly aqueous coating agent.

Therefore, to have a more favourable environment for the nanowires, the latter were dispersed in a greater quantity of ethanol after which they were introduced into the aqueous solution before the addition of chitosan; although the nanowires appeared to be stable and did not precipitate, making the solution slightly pink, the problem shifted to the chitosan solubilisation. In fact, the amount of ethanol causes the increase in volume of the entire solution and consequently the decrease in the concentration of acetic acid, making it unable to protonate all the amino sites of the chitosan, which is therefore slightly soluble. The solution thus prepared is difficult to deposit as it appears to be composed of large transparent and gelatinous fragments of chitosan (Fig. 39a).

Reiterating the concept according to which a homogeneous film can only be generated from a homogeneous solution, the alcoholic dispersion of nanowires was added after the complete solubilisation of the chitosan. Unfortunately, even in this case, the hostility towards the aqueous environment did not allow the nanowires to disperse in the solution, in which they were strongly aggregated despite hours of magnetic stirring or sonication (Fig. 39b).

As previously operated, the nanowire dispersion was first diluted in a greater quantity of ethanol and subsequently added to the aqueous solution with the already dissolved chitosan; when the nanowires are dispersed in a greater volume, the distance between them increases and therefore their aggregation is prevented. Through this expedient, the resulting solution was perfectly homogeneous and clear, slightly pink coloured, a sign that nanowires were evenly dispersed without forming aggregates (Fig. 39c).

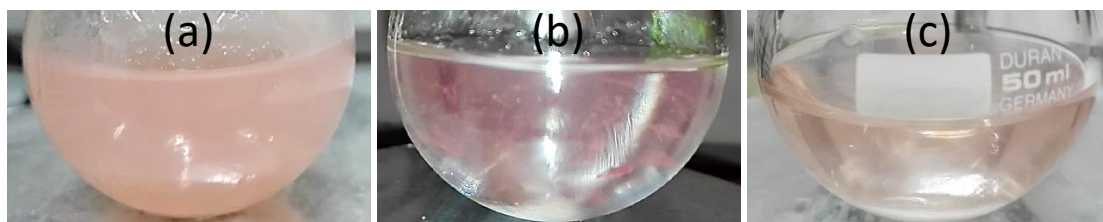


Figure39 – Attempts to add the nanowires: (a) before the chitosan solubilisation; (b) after the chitosan solubilisation and CuNWs dispersed in a small amount of ethanol; (c) after the chitosan solubilisation and CuNWs dispersed in large amount of ethanol.

As previously stated (§2.2), ethanol is not only useful for adding nanowires, but it is also beneficial for increasing the affinity of the solution with the substrate electrodes, allowing for better coating.

On the contrary, the pink colour of the solution, an indication of the excellent dispersion of the copper nanowires, is not useful for our purpose; this will generate a pink film, therefore the quantities of nanowires must be modulated in order to have their presence in the final film, without compromising its colourlessness. The calibration of the quantities of CuNWs and all other species to be used will be extensively discussed later, in a dedicated section (§2.5.3.4).

At this point glycerol and TMPD can be added without any problems for their dissolution and after a few minutes of stirring the film-forming solution will be homogeneous and blue/purple.

Although the goal of an all-in-one solution was achieved, it was decided to make its preparation easier and faster. Starting from the assumption that in any case, it is necessary to start from two different solutions, an acidic aqueous where the solubilisation of the chitosan occurs and the other alcoholic to allow the appropriate dispersion of the CuNWs, it was decided to add the other species in one of the two solutions just mentioned.

To facilitate understanding what has been done, a scheme is shown in figure 40. The

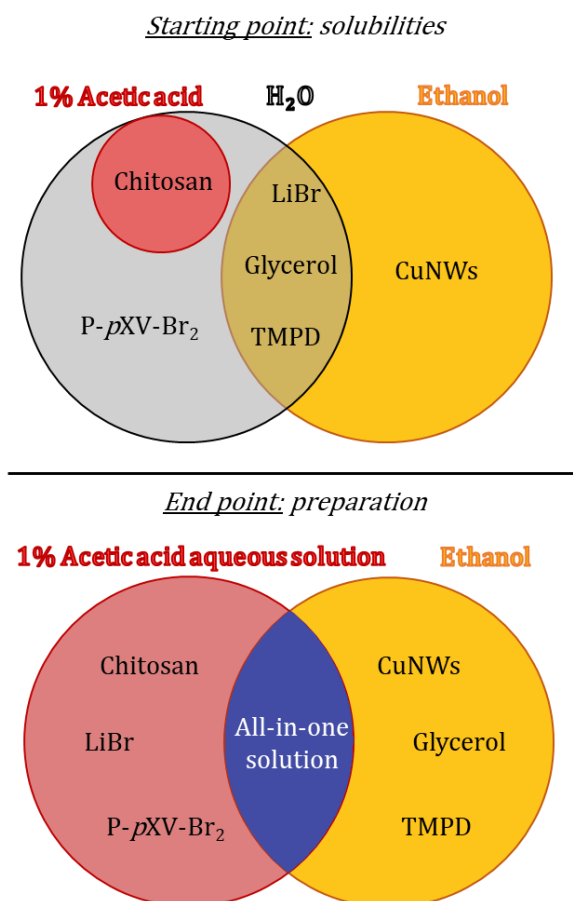


Figure 40 – Top: the solubilities of the species in the different solvents represented by circles. Bottom: the two solutions with solubilised species from the mixing of which the single film-forming solution is obtained.

starting point is developed from the solubilities of all the species in the chosen solvents, while the final point is the elaboration of the two different solutions from which the all-in-one film-forming solution is obtained.

Basically, a 1% aqueous solution of acetic acid is prepared and LiBr, polyviologen and chitosan are added there (Fig. 41a); separately CuNWs, glycerol and TMPD are added in ethanol (Fig. 41b). After all the species in both solutions are well solubilized, the two solutions are mixed to obtain the all-in-one film-forming solution (Fig. 41c).

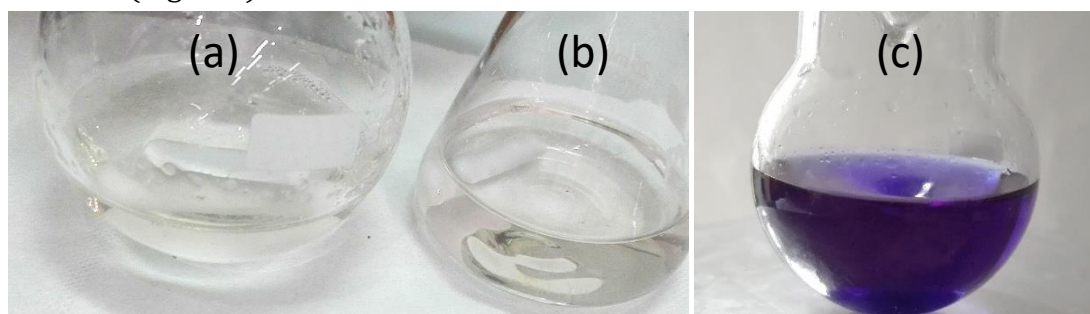


Figure 41 – (a): Aqueous solution; (b): Alcoholic solution; (c): All-in-one film-forming solution.

It is immediately evident that while the aqueous and alcoholic solutions are almost transparent, the two mixed together are strongly coloured; this is due to the TMPD which in ethanol is colourless because in the neutral state, while in water it is coloured because it oxidizes and switches into the radical form. Further details will be discussed in the dedicated section (§2.5.3.3).

Furthermore, it can be noted that the solution containing the CuNWs (Fig. 41b) is much less coloured than the one previously prepared during the nanowire embedding tests (Fig. 39c); this is because figure 41 illustrates the preparation of the single film-forming solution with the optimized quantities of all the species used.

Only now that the correct method of adding the various species has been found, to obtain a clear and homogeneous solution, we can proceed by adjusting the physical quantities of the components of the solution; the objectives are to use as few materials as possible and to allow the functioning of the final device avoiding the technical and practical problems that could arise.

The calibration of the amounts of each species will be discussed in the next sections, as well as the techniques of deposition and drying of the film and the electrochromic device assembly.

2.5. OPTIMIZATION

The practical procedure for obtaining the film-forming all-in-one solution was described in the previous section. This solution deposited on the substrate electrodes will generate a film whose chemical-physical properties derive from the materials used. Furthermore, the amounts of species present in the solution and the techniques of film deposition and device assembly are decisive for the quality and functioning of the entire electrochromic system.

In fact, deposition starting from a composite solution, such as the elaborate film-forming one, is not simple and requires various precautions to avoid inhomogeneity or compromise the desired characteristics.

The main problems encountered during the formation of the film and the assembling of the device will be described below. Following the observation and characterization of the deposited films, the quantities of each species used were adjusted, verifying each time the improvement in the film and ascertaining its functioning.

These problems were solved as appropriate either by acting directly on the all-in-one solution or by operating on a preliminary stage of the same, to avoid wasting materials; in the latter case, the improvements obtained have been verified to work even when transposed to the all-in-one solution.

Due to the multitude of components in the solution, it is important to clarify that many times, when looking for the optimal amount of one species it was necessary to modify the quantity of another. Therefore, the optimization process involved the entire research period and led to continuous adjustments of the quantities of each species.

Photographs of deposited films with various defects will be shown and, after a rational analysis of the problem and through various tests, they will be corrected.

Consequently, the next sections will be dedicated to problem-solving, which will result in technical procedures for the best deposition and optimization of the amount of species used.

2.5.1. FILM DEPOSITION

As mentioned in section 1.7., the deposition of the solution on the electrode surface takes place by solvent-casting technique. Although the knife-coating method is considered more appropriate, the lack of doctor blade instrumentation made us opt to use this similar deposition in the laboratory.

To obtain a homogeneous film it is not sufficient to remove the solvents, but this must be done slowly and limiting as much as possible the formation of turbulences in the deposited liquid layer responsible for uncontrolled precipitation of the species on the substrate, which would lead to the realization of a fragmented or irregularly thick film.

First of all, the evaporation of the solvents must take place gradually and without particular forcing, to avoid convective motions harmful to the formation of the film; since in our case we have a solution of water and ethanol, it is sufficient to work at room temperature or slightly higher. This aspect acquires greater importance from an industrial perspective because it would save on high-temperature processing costs.

Unfortunately, although operating carefully during the casting step, the drying returns an inhomogeneous film due to the different tendency of the two solvents to vaporize. Ethanol, having a vapour pressure higher than that of water, is more volatile and leaves the wet layer before the other solvent. Water evaporates more slowly, causing the concentration of the chitosan and therefore an increase in the viscosity of the aqueous phase; this does not allow the latter to spread uniformly over the entire surface of the substrate, generating a patchy film similar to that generated by the ethanol-free solution and shown previously in figure 21.

It was decided to add a very small amount of dimethyl sulfoxide (DMSO) inside the all-in-one solution to solve this problem. The idea is to exploit its low volatility and its complete miscibility in the other two solvents to maintain a very thin homogeneous wet layer always present on the entire surface of the substrate throughout the drying phase. Although DMSO is a difficult solvent to remove, the film obtained with this method is perfectly solid. This is because DMSO, the prevailing solvent in the final drying phase, is so thinly spread that it has a very large

surface/volume ratio; as evaporation takes place on the surface, DMSO can evaporate despite its low vapour pressure.

The various tests carried out have verified that the optimal quantity of DMSO is approximately 6%_(V/V) of the whole solution; for much larger quantities, the drying of the film is compromised, while for much below amount its beneficial role is not enough appreciated.

From a technical point of view, a homogeneous film is obtained if the bench on which the deposition takes place is perfectly level and parallel to the floor, to prevent the deposited solution from accumulating on one side of the substrate after casting, as shown in figure 42a. In the absence of a suitable workbench, it can be remedied by using a smooth and flat plate with height-adjustable feet and a bubble level.

Another practical precaution was used in the laboratory to slow evaporation and protect the delicate drying phase, by doing it under an inverted funnel (Fig. 42b).

Thanks to all the measures adopted, the wet layer in the drying phase remains homogeneous until the end of the process (Fig. 42c), producing a film free of macroscopic defects.

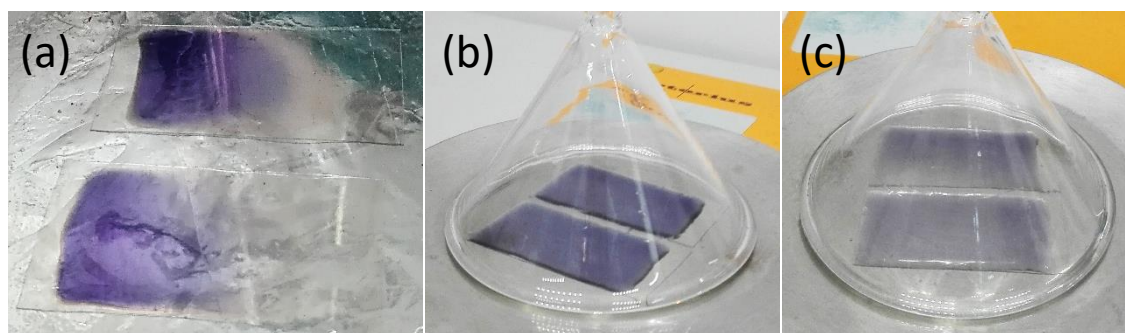


Figure 42 –(a): Uneven drying due to the slope of the bench; (b): Levelled bench and inverted funnel method; (c): The same samples in the terminal drying phase.

This drying method at room temperature takes about an hour or even less if the terminal phase is carried out at 35-40 °C.

Furthermore, it is interesting to note that as the film dries, it gradually loses the colour of the all-in-one solution; this is because TMPD returns to the neutral form, indicating that there is no presence of free water in the dry film.

The solid feature of the film is clearly shown in figure 43 in which it can be seen that it is irreversibly pierced if pricked with tweezers.

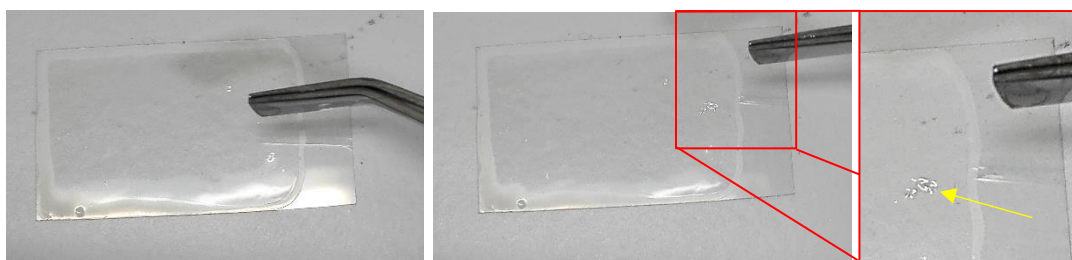


Figure 43 – From left to right: film dried and just before pricking; film after damage; magnification of the irreversible lesion caused. If the film was still in a liquid or gel state, the hole would have closed.

Figure 43 also highlights the great transparency of the deposited film which is clearly visible only when viewed in the backlight. Due to the deposition and drying techniques, the edge of the film is thicker than its central part and appears slightly opaque. In fact, from the observation under an optical microscope (Fig. 44), it can be excluded that the opacity is caused by the peripheral fragmentation of the film. Two other very interesting pieces of information can be collected from figure 44: the first is that the thickness of the substrate is much greater than that of the film; the second is the stratigraphy of the electrode, in which the surface coating of ITO shows itself in all its scaliness along the cutting site.

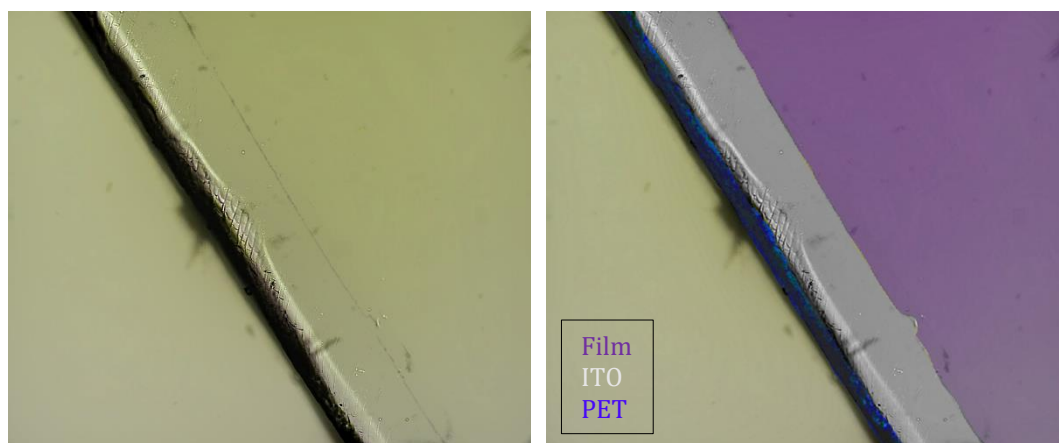


Figure 44 – Left: Optical microscope image of the film on the substrate. Right: same image in distorted colours to highlight the stratigraphy of the functionalized electrode.

A factor that acquires considerable importance for the operation of the device is the thickness of the electrochromic film. In fact, even if adequately deposited, a film that is too thick obstructs the flow of charges between the electrodes, requiring a greater potential difference to function; on the contrary, a film that is too thin has less

physical resistance, so it will be more prone to damage as well as showing less optical contrast between the on and off state.

Having a doctor blade available, the thickness of the film produced can be modulated by finely adjusting the distance of the blade from the substrate; the different volumes of the solution spread on the electrode surface will lead to films of different thicknesses.

By transposing this concept to the solvent casting technique, the final film thickness will depend on the volume of solution cast on the substrate.

To optimize the amount of solution to be deposited, we proceeded to cut different electrode substrates having the same dimensions, i.e. $2.5 \times 5 \text{ cm}^2$, on which different quantities of film-forming solution were deposited and taking care to leave a free area equal to about $0.8 \times 2.5 \text{ cm}^2$ to apply the electrical contacts (Fig.45).

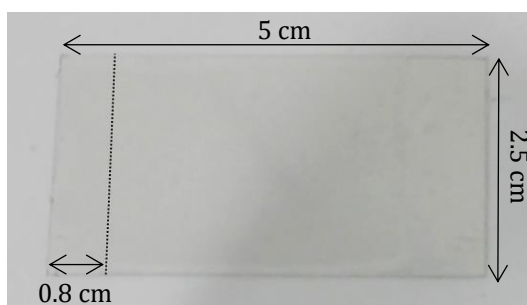


Figure 45 - Substrate electrode in ITO/PET ready for deposition.

Subsequently, the films obtained were evaluated by assembling the devices and testing them. Despite what has been said about the deposition of the film, the search for the best amount of solution to be cast cannot be separated from the assembly of the device and the related problems, which are the subject of the next section.

In conclusion, it should be noted that although these operating modes lead to the formation of an acceptable film with great transparency and homogeneity, operating with a laboratory doctor blade, preferably having a heating plate, is certainly more appropriate and would give a better result.

2.5.2. DEVICE ASSEMBLY

In the previous section, the necessary precautions for obtaining a thin and homogeneously distributed film on the substrate electrode were shown. Unfortunately, achieving a good film deposition does not mean obtaining a performing device.

Although having a potentially functional film, the operation of the device is largely due to the efficiency in electrical conduction which in turn depends on the quality of the contact between film and electrodes.

Having one of the electrodes functionalized with the electrochromic film, the difficulty consists in making the other electrode adhere to the first one, but in a non-aligned way, to allow the application of crocodile clips at the ends (Fig. 46). For this reason, the assembly of the device is another very delicate operational step, especially if carried out without the aid of adequate instrumentation.

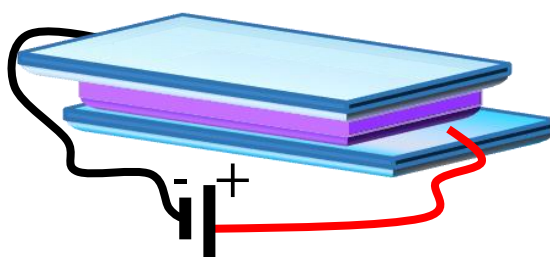


Figure 46 – Representation of a device assembled and connected to the power supply.

If this action is not carried out accurately, air bubbles can become embedded in the device, causing patchy colouration during operation. A similar result occurs when, while paying the utmost attention, the bare electrode does not adhere completely to the film. The observation under the optical microscope clearly confirmed that the activation of the electrochromic species occurs only in the portions of the film in contact with both electrodes, allowing the closure of the electrical loop (Fig. 47).

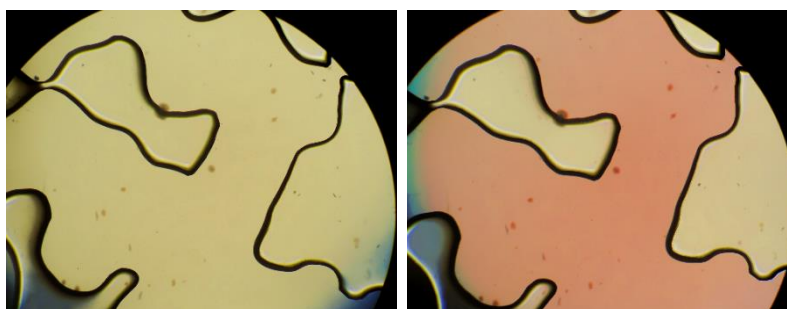


Figure 47 – Optical microscope images of a device in which there are defects in the film-electrode contact. Left: OFF mode. Right: only the parts of the film that are in contact with both electrodes are coloured in the ON mode.

This drawback is partly due to surface irregularities and partly to the thickness not being perfectly equal along the whole film.

Furthermore, in our case, we have already seen in the previous section how the thickness of the film is very small compared to that of the substrate; the latter, although flexible, can be considered a "hard" material compared to the "soft" film. Therefore, the bare electrode approaches the film with a certain rigidity and contact is formed only in certain areas (Fig. 48a).

To solve this problem, a film was deposited on both electrodes, which were then assembled in a single device after drying. During assembly, the "soft" films lay one on top of the other and, by pressing slightly, the surface irregularities interpenetrate each other self-sealing the device and producing continuity of contact (Fig. 48b).

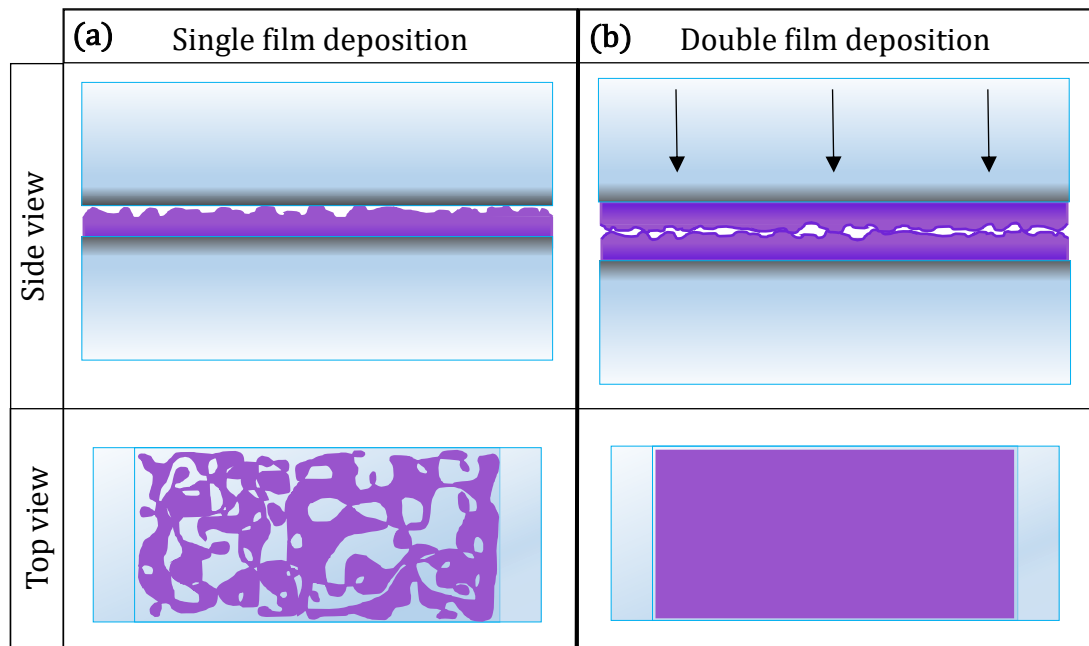


Figure 48 – Side and top view representations comparing devices with single (a) and double (b) deposition.

Also in this case it should be noted that the laboratory adaptation of the double deposition would probably have been avoided by using a doctor blade.

Anticipating the results that will be discussed in the next chapter (§ 3.2), we declare that the optimal volume of solution to be deposited on each electrode is 0.4 ml and that the resulting device will respect the characteristics established in the introductory chapter.

2.5.3. OPTIMIZE SPECIES

The transformation of the film-forming solution into a solid film derives from the loss of the solvents by evaporation, thus in the resulting dense layer the species will be more concentrated than in the starting solution as shown in figure 49.

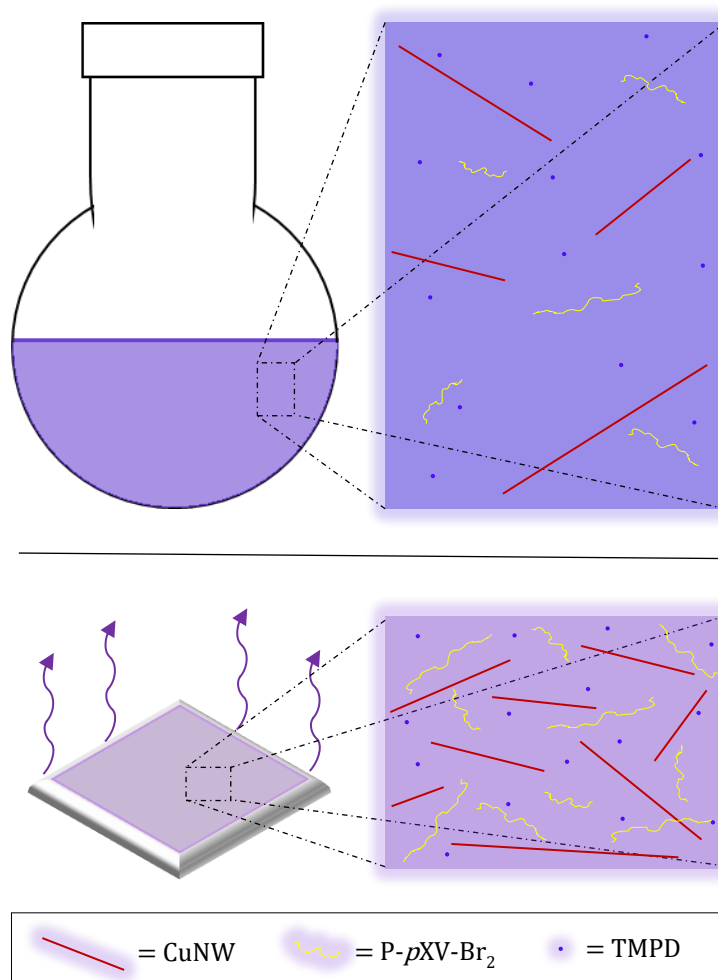


Figure 49 –In the film-forming solution the species are diluted (top), while in the film they are more concentrated due to the evaporation of the solvents (bottom).

The increase in the concentration of species, even if it is a trivial consequence of the drying of the film, is an aspect to which we must pay close attention, as it could compromise some properties of it. Therefore, the problems encountered are now analysed and the actions taken for their resolution are reported, leading to optimizing the amounts of each species introduced in the all-in-one solution.

2.5.3.1. GLYCEROL AND LITHIUM BROMIDE

The first species to be optimized are those forming the electrolyte matrix. Since the polymeric matrix constitutes the major part of the composite film of our purpose, obtaining a homogeneous film by drying the electrolytic solution is the first step to achieve the defect-free electrochromic film.

In the beginning, the optimization of the species was carried out in a solution with only chitosan, lithium bromide and glycerol, therefore without electrochromes and nanowires; only after verifying the obtainment of the film with good characteristics, these species were introduced in the all-in-one solution with the optimized quantities, verifying both the formation of a homogeneous film and its functioning.

We proceeded by keeping the amount of chitosan constant and varying the amount of glycerol; following various tests with different weight percentages, films with different physical behaviours were obtained. As already discussed in section 1.5.1.1 the greater the amount of glycerol, the more elastic the film obtained.

Unlike the other works previously mentioned, our film is rich in plasticizer because it is made with 35%_(w/w) chitosan and 65%_(w/w) glycerol. Despite this, the film obtained is perfectly solid (Fig. 50a), while the further addition of plasticizer leads to the formation of a gel-like film with a conspicuously inhomogeneous morphology (Fig. 50b).

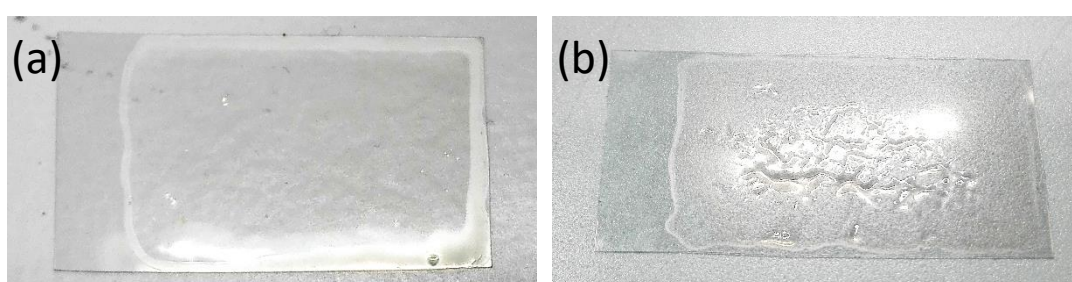


Figure 50 – Comparison between one film obtained with the optimized amounts (a) and another with excess glycerol (b).

Repeating what has already been said, the species in the optimized quantities were used in the preparation of the all-in-one solution, returning a functioning electrochromic film with an increased elasticity compared to that derived only from chitosan.

After obtaining this important result, we proceeded by gradually decreasing the quantity of LiBr; the goal was to find the minimum quantity necessary for the electrochromic film to function.

Probably due to the increase in elasticity of the film, it has been verified that the necessary amount of LiBr to be used is about half of the previous one, which means an important reduction in costs.

To summarise, the optimal amounts for preparing the electrolyte matrix are 300 mg of chitosan dissolved in about 23 ml of 1% aqueous solution of acetic acid, 554 mg (or 0.44 ml) of glycerol and 50 mg of LiBr.

2.5.3.2. POLYVIOLOGEN

The decrease in the available volume due to the evaporation of the solvents causes an increase in concentration and some species may become saturated and precipitate, causing a reduction in transparency of the film.

The polyviologen chosen, being a quaternary ammonium salt (§2.1), has this behaviour and if it concentrates up to saturation, it forms microcrystals that precipitate and give the film an opaque and slightly yellowish appearance.

This event does not affect the electrochromism of the film because not all the viologen precipitates, but it affects the effectiveness of the final device as it is not transparent enough for our purpose.

Also to resolve this drawback numerous observations under the optical microscope have been carried out. The crystalline formations causing the opacity were initially identified; they were later attributed to viologen salts, thanks to the accentuated purple colour assumed when the device was switched on (Fig. 51a).

At that point, it was sufficient to gradually reduce the amount of viologen in the film-forming solution until the absence of macroscopic opacity and crystalline formations under the microscope was verified (Fig.51b).

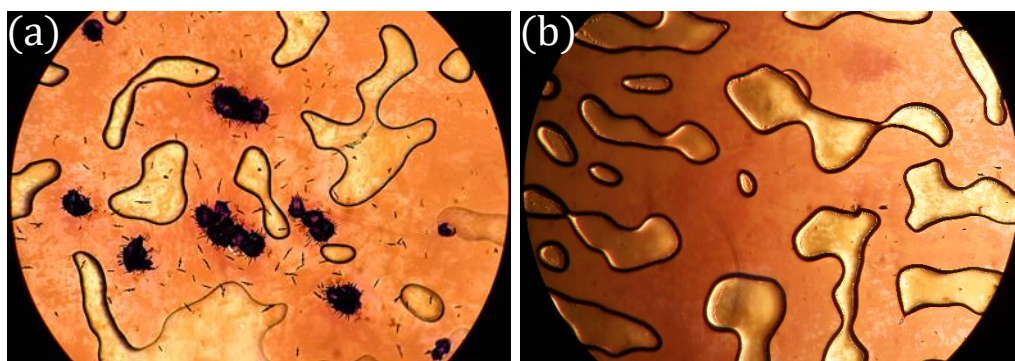


Figure 51 –Optical microscope images showing a device with precipitated viologen salts (a) and another in which the electrochrome is perfectly solubilized inside the matrix (b).

The optimized amount of polyviologen, derived from the experimental method just described, is 50 mg. Remember that all the optimized quantities shown, refer to processing our all-in-one film-forming solution.

2.5.3.3. TMPD

For the calculation of the optimal amount of TMPD, counter-species of the polyviologen, it was not possible to reason in terms of equimolarity due to the high polydispersion index of the polymer, which did not allow to quantify the electrochemically active sites per unit of mass.

The molecular weight of monomeric viologen was taken as a starting point (i.e. 418 g/mol), then a mass of 20 mg was calculated for an equimolar quantity of TMPD (MW = 164 g/mol).

Aware of operating guided by an approximation, the above amount of TMPD was added to the film-forming solution and the tests on the resulting device returned good results.

However, trials with both double and half the amount of TMPD were conducted to investigate the role of the counter-species in the device.

Although the film-forming solution acquired an intense blue tint, the double amount of TMPD did not compromise film deposition. On the contrary, the excess of the counter-species has generated a device with a marked tendency to degradation; in fact, the latter after a few on/off cycles showed a permanent blue halo, probably due to the adsorption of electrochrome on the electrodes.

Furthermore, the film-forming solution also showed signs of degradation, acquiring red shades after a few hours and becoming completely red a few days later (Fig. 52).

This red solution showed no electrochromic properties.



Figure 52 – Left: the freshly prepared film-forming solution, with double amount of TMPD. Right: the same solution degraded after a few days.

In the following chapter, the cause of this degradation will be investigated, through dedicated tests.

Returning to the optimization of the counter-species, the solution having half amount of TMPD produced a film which, when tested in the device, showed a behaviour similar to the first.

Furthermore, the introduction of a smaller quantity of TMPD avoided the rapid degradation of the film-forming solution, making it even more stable than that obtained with 20 mg of TMPD.

Since the further decrease of the counter-species worsened the electrochemical activity of the film, it was established that the optimal amount of TMPD is 10 mg.

2.5.3.4. COPPER NANOWIRES

In section 2.4 we have already mentioned that a large presence of CuNWs causes a pale pink colour to the solution (Fig. 39). Although this slight colouring indicates the successful dispersion of the nanowires inside the solution, during the drying phase it becomes more charged and the film obtained undoubtedly appears pink.

Having pink film rich in nanowires can have several advantages but, at the same time, it limits the optical contrast between the on and off mode, as well as being aesthetically questionable. Therefore, it is necessary to carefully balance the amount of nanowires to be added to the solution, in order to have a film that is not excessively coloured.

To optimize the amount of CuNWs, the tests were carried out in a solution of only chitosan and glycerol, in order to avoid the waste of the other species. Once the right amount was established, compatibility with the all-in-one film-forming solution was successfully verified.

Remembering that the storage alcoholic dispersion of CuNWs is very concentrated, i.e. 1 mg/ml (§ 2.3.3), the small variation in volume will produce large differences.

Initially a volume of nanowire dispersion equal to 0.5 ml was added to the solution; in this way, a very coloured film was obtained, therefore the amount of CuNWs was gradually reduced until a very weak colour was achieved. The colour is more accentuated in the devices due to the film deposition on both electrodes. (Fig. 53).

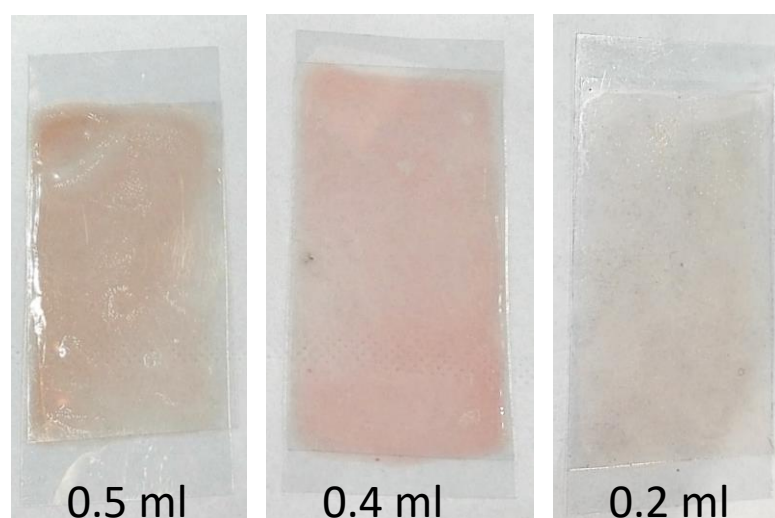


Figure 53 – Devices made with double film deposition starting from solutions with different amounts of CuNWs; 0.5 ml 0.4 ml and 0.2 ml from left to right.

Although all the devices produced show excellent transparency, adding 0.2 ml of CuNWs dispersion leads to a device with a sufficiently weak colour which is visible only if placed on a white background. Minor amounts of CuNWs dispersion are not detectable with the naked eye.

Figure 54 shows the optical characteristics of the devices produced by adding 0.3 ml of CuNWs dispersion, which are transparent despite being coloured.

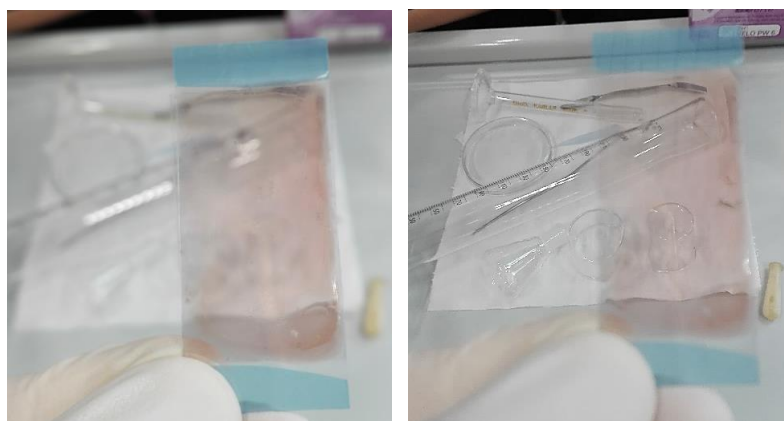


Figure 54 – Photographs with different focus of a same device to appreciate its transparency. On the left: close-up; on the right: out-of-focus.

The observation under an optical microscope confirms the presence of nanowires even in devices with the minor addition of CuNWs dispersion (Fig. 55).

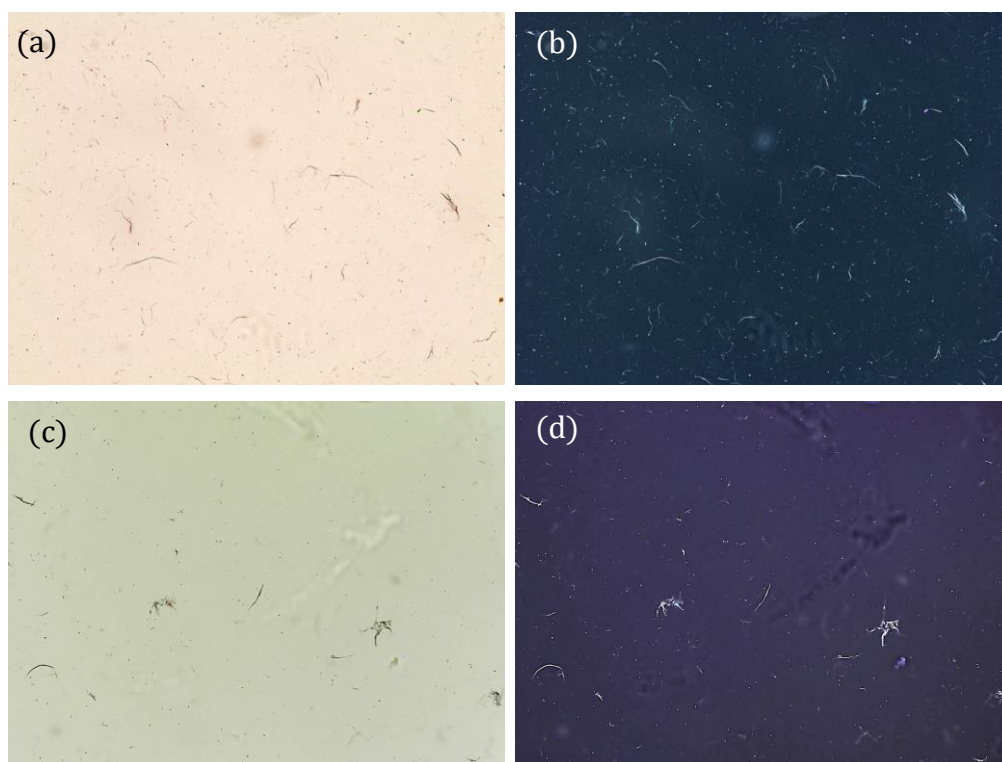


Figure 55 – Optical microscope images of devices having 0.5 ml (a) and 0.2 ml (c) of CuNWs dispersion in film-forming solutions; (b) and (d) are colour-inverted images to highlight the nanowires.

From these tests, it is established that the optimal amount of alcoholic dispersion of CuNWs in the all-in-one solution is 0.2 ml.

Now that the optimal quantities of all the species, the methods for the preparation of the solution, those for the deposition of the film and those for the assembly of the device have been found and having verified the operation of the devices produced several times, it is possible to proceed to the chapter about the characterizations. First, however, it is considered appropriate to summarize the synthetic protocol in the next section.

2.5.4. SYNTHETIC PROTOCOL

Chitosan (medium molecular weight 100-300 kDa, degree of deacetylation $\geq 75\%$) were purchased from Acros Organics© and used as received without further purification. *N, N, N', N'-Tetramethyl-1,4 - phenylenediamine (TMPD)*, *lithium bromide (LiBr)*, glycerol, glacial acetic acid, dimethyl sulfoxide (DMSO), and ethanol were purchased from Merck© and used as received without further purification.

P-pXV-Br₂ and *CuNWs dispersion* were obtained as described in sections 2.1.1 and 2.3.3 respectively.

Initially, as described in section 2.4, two solutions are prepared, one aqueous and the other organic, from the mixing of which the all-in-one film-forming solution is obtained.

Aqueous solution

In a flask of suitable size (e.g. 100 ml), under magnetic stirring, put distilled water (e.g. 23 ml), *P-pXV-Br₂* (e.g. 50 mg), and LiBr (e.g. 50 mg). After complete dissolution of the species add glacial acetic acid (e.g. 0.24 ml) and chitosan (e.g. 300 mg).

Wait about half an hour for the chitosan to be completely solubilised and the solution to be clear and colourless; in the meantime, you can proceed with the preparation of the organic solution.

Organic solution

In another flask of suitable size (e.g. 100 ml), under magnetic stirring, put ethanol (e.g. 23 ml), CuNWs dispersion (e.g. 0.2 ml), glycerol (e.g. 0.44 ml), TMPD (e.g. 10 mg) and DMSO (e.g. 3.3 ml).

The introduced species easily dissolve and the solution becomes clear and slightly pink.

All-in-one film-forming solution

Slowly, mix the two previously prepared solutions under magnetic stirring and wait about two hours for the solution to be clear, homogeneous and deep purple.

The total volume obtained by following the suggested amounts is about 40 ml due to the hygroscopicity of the species used.

The deposited films and consequently the assembled devices show excellent transparency and lack of macroscopic defects (Fig. 56).

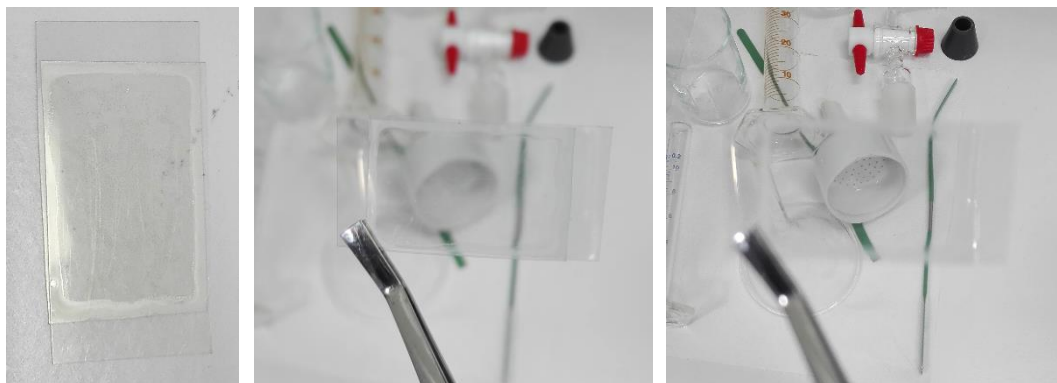


Figure 56 – Photographs with different focus demonstrating the transparency and homogeneity of the device, designed and developed as described up to now.

To retard the degenerative phenomena and preserve the all-in-one solution it can be stored in a freezer (-15 °C) and will be stable for over two months.

With the latest synthetic-operational information provided, this chapter ends. In the next, the device will be tested with different instruments with the aim of characterizing it and verifying whether the results obtained satisfy the pre-established purposes.

3. RESULTS AND DISCUSSIONS

The synthetic protocols and methods for obtaining a functioning electrochromic device were illustrated in the previous chapter; in there it was considered appropriate to include all the characterizations necessary to validate the synthesized species and the choices made for the development of the device.

Instead, in the following sections, the experimental results relating to the operation of the device will be presented and in some cases, information will be obtained from the comparison between slightly different devices.

The differences between the devices consisted in the presence or absence of some species or the use of different thickness films resulting from the same film-forming solution.

Therefore, the data obtained will provide qualitative or quantitative information and be able to confirm what has already been verified or will offer totally new indications.

As already stated in chapter 2, the films that were found to be suitable after drying constituted devices, the operation of which was verified through the application of the potential.

Consequently, it is considered appropriate to start with a section illustrating the crucial indications provided by this simple practical test.

Electronic and morphological characterization will be performed to determine the film thickness and the response of the device between the on and off modes.

Optical and electrochemical behaviours will be recorded and discussed; finally, investigations will be carried out to understand what causes the degradation of the film-forming solution.

3.1. MONITORING THE SWITCHING POTENTIAL

The switching potential for an electrochromic device is the potential difference to be applied to observe the switching of the transparent to the coloured state. The lower the switching potential, the higher the efficiency of the device.

For this reason, since the beginning of the development phase, this parameter has been constantly monitored for all the samples produced; when the colour change appeared to take place at high potentials, we worked on its lowering.

The first tests concerned the correct inclusion of the polyviologens in the chitosan-based biopolymer electrolytic matrix; once the correct film formation was achieved, the devices were assembled and tested by applying an increasing potential difference until the colour change was seen.

Tests were conducted on all four synthesized polyviologens, yielding the same result. The P-*p*XV-Br₂ was chosen as, unlike the others, its more rigid structure and its growth in extension probably lead it to occupy more sections within the electrochromic film.

Contrary to what one might think, the devices having only a polyviologen without counter-species showed electrochromism; the biggest problems were the high switching potential of 3.1 V and the very slow return to the transparent state, which took over half an hour.

In fact, unlike the asymmetrical type devices, the one under development does not allow the polarity reversal as a bleaching method.

Although the switching potential was lowered for the thinnest films, this was at the expense of the intensity of colour assumed by the device. Therefore, the use of metal nanoparticles was tested, considering them useful conductors of electrons.

Spherical or rod-like nanoparticles of both gold and silver were placed in the film-forming solution and the resulting devices were tested.

Surprisingly, the same result was obtained, regardless of the different metals and different shapes. Despite this, the switching potential had dropped to 2.8 V and the devices all exhibited a more homogeneous colouration.

Therefore, it was decided to introduce nanoparticles with a higher aspect ratio, based on the cheaper metal copper. The switching potentials recorded for these devices were 2.6 V, with the same concentrations and thickness (or rather obtained by depositing 0.5 ml of film-forming solution on each electrode) as the previous ones.

Despite these advances, the switching potential was still too high and the return to the transparent state of the device remained equally slow.

A big improvement was finally achieved through the use of TMPD as a counter-species of the polyviologen; acting in an electrochemically complementary manner, it lowered the switching potential of the device to 0.8 V.

In addition, the return to the transparent state was much improved, taking less than a minute.

Table 4 summarizes the improvements just described; starting from a switching potential of 3.1 V we arrived at a device whose activation is observed at 0.8 V, improving the parameter by 74%.

Tests	Polyviologens	Nanoparticles	Counter-species	ΔV (V)
I	P-propV-Br ₂	/	/	3.1
	P-dodecV-Br ₂	/	/	3.1
	P- <i>o</i> XV-Br ₂	/	/	3.1
	P-<i>p</i>XV-Br₂	/	/	3.1
II	P- <i>p</i> XV-Br ₂	AuNPs	/	2.8
		AgNPs	/	2.8
		CuNWs	/	2.6
III	P- <i>p</i> XV-Br ₂	CuNWs	TMPD	0.8

Table 4 - Materials present in the tested devices and related switching potentials.

Although these basic tests were carried out only with a DC power supply and through observation with the naked eye, they were of fundamental importance in directing the search path. In the next sections, the data obtained using instrumental analyses will be shown, which will better describe the characteristics of the developed device.

3.2. ELECTRONIC MEASUREMENTS

At the end of section 2.5.2. it was anticipated that the optimal volume of film-forming solution to be cast on each electrode is 0.4 ml while in the previous section the data of the films obtained by depositing 0.5 ml were shown; in this section, the results of the measurements that led to fixing this value will be presented.

Let's start by remembering that the electrochromic device works thanks to a DC power supply, so it is a component of an electrical circuit. Analysing the device from an electronic point of view represents the necessary in-depth study of what is indicated by the observation of the switching potential.

The experimental setup developed for data collection is schematized in figure 57 and involved an oscilloscope, a DC power supply and a reference resistor.

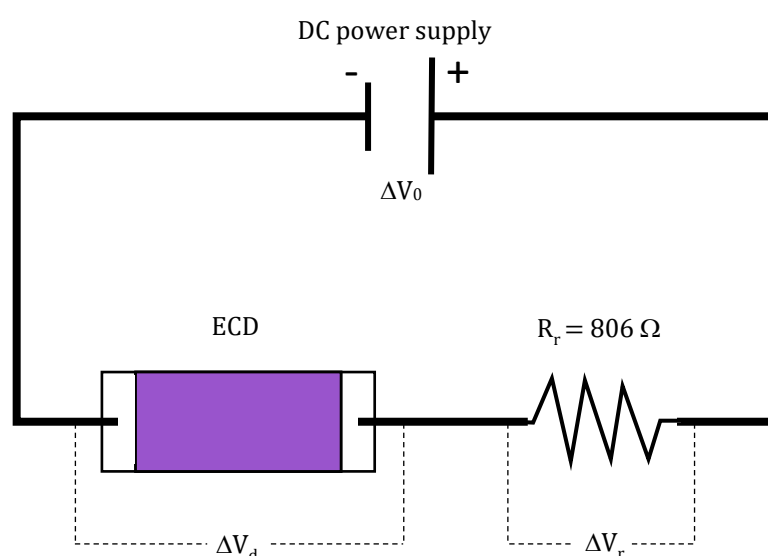


Figure 57 – Representation of the experimental setup circuit.

The reference resistor and the electrochromic device (ECD) are placed to form a series circuit, powered by a direct current power supply (ΔV_0), the voltage drops across the resistor (ΔV_r) and the device (ΔV_d) are recorded by the oscilloscope.

The first test carried out consisted in recording the voltage drop on devices resulting from the deposition of different volumes of the same film-forming solution, which had been prepared as described in the previous chapter.

Samples deriving by depositing 0.5 ml, 0.4 ml and 0.3 ml per electrode of the same solution were produced and named respectively D5, D4 and D3. The D3 devices

exhibited poor colouration during the preliminary tests; although functioning, the D3s did not show sufficient optical contrast, so they were excluded from the electronic analysis as ineffective devices.

This is already the first indication that helps determine the optimal volume of the film-forming solution to be deposited.

The D5 and D4 devices have been successfully tested in the circuit described above and their behaviour in an ON/OFF test has been recorded. This test involves powering the circuit by applying a constant potential (ΔV_0) for a certain time, after which the power is turned off; during this period, the values of the potential drop across the device (ΔV_d) and the resistor (ΔV_r) will be recorded step by step. Figure 58 provides an example of the raw data obtained by this analysis.

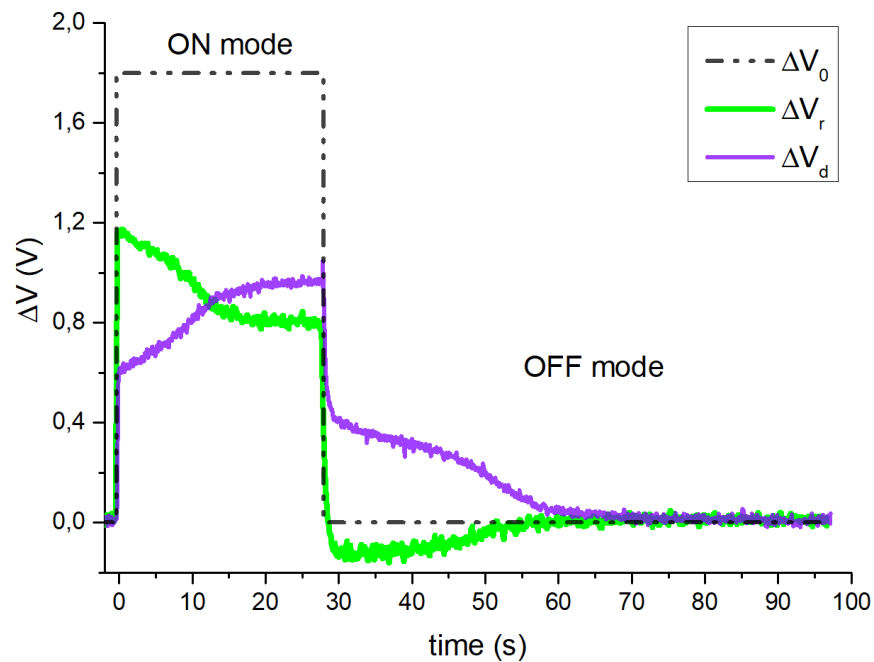


Figure 58 – Changes in potential drops during an ON/OFF test conducted on a sample D4.

The first experimental evidence acquired and expected is that the circuit is not purely resistive, because otherwise, the potential drops across the two components would have varied coherently with the applied potential.

Secondly, it is observed that the device reacts oppositely concerning the resistor. Remembering that the greater the resistance of a component, the greater the voltage drop across it, changes in potential drops indicate an increase in the resistance of the device.

Considering that the trends of ΔV_d are the same for all tested devices, an explanation can be proposed by analysing the potential drop across the device.

Figure 59 shows the generic trend of the ΔV_d of our electrochromic devices during the ON/OFF test. The blue points on the curve represent different phases of electrochromic operation.

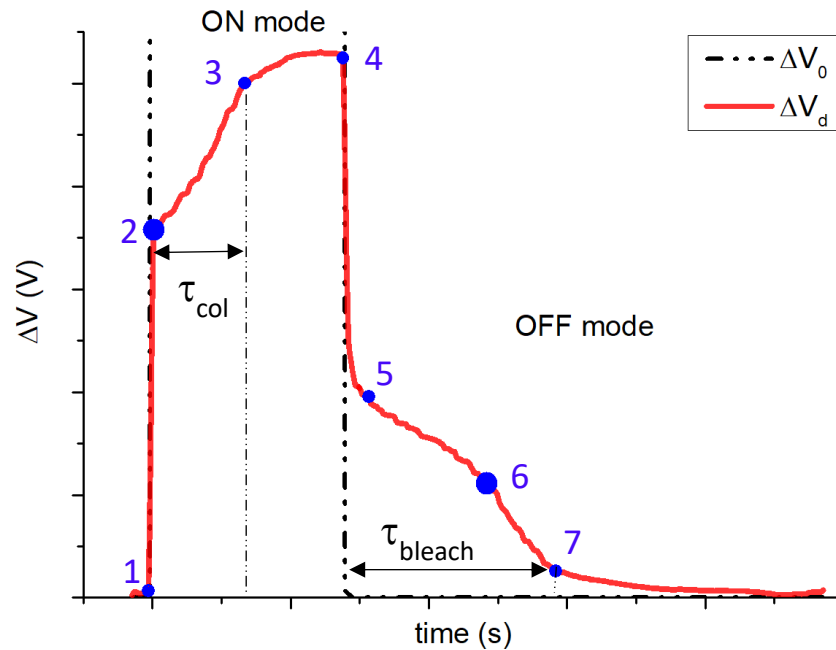


Figure 59 – Trend of potential drops across our generic ECD during an ON/OFF test.

The points selected on the curve are not only an expression of the electronic behaviour of our ECD, but often correspond to variations in its optical properties.

1. **Turning on.** Due to the applied potential difference (ΔV_0), charges begin to accumulate on the electrodes of the ECD.
2. **Switching potential.** The potential difference on the electrodes is enough to initiate the transfer of charges in the film; electrochromes acquire or release electrons and colour switching is observed.
3. **Equilibrium phase.** Close to the electrodes, most of the electrochromes are activated. The potential drop slowly reaches a plateau.
4. **Turning off.** By resetting ΔV_0 , the charge accumulation on the electrodes is quickly exhausted and the potential drop across the device collapses.
5. **Discharge phase.** Electrochromes still charged switch to the neutral state slowly, through the exchange of electrons.

6. **Bleaching point.** Many of the electrochromes return to their neutral state, so the device appears to gradually bleach.
7. **Deactivation phase.** There are very few charges within the film, and the ΔV_d exponentially tends to zero, so the device switches completely to a transparent state.

In addition to accurately determining the switching potential, as shown in figure 59, other information can be obtained with the ON/OFF test such as the colouring time (τ_{col}) and the bleaching time (τ_{bleach}); these data are fundamental to defining the properties of an ECD. The shorter these times, the faster the device will respond.

In light of the above, we just have to compare the data obtained from the D5 and D4 devices and evaluate the differences.

The devices were tested under the same conditions, then subjected to the same ΔV_0 for the same time. (Fig. 60).

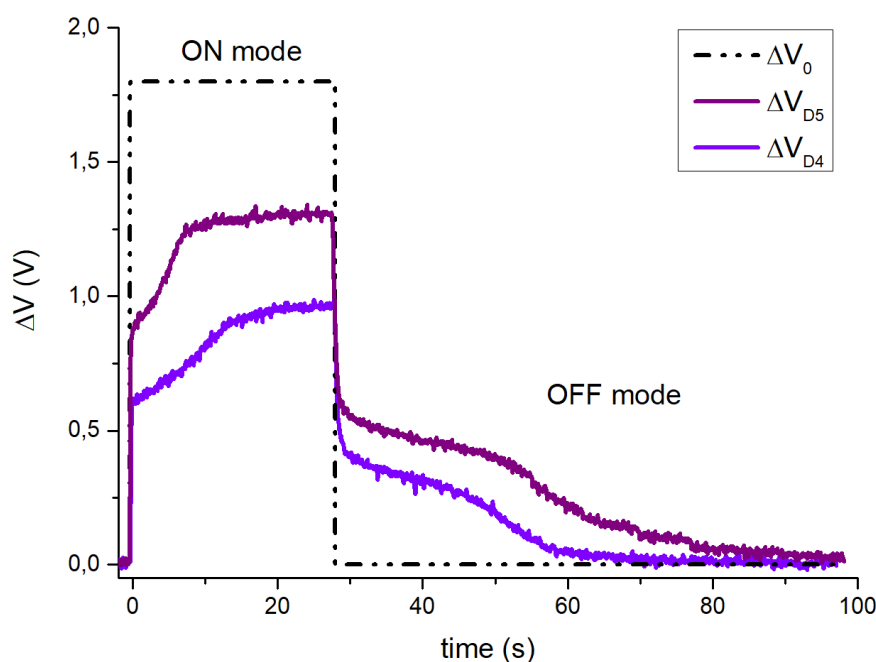


Figure 60 – Comparison between devices D5 and D4 at the ON/OFF test.

By comparing the behaviour of the two devices, it can be seen that the switching potential is greater for the thicker film; in fact, this value is 0.85 V for the film obtained by depositing 0.5 ml of solution (which matches the one obtained by empirical observation), while the switching potential of the film deriving from the deposition of 0.4 ml of solution is 0.60 V.

As regards the response times, it is observed that D5 has a shorter τ_{col} than D4, respectively 9 s and 15 s. On the contrary, the D5 has a significantly longer τ_{bleach} of 50 s compared to the 30 s of the D4.

Overall, it can be said that the D5 ends the ON/OFF test after about 80 s while the D4 after only about 60 seconds.

To summarize the data obtained, we can state that, due to the lower switching potential, and the higher response speed, the ON/OFF tests are in favour of the D4 devices; therefore 0.4 ml is considered the optimal volume of film-forming solution to be deposited on each electrode.

It is possible to carry out another type of measurement through the same experimental setup. Indeed, knowing the resistor resistance ($R_r = 806 \Omega$) and measuring its potential drop (ΔV_r), it is possible to calculate the current intensity passing through the resistor, using Ohm's law:

$$I = \frac{\Delta V_r}{R_r} \quad \text{where} \quad \begin{array}{l} I = \text{current intensity} \\ \Delta V_r = \text{resistor potential drop} \\ R_r = \text{resistor resistance} \end{array}$$

Since the current flowing in a series circuit is equal in every part of the circuit, by measuring the voltage drop across the device (ΔV_d) we can calculate the value of its resistance (R_d):

$$R_d = \frac{\Delta V_d}{I} \quad \text{where} \quad \begin{array}{l} R_d = \text{device resistance} \\ \Delta V_d = \text{device potential drop} \\ I = \text{current intensity} \end{array}$$

By varying the applied potential, recording the potential drops and applying Ohm's law, it is possible to observe the variations in the resistance of the D4 devices (Fig. 61) and the current flowing through them.

Initially, the application of a potential corresponds to a sudden decrease in the resistance value of the device. Electrochromic activity is triggered when the further increase of ΔV_d reaches the switching potential. At higher potential, the electrochromes near the electrodes are charged and this corresponds to the achievement of a minimum in the resistance function.

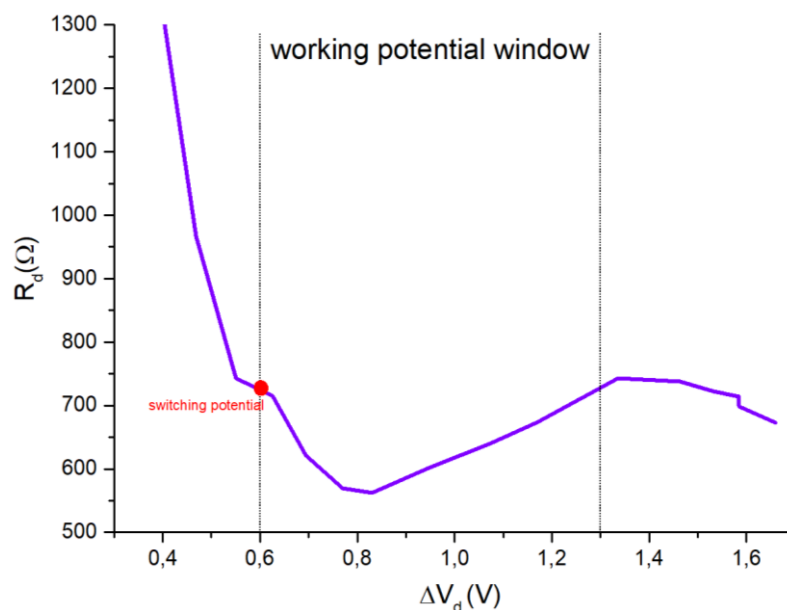


Figure 61 – Device resistance trend as a function of the applied potential.

From this point on, the activated electrochromes hinder the exchange of charges and the resistance of the device increases until it reaches a maximum. Further increasing the applied potential means forcing the passage of charge in the film, causing degradation effects. Therefore, the operation of the device is reversible within a potential range, called working potential window, which for D4 devices is between 0.6 V and 1.3 V

The final considerations to be made concern the current intensity flowing through the device. As shown in figure 62, the current in the working potential window varies between 0.8 to 1.8 mA, common values for most electrochromic devices.

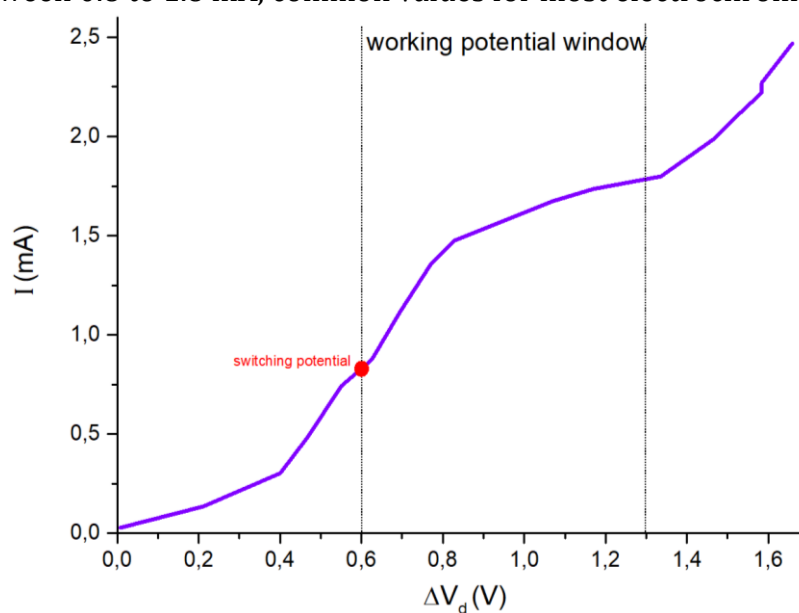


Figure 62 – Current intensity trend as a function of the applied potential.

3.3. FILM THICKNESS AND MECHANICAL BEHAVIOUR

In previous section the optimal volume of film-forming solution to be deposited has been set; the electronic behaviour of the resulting device was characterized and analysed. In this section, specific measures to determine the film thickness will be exposed.

As stated in the introductory chapter, a thin film is preferred to allow the final device to easily fit into pre-existing windows.

Not being able to change the thickness of the electrodes, we can only adjust the film. Due to the solvent-casting deposition technique, the parameter that allows us to regulate the thickness of the film is the volume of solution cast onto the electrode.

Obtaining a very thin electrochromic film would mean poor colouring, i.e. a low optical contrast, which would render the device ineffective.

As we have seen in the two previous sections, monitoring the switching potential and the electronic measurements indicated the validity of the films resulting from the deposition of 0.4 ml of film-forming solution on each electrode.

In this section, the thickness will be quantified and considerations of its mechanical behaviour will be made.

Let's start by informing that a single ITO/PET sheet, from which the electrodes for our device are obtained, has a constant thickness of 128 μm ; since the electrodes are two, the thickness of the device will certainly be greater than 256 μm .

Remembering that the device is obtained by sandwiching the two functionalized electrodes (§ 2.5.2), it follows that the resulting film is the sum of the two depositions.

The thickness measurements were initially conducted using a micrometer by measuring different devices on several parts. By subtracting 256 μm from the collected values, due to the thickness of the electrodes, an average thickness of about 68 μm per film is obtained. All the films measured gave the same data but unfortunately, they also showed a non-homogeneity of thickness between various parts of the same film.

The cause of this is attributed to the deposition and drying methods not supported by doctor blade instrumentation.

To obtain further information, observations were carried out using SEM microscopy (Fig. 63); The sample was obtained by gently opening the device and peeling the film from the electrodes. Being an analysis to be conducted under vacuum, a shrinkage of the film was observed, probably due to the solvent molecule's desorption from the bulk of the film.

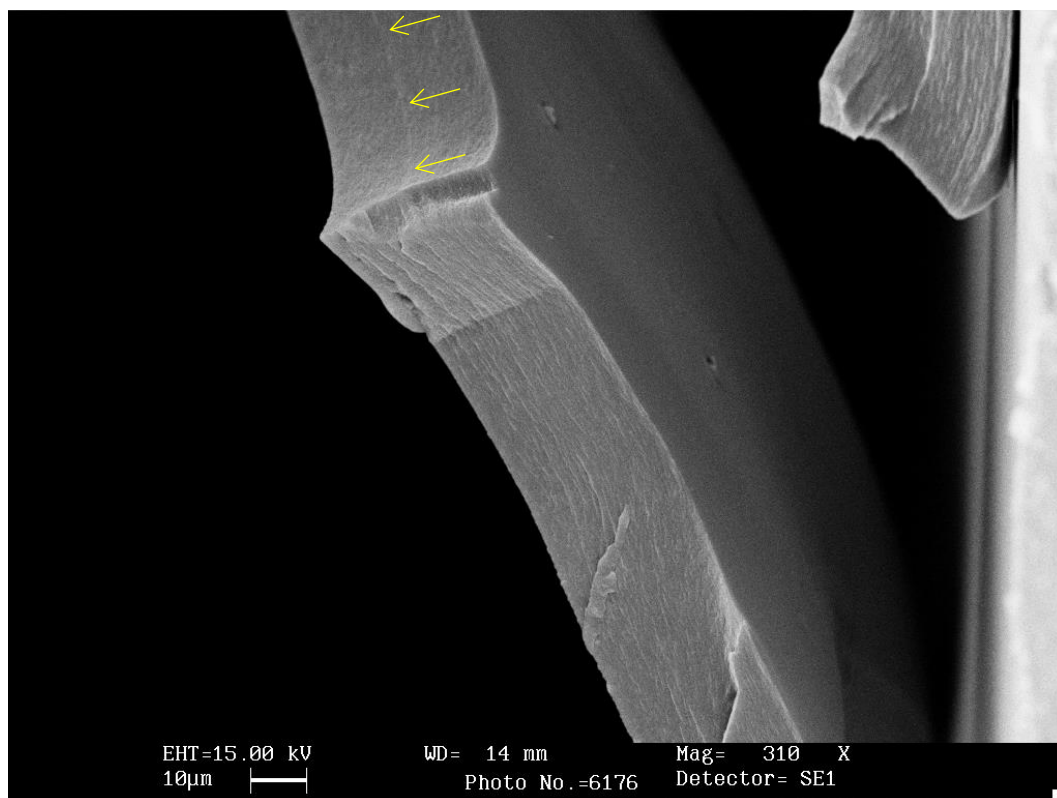


Figure 63 – SEM image of the electrochromic film; the yellow arrows indicate the area where the two depositions merge.

The graphical measurement of the thickness provides an average value of 30 µm, confirming what was observed during the vacuum draft.

In the image above, highlighted by the arrows, the area where the two depositions merged to form a single film is visible. This demarcation is not appreciated everywhere, proving that there is continuity between the two original layers. This, combined with the good adhesion of the film to the electrodes, allows the assembly of the device without the use of any sealant.

The self-sealing is strong enough to allow the device to work even when bent, without detaching (Fig. 64). In fact, the detachment of the device occurs only if deliberately caused.



Figure 64 – Photographs of a device working without mechanical stress (left) and bent (right).

Another desired and achieved feature of the film is its great flexibility; even when the device is excessively stressed, the film accompanies the bending. This film is so stretchable that it can potentially adapt to electrodes more flexible than ITO/PET.

The photographs above, in addition to showing the flexibility of the device, also indicate a good level of colouring. This topic, fundamental for an electrochromic device, needs to be explored and will be the topic of the next section.

3.4. OPTICAL MEASUREMENTS

As stated from the beginning, we aim to develop an electrochromic device intended for application on windows. For this reason, maximum transparency was pursued in OFF mode and maximum colouring in ON mode.

Even in achieving this characteristic, the first screening consisted in critical observation of the samples produced; devices exhibiting opacity or colouring in OFF mode or weak colouring in ON mode were consequently discarded. Only the devices that appeared to be the best with the naked eye were analysed with the spectrophotometer.

Before showing the optical behaviour of the devices, it should be pointed out that humans define as transparent everything that allows them to see beyond. For example, the electrodes used, although declared transparent, still absorb part of the incident radiation, as already seen from the spectra presented in section 1.3. For this reason, observation with the naked eye has always been considered a valid tool.

Closing parenthesis, the measurements were collected in percentage transmittance mode (T%) versus air, since it is more immediate to link the amount of electromagnetic radiation that crosses the device to its future application.

For the same reason, the range of wavelengths in which the analyses were carried out corresponds to the visible spectrum (390-760 nm).

The complete device, obtained as described in section 2.5.4, was connected to the power supply and inserted into the spectrophotometer to record the spectral features at various applied potential differences.

As learned from all the literature consulted and as verified several times during the research, it is expected that higher potentials induce a deeper colour of the device.

The device was tested in the working potential window, i.e. between 0.6 - 1.2 V, established through the analyses in section 3.3; after which the collected data were aggregated and plotted in a single graph (Fig. 65). After the test, the device was checked again and the reproducibility of the results indicated the excellent reversibility of the electrochromic processes.

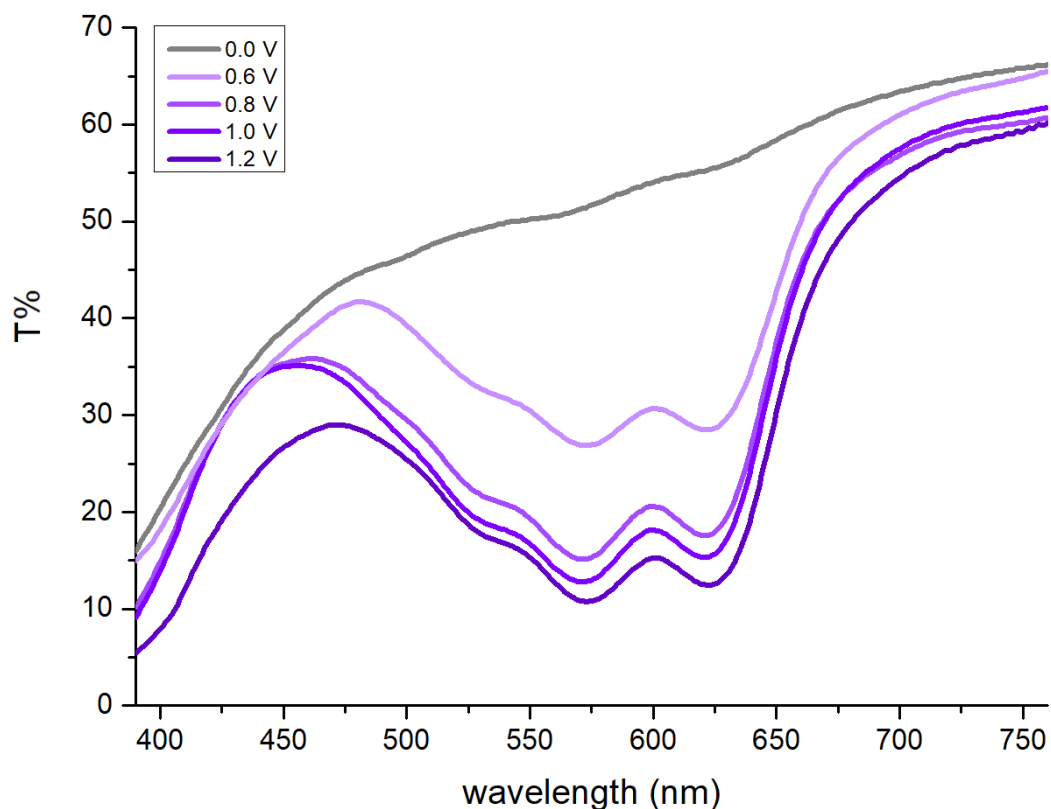


Figure 65 – Transmittance spectra of our device at different applied potentials.

Observing the spectra in figure 65, as expected, we can observe the decrease in transmittance at increasing ΔV . Interestingly, the distance between the curves is smaller at potentials greater than 0.8 V, presumably because it is already sufficient to activate most of the electrochromes in the film.

The loss of transmittance during the ON mode is mainly between 475 - 675 nm and this variation gives our device the characteristic blue/purple colour.

To investigate the assignment of the band, two other devices were produced, one with only the polyviologen and the other with only the TMPD; the latter showed no electrochromic activity (being a type I electrochrome, § 1.4), while the other was successfully characterized.

Plotting in the same graph (Fig. 66) the spectra of the complete device (D_c) and the one with only the polyviologen (D_v) during ON mode and OFF mode, some important information can be obtained. Plotting the spectrum of a pair of electrodes can also be useful as it represents the starting point of the devices.

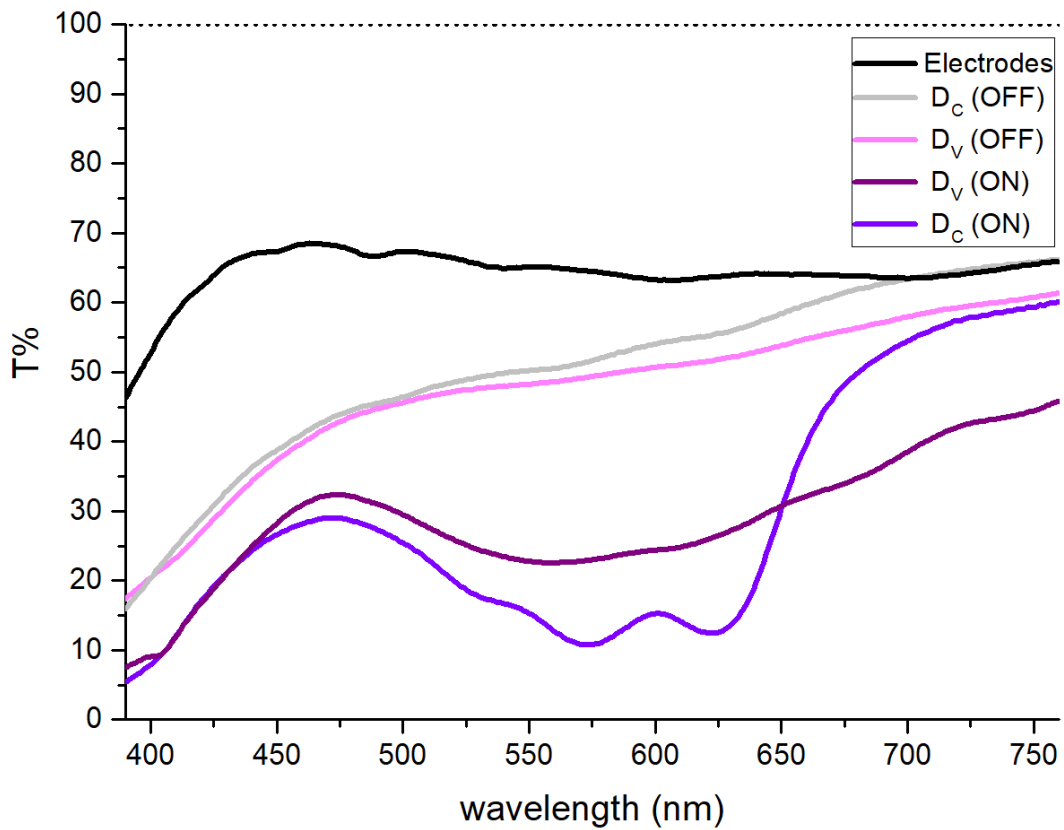


Figure 66 – Transmittance spectra of the two devices during ON mode and OFF mode.

Comparing the spectra in figure 66 it is possible to observe almost the same optical response of the two devices in OFF mode; this implies that even with the naked eye the two devices are not distinguishable. Differently, comparing the devices in ON mode, different spectral features are noted, although both bands fall almost entirely in the same wavelength range. To confirm what has been said in figure 67, the two devices in OFF and ON mode are compared.

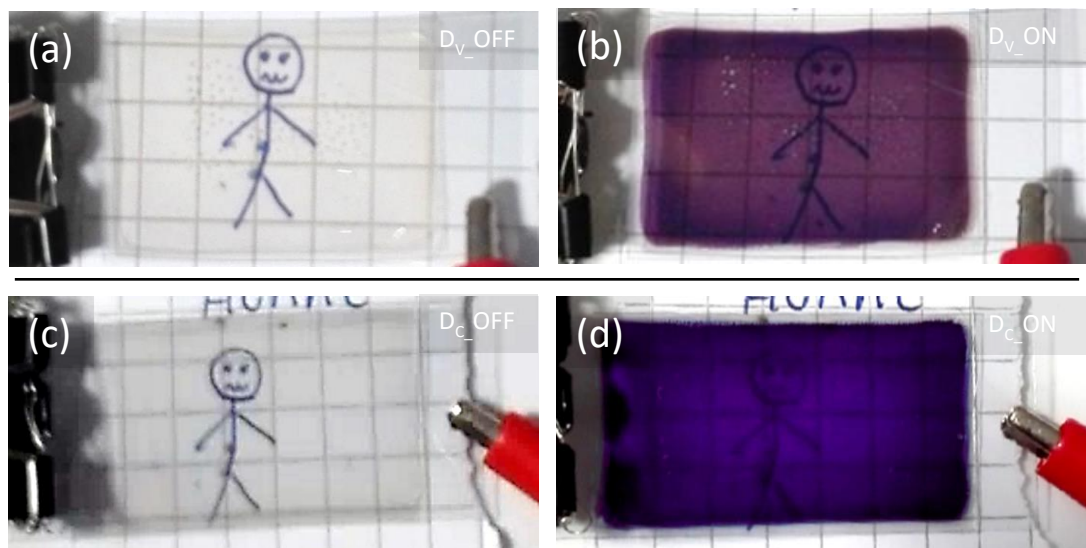


Figure 67 – Visual appearance of the D_v (top) and D_c (bottom) devices, in OFF mode (a) and (c) and ON mode (b) and (d) respectively.

The photographs show good transparency in OFF mode and intense colour in ON mode for both devices. The D_v device tends to purple, while the D_c device has shades of blue due to the presence of TMPD in the latter.

Furthermore, the D_v device appears a little more transparent than the other, which is also confirmed by the spectra in figure 66. Wanting to quantify what has been said, it is necessary to calculate the optical contrast of both devices. While this value is the same, the D_c device achieves it by applying a potential of 1.2 V while D_v needs 3.7 V.

Generally, in the literature^{4,163-165}, this property is determined by examining only the wavelength at which the greatest transformation of the spectrum occurs between the OFF and ON modes. Instead, in this work, it is considered more suitable to compare the areas underlying the spectra, also because of the diversity in the spectral features of the two devices.

To do this, the entire area of the graph is calculated and assumed as a value of 100% transmittance. By simple proportion with the maximum area, the areas subtended by the spectra will provide the values in T% of the respective devices.

Analysing the spectra in this way, it results that the pair of substrates constituting the devices have a T=66%, confirming what is stated in §1.3; D_v and D_c in OFF mode have T=47% and T=50% respectively, while in ON mode T=29% for both. While this value is the same, the D_c device achieves it by applying a potential of 1.2 while D_v needs 3.7 V.

Consequently, the optical contrast ($\Delta T\%$) is 18% for D_v and 21% for D_c. if we compare the loss of transmittance between the OFF and ON modes we will have a variation equal to 40% for D_v and 43% for D_c.

3.5. ELECTROCHEMICAL MEASUREMENTS

In the previous section, the reversibility of the device was demonstrated by comparing the transmission spectra; here the use of an electrochemical analysis such as cyclic voltammetry, is useful to establish whether the red-ox processes are effectively reversible.

Before testing the device, it was considered useful to measure the behaviour of the electrochromic film by placing it in an electrochemical cell with 0.1 M electrolytic solution of tetrabutylammonium hexafluorophosphate (Bu_4NPF_6) of anhydrous dichloromethane (DCM); the transparent cell allows to monitor the colour changes of the film during the analysis and no degradation phenomena were observed in the immersed film during the measurements.

The film was deposited on the ITO/glass working electrode (WE) as the PET substrate is damaged by DCM; a platinum wire as a counter electrode (CE) and a silver wire as a pseudoreference electrode (RE) close the electrical circuit. A photograph of the experimental setup is shown in the figure 68 below.

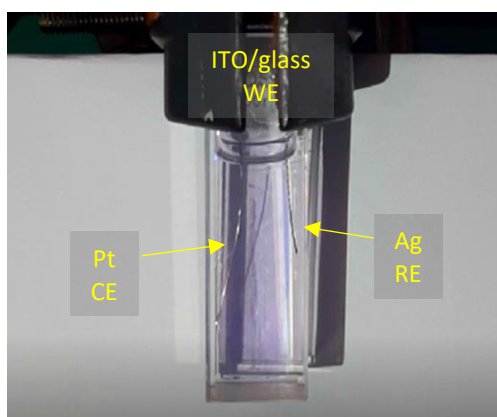


Figure 68 – Experimental setup for electrochemical measurements.

The cyclovoltammetric measurements were conducted between -0.6 and +1.2 V at a scan rate of 100 mV/s. The voltammogram in figure 69a shows one peak in reduction at -344 mV and one peak in oxidation at -40 mV, with a ΔV of 304 mV.

With the same experimental setup, it was also conducted chronoamperometric analysis (fig. 69b). Two potentials, i.e. -0.6 V and +1.0 V, were applied to the WE alternately for 20 seconds. After 10 repetitions, no changes in the currents are evident, indicating the reversibility of the electrochemical reactions.

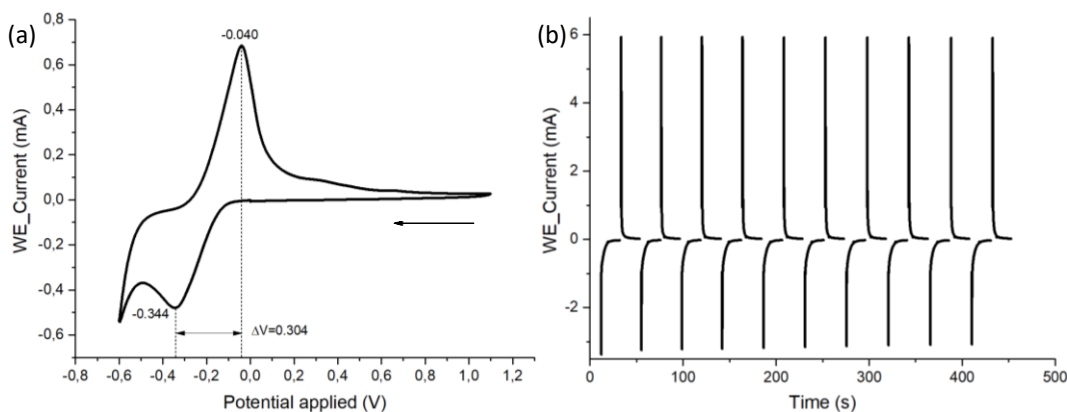


Figure 69 – Voltammogram (a) and amperometric repetitions (b) of electrochromic film.

Another confirmation of reversibility is obtained by comparing a further five voltammograms under the same conditions like the one in figure 69a. After more than 50 total cycles performed during measurements, the five curves appear perfectly superimposable and no peak shift is observed (Fig. 70a).

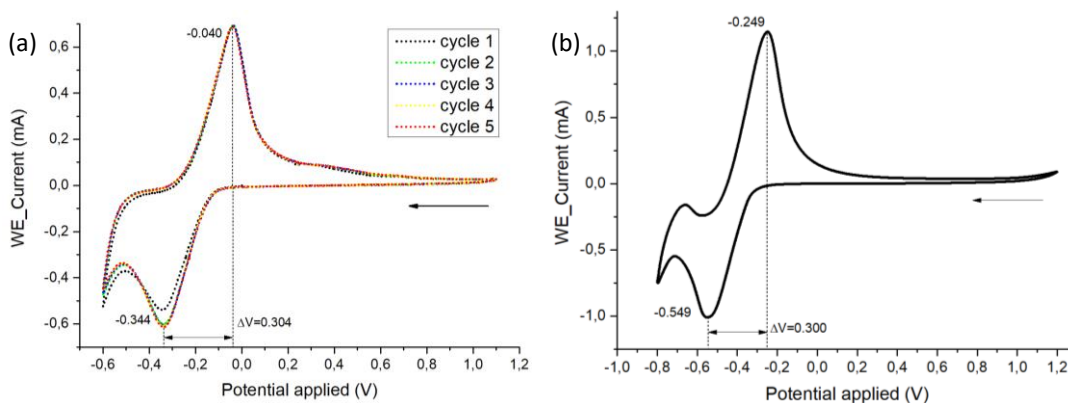


Figure 70 – Cyclic voltammograms of the electrochromic film (a) and of our device (b).

After the film, the device was also subjected to cyclic voltammetry; the two ITO/PET electrodes were respectively WE and CE while a graphite tape was inserted into the device as RE during the assembly phase. Despite the difficulties due to the suboptimal sealing of the device and the application of the crocodile clips, the voltammogram was successfully recorded (Fig. 70b).

The device was analysed between -0.8 and +1.2 V at a scan rate of 100 mV/s. The voltammogram shows one peak in reduction at -549 mV and one peak in oxidation at -249 mV, with a ΔV of 300 mV.

Although the reduction and oxidation peaks in the device occur at lower potentials than those of the film, the potential difference between them remains constant, a sign of the reliability of electrochemical processes.

3.6. INVESTIGATIONS ON SOLUTION DEGRADATION

Previously in section 2.5.3.3 a degradation phenomenon of the all-in one-film solution was observed, evidenced by the colour change from blue/purple to red. It has been verified that due to this transformation the solution loses its electrochromic behaviour. During the research activity it was considered appropriate to investigate the cause of the problem, to find a way to avoid, or delay, this degradative phenomenon.

Since the degradation is connected with a change of colour, attention has been focused on the electrochromes and their stability in solution.

The polyviologen P-*p*XV-Br₂, obtained as a yellow powder (Fig. 71a), is soluble only in water; the resulting aqueous solution is stable, clear and slightly yellowish if the amount of dissolved polymer is considerable (Fig. 71b).

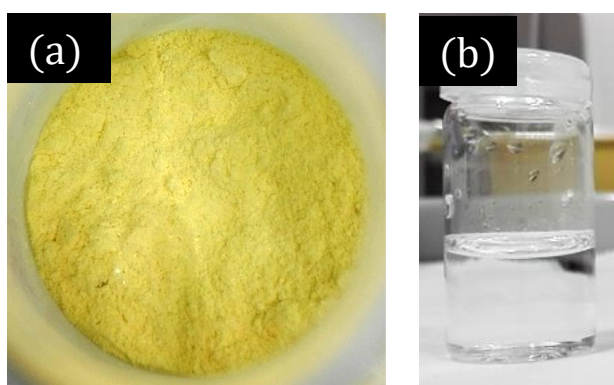


Figure 71 – Polyviologen in solid state (a) and in aqueous solution (b).

TMPD, on the other hand, occurs as flakes powder, coloured off-white to brown (Fig. 72a); it is soluble in both water and ethanol and the resulting solutions are stable but deep blue or yellow, respectively (Fig. 72b,c).

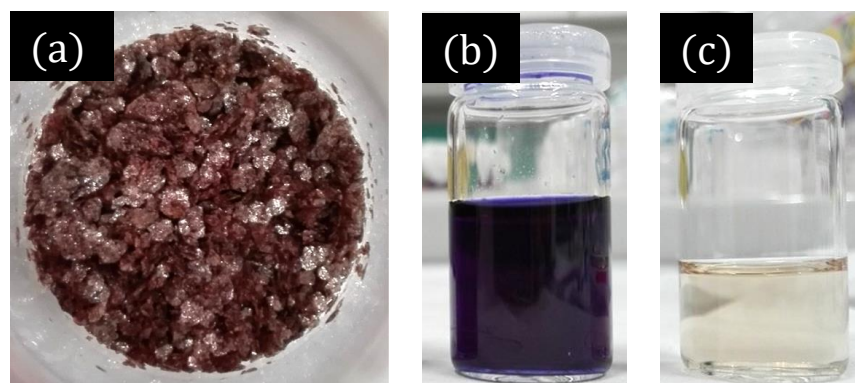


Figure 72 – TMPD in solid state (a), in aqueous solution (b) and in ethanol (c).

By mixing the aqueous solution of polyviologen and the ethanolic (or aqueous) solution of TMPD, a gradual change of colour is observed which leads from blue to purple, to red in just four hours (Fig. 73).

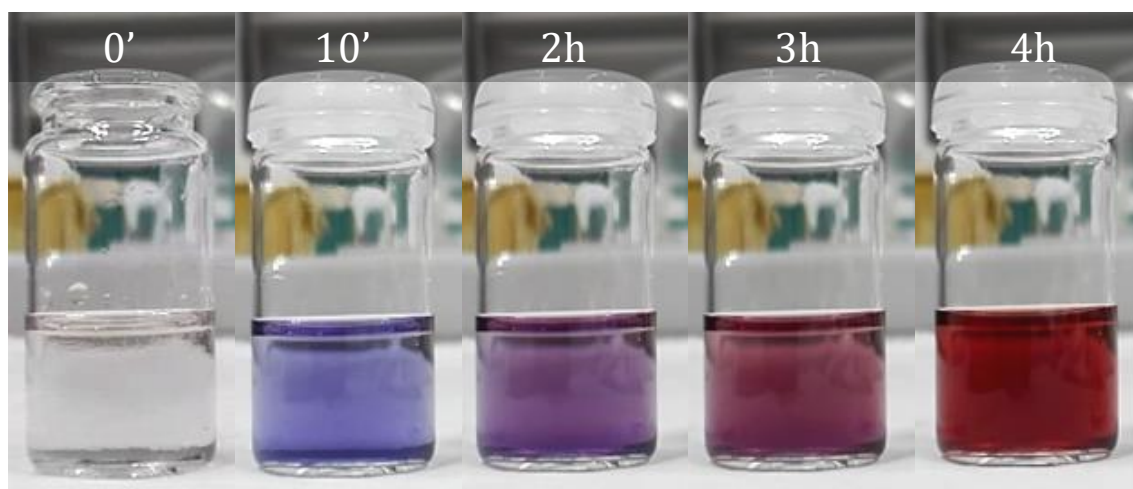


Figure 73 – Colour change of the mixture solution containing polyviologen and TMPD.

The spectroscopic analyzes carried out (Fig. 74) attribute the colour change of the solution to a decrease in the absorption bands at 560 and 620 nm and the simultaneous appearance of a band at 460 nm.

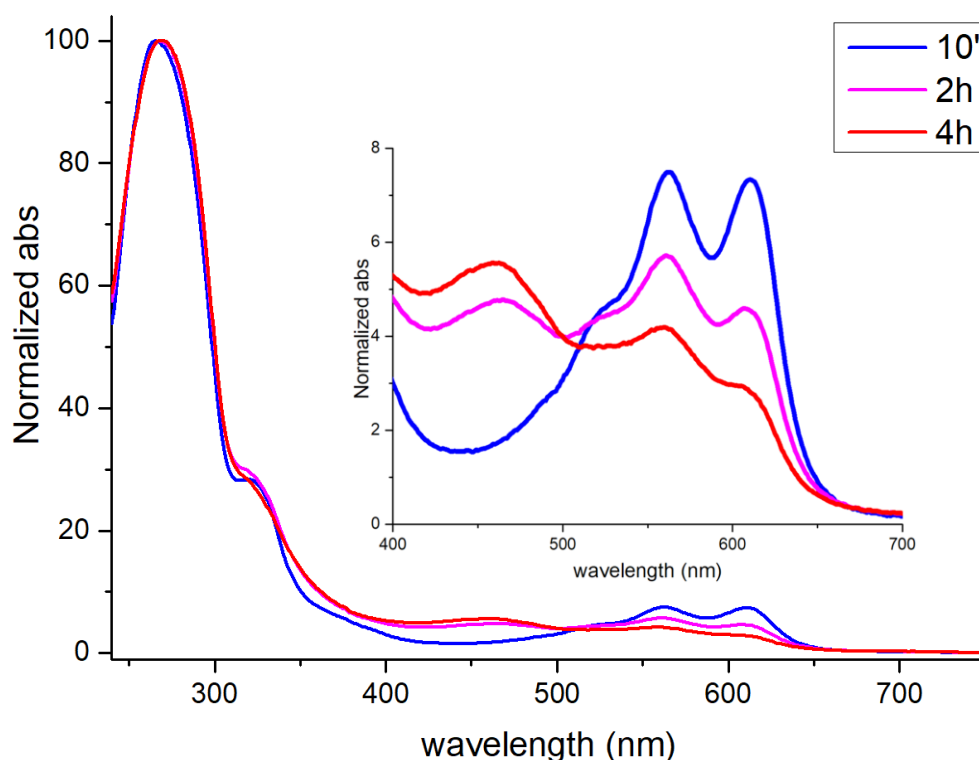


Figure 74 – Absorption spectra of the solution during different steps of the colour change. In inset: Magnification of the range 400-700 nm.

For comparison, the absorption spectra of each electrochromic species were acquired and plotted together (Fig. 75). By observing the spectra, the common

absorption band at 320 nm is observed with the exception of the polyviologen. One might think that TMPD is the main protagonist of the degradative phenomenon, but it must be remembered that this occurs only in the presence of polyviologen.

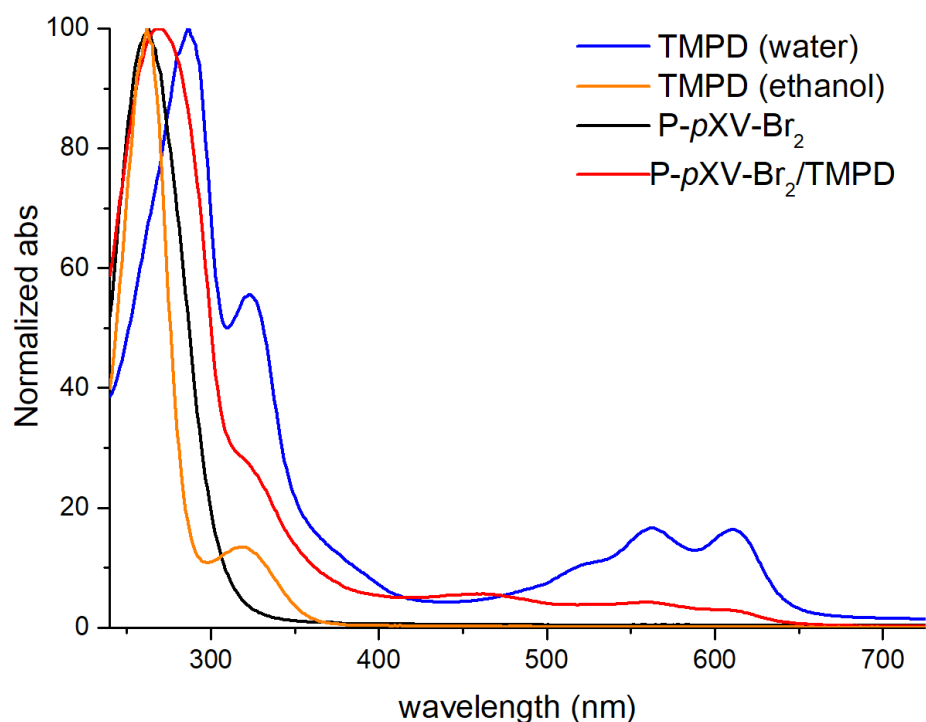


Figure 75 – Comparison between the absorption spectra of electrochrome solutions and that of the mixture solution.

In the attempt to obtain additional information, the three solutions containing TMPD, polyviologen and the red one were deposited and left to dry, to be observed under a polarized light microscope (Fig. 76).

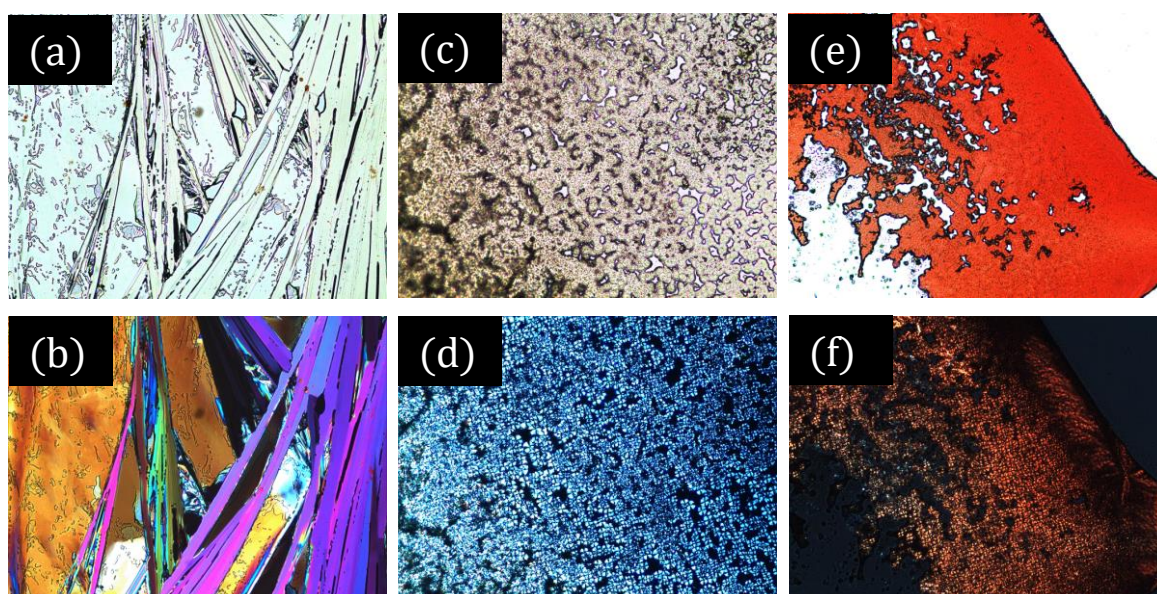


Figure 76 – Optical microscope images of TMPD, polyviologen and red product in non-polarized light (a), (c), (e) and in polarized light (b), (d), (f).

Contrary to the spectroscopic analyzes, the microscopic ones suggest a greater similarity of the product obtained with the polyviologen rather than with the TMPD. By heating the samples to the melting point of the TMPD and above ($T > 51\text{ }^{\circ}\text{C}$) the transition to the liquid phase in the sample under study is not observed; this clearly indicates the absence of free TMPD and suggests an interaction between the two electrochromes.

Further investigation was possible, isolating the solute from the solution by precipitation and filtration. The product obtained in the form of red powder was compared with the two electrochromes in solid state, by means of thermogravimetric analysis (Fig. 77). All data were collected from $25\text{ }^{\circ}\text{C}$ to $500\text{ }^{\circ}\text{C}$ with a scan rate of $5\text{ }^{\circ}\text{C}/\text{min}$.

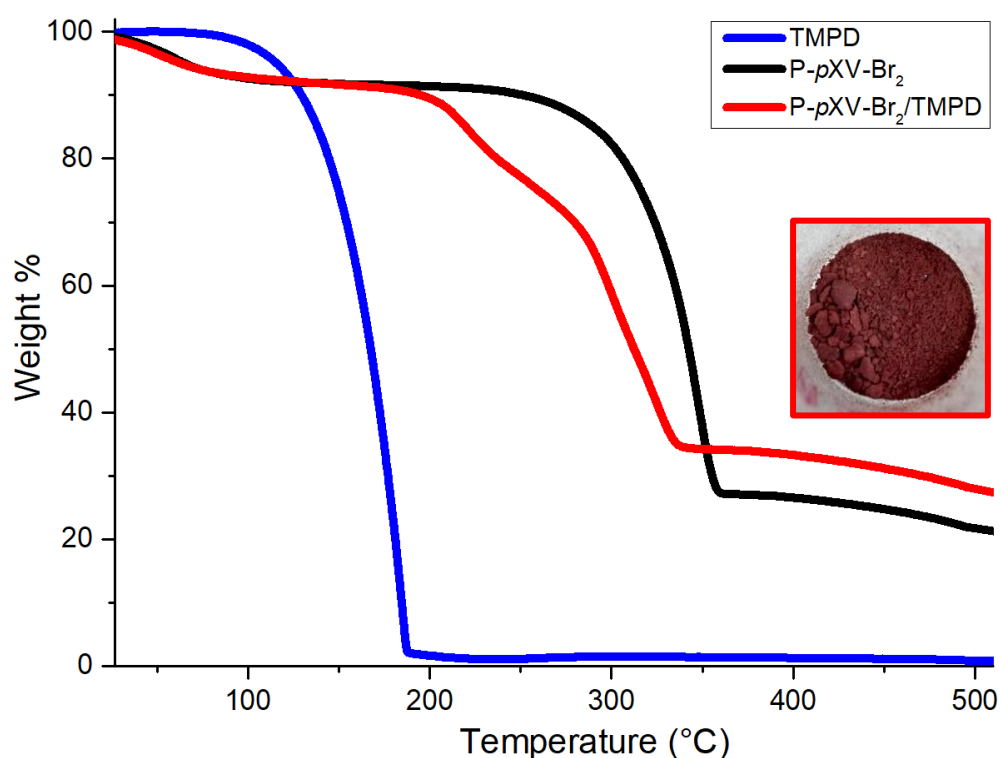


Figure 77– Thermogravimetric profiles of TMPD (blue line), P-pXV-Br₂ (black line) and red powder (red line). In inset: photograph of the red powder to be investigated.

As the temperature increases for the TMPD sample, a mass loss of 98% is observed in the range $90\text{--}190\text{ }^{\circ}\text{C}$; in this range there is no mass loss in the P-pXVBr₂/TMPD mixture, further confirming the absence of pure TMPD in the red powder.

Both polyviologen and red powder have a weight loss of 7% around 80 °C, which can be explained by the desorption of water from the two hygroscopic powders.

At higher temperatures the polyviologen loses 63% of the mass in the range 245-370 °C in a single step and at a temperature of 500 °C it has a residual mass equal to 20% of the initial mass.

The red powder behaves differently, with a mass loss of 57% between 175 °C and 345 °C through a multi-step decomposition process; at a temperature of 500 °C the residual mass is 26%.

From the various analyzes carried out, it seems plausible that the solution degradation is due to a strong and irreversible interaction between the electrochromes. Unfortunately, contrary to what others have hypothesized⁴⁸, in this specific case, the interaction between anodic and cathodic species does not seem to favor electron-transfer and undoubtedly cancels electrochromic activity.

It is beyond our purpose to determine what type of interaction is established between electrochromic species; on the contrary, it was considered appropriate to decide how to counteract the loss of the electrochromic properties of the all-in-one film-forming solution.

Since the interaction occurs spontaneously and is therefore thermodynamically favoured, lowering its degradation kinetics is a possible remedy.

Although in the film-forming solution the interaction kinetics are lower due to the high presence of other species, storing it at -15 °C is recommended to increase its duration. After the deposition and drying of the film, the two electrochromes are blocked and spaced apart thanks to the biopolymer matrix and their degradative interaction is inhibited.

3.7. INSTRUMENTS

- A Digimess HY3003-2 was used as DC power supply with double output.
- Optical microscopy observations were performed with a Leica DMLP polarizing microscope equipped with a Leica DFC290 camera and a CalCTec heating stage.
- Photophysical characterizations of the samples were performed at room temperature using spectrofluorimetric grade solvents. Absorption spectra were recorded with a Perkin–Elmer Lambda 900 spectrophotometer.
- Size and morphology of the copper nanowires were measured using a transmission electron microscope (Jeol JEM-1400 Plus 120 kV). The samples for transmission electron microscopy (TEM) were prepared by depositing a drop of a diluted solution on 300 mesh copper grids. After evaporation of the solvent in air at room temperature, the particles were observed at an operating voltage of 80 kV.
- Electronic measurements were collected through PicoScope 4262 oscilloscope, 2x 5MHz, 10MSPS, Pico Technology.
- Electrochemical measurements were performed with an Autolab Potentiostat-Galvanostat controlled by the NOVA 1.1 software. A conventional 3 ml three-electrode cell was employed, with a Pt wire as counter-electrode, an Ag wire as pseudoreference electrode and a ITO/glass slide as working electrode. NBu_4PF_6 (0.1 M) was used as supporting electrolyte and experiments were performed in a dry, and degassed (Ar) dichloromethane solution.
- TGA analysis was performed on a Perkin Elmer Pyris 6 Thermogravimetric Analyzer. Approximately 3 mg of each sample was placed in an alumina crucible and heated from 25 °C to 500 °C, at a heating rate of 5 °C/min.

3.8. COST ANALYSIS

In this chapter, through tests and observations, the amounts of the species to be used to produce the all-in-one film-forming solution have been optimized. The assembly method has been described in detail and the optimal volume of film-forming solution to be deposited to create the electrochromic device our purpose has been calibrated. Its properties have been characterized through different analyses, demonstrating the validity of the developed device.

In this last section, with a view to industrial scalability, it is considered appropriate to evaluate the production costs of our device.

We start by reporting the retail prices of all the reagents and solvents used, adjusting the costs with the amounts used for the production of polyviologen P-*p*XV-Br₂ (Table 4) and the ethanolic suspension of CuNWs (Table 5).

Polyviologen synthesis				
Reagents or solvents	Pack size [g] or [ml]	Price €	Used amount [g] or [ml]	Price €
4,4' bipyridine	10	52.20	0.300	1.57
Dibromo-p-xylene	25	63.50	0.507	1.29
Acetonitrile	100	79.00	40	31.60
Product				
P- <i>p</i> XV-Br ₂	0.621	34.45		

Table4- Production costs of the polyviologen.

CuNWs synthesis				
Reagents or solvents	Pack size [g] or [ml]	Price €	Used amount [g] or [ml]	Price €
EtOH	1000	117.00	10	1.17
CuCl ₂ ·H ₂ O	100	36.00	0.063	0.02
Glucose	25	12.70	0.15	0.08
HDA	100	21.60	0.54	0.12
CHCl ₃	1000	107.00	5	0.53
Product				
CuNWs dispersion	10	1.92		

Table5- Production costs of the copper nanowires dispersion.

The same approach applies to estimate the costs of preparing the all-in-one film-forming solution (Table 6).

All-in-one film-forming solution (FFS)				
<i>Aqueous solution</i>				
Reagents or solvents	Pack size [g] or [ml]	Price €	Used amount [g] or [ml]	Price €
P- <i>p</i> XV-Br ₂	0.621	34.45	0.05	2.77
LiBr	100	53.60	0.05	0.03
Acetic acid	1000	55.80	0.24	0.01
Chitosan	100	96.00	0.30	0.29
<i>Organic solution</i>				
Reagents or solvents	Pack size [g] or [ml]	Price €	Used amount [g] or [ml]	Price €
EtOH	1000	117.00	23	2.69
CuNWs dispersion	10	1.92	0.2	0.04
Glycerol	100	53.90	0.44	0.24
TMPD	5	38.50	0,01	0.08
DMSO	1000	222.00	3.3	0.73
Product				
FFS	40	6.88		

Table 6– Production costs of the all-in-one film-forming solution.

For the assembly of the device, the cost of flat, transparent ITO/PET electrodes must be taken into account; thus the laboratory device having an area of 12.5 cm² is determined and proportionally it is possible to calculate the cost of a much larger device having an area of 1 m² (Table 7).

Device assembly				
<i>Laboratory device</i>				
Component	Pack size [cm ²] or [ml]	Price €	Used amount [cm ²] or [ml]	Price €
ITO/PET (1 sheet)	930.25	22.40	25	0.60
FFS	40	6.88	0.8	0.14
Product				
Device (12,5 cm ²)	12.5	0.74		
<i>Industry device</i>				
Component	Pack size [cm ²] or [ml]	Price €	Used amount [cm ²] or [ml]	Price €
ITO/PET (21,5 sheet)	20000	481.59	20000	481.59
FFS	40	6.88	640	110.05
Product				
Device (1 m ²)	10000	591.65		

Table 7– Production costs of the electrochromic devices of different sizes.

Before starting the discussion on costs it is necessary to specify that those attributed to substances are retail prices; the purchase of a large quantity of materials certainly lowers their cost.

On the other hand, the tables do not show the cost of the energy necessary for the production instruments to work; certainly having discarded procedures using high temperatures or long syntheses reduces this economic impact.

Therefore, the costs shown are not to be considered absolute, but are a first useful indication for a possible industrial development.

From reading the tables, one can immediately observe the cheapness of the raw reagents used; on the contrary, the cost of the electrodes appears high and preponderant in determining the final cost of the device.

Taking into consideration the 1 m² device, which costs € 591.65, it cannot be ignored that € 481.59 come from the electrodes. With a weight equal to 81.4% of the final cost, it is clear that research on alternative electrodes is necessary to reduce production costs.

Furthermore, finding an alternative to ITO/PET sheets could lead to much more flexible electrodes, on which our electrochromic film could be deposited, allowing for new applications in various industrial sectors.

With these considerations this chapter ends. The final chapter will follow, in which the properties of our electrochromic device will be summarized and the results achieved will be compared with our initial purpose.

4. CONCLUSIONS

The research activity was focused on the design and development of an electrochromic device having the characteristics predetermined in section 1.1.

Understanding how to develop a single solution starting from species with different solubilities was a difficult challenge but successfully overcome.

A very important activity was to correctly choose each material to be used, to give the device a specific characteristic, without compromising another.

At the end of this experimental path and with the device produced and characterized, it appears important to return to the portion of section 1.1, in which the properties to be given to the device under development were listed, in order to verify its achievement.

- **Transparency** - the device in OFF mode has a transparency of 50%; considering that the two ITO/PET electrodes alone have a $T\% = 66\%$, it follows that the film produced absorbs only 16% of the incident radiation. Although it may seem a rather high value, observing the acquired photographs, the entire device appears transparent to the naked eye and this can be considered an excellent result.
- **Good optical contrast** - between the OFF and ON modes of the device, the absolute value of the percentage transmittance is lowered from 50% to 29%, averaged over the entire visible range. However, if we consider the loss of transparency of the device between the OFF and ON modes, we have an optical contrast $\Delta T\% = 43\%$, very visible to the naked eye.
- **Low working voltage** - by means of electronic measurements, a working potential window was estimated to be within 0.6-1.3 V; this value and the low measured operating current intensity, below 2 mA, characterize the low-energy device.
- **Fast and reversible switching** - our ECD switches between OFF and ON modes reversibly and quickly, with coloring time $\tau_{col} = 15$ s and bleaching time $\tau_{bleach} = 30$ s.

- **Thinness** - through graphic measurements on SEM images and by means of a micrometer, a thickness of the device of 350 μm was estimated, of which $67 \pm 20 \mu\text{m}$ consist of the film.
- **Flexibility** – thanks to the use of glycerol plasticizing agent for chitosan, the film produced has a high flexibility, greater than that possessed by the ITO/PET electrode.
- **Scalability** -the synthesis and deposition methods of the film have been carefully selected in order to easily adapt to the industrial application. While not using depositor instrumentation in the laboratory, the use of the doctor blade for the industrial scale is envisaged.
- **Produced with safe solvents** - the main solvents used are water and ethanol; the latter can potentially be replaced with another cheaper alcohol.
- **Processed in a few steps** - The syntheses of polyviologen and CuNWs take place in a single step; the preparation of the film-forming all-in-one solution takes place by mixing two solutions both prepared in a few minutes. There are no long deposition and assembly times and they can be further reduced by using the correct instrumentation.
- **Low total production cost** - the total cost for a 1 m^2 device is approximately € 591; the solution impacts only 18.6% of the total cost, therefore finding new electrodes is the key to greatly reduce the cost of the device.
- **Mild process conditions** - All syntheses take place at room temperature or in any case always below 100 °C; no strong acids or bases are used nor highly dangerous substances.
- **Environmentally friendly** - Most of the mass of the electrochromic film has an electrolytic matrix based on chitosan and glycerol, two natural molecules readily available. The solvents used are little or non-polluting and the syntheses do not require a high amount of energy. Our electrochromic device can be easily powered by renewable sources, being low in energy consumption and powered by direct current.

- **Self-sealing** - This property, not unintentionally conferred, has been observed and is an added value for the device.

As just described, the electrochromic device developed satisfies all the requirements of our purpose; its properties are summarized in table 8.

Properties	Values	
Switch potential	$\Delta V =$	0.60 V
Colouring time	$\tau_{col} =$	15 s
Bleaching time	$\tau_{bleach} =$	30 s
Working potential window	$\Delta V =$	0.6 - 1.3 V
Operating current intensity	$I =$	0.8 - 1.8 mA
Device thickness	$h_D =$	350 μm
Film thickness	$h_f =$	$67 \pm 20 \mu\text{m}$
Percentage transmittance (OFF mode)	$T_{OFF}\% =$	50%
Percentage transmittance (ON mode)	$T_{ON}\% =$	29%
Absolute optical contrast	$\Delta T\% =$	21%
Device optical contrast	$(\Delta T\%)_{OFF/ON} =$	43%
Tested reversibility	Cycles \geq	50
Others	Flexibility	
	Self-sealing	

Table 8- Data sheet of the developed electrochromic device.

Other analyzes and measurements of the device can further enrich the technical data of the same and quantify its effective duration.

One thing worth noting is that the approach suggested in this work can be used with very different species; for example, a laboratory device having an ethylcellulose matrix and emeraldine as an electrochrome has been successfully developed from chloroform.

If the development through manual procedures may have brought some defects to the device, on the other hand it means that producing the same in an automated way can only improve its properties and performances.

The transposition to production on a larger surface was not possible due to the lack of availability of suitable instrumentation such as a doctor blade coater.

The problems that could be encountered in this phase can be many; they will be discussed below and for some of them possible solutions are proposed.

First of all, it is necessary to find the right distance between the electrode to be coated and the depositor knife, so that the amount of film-forming solution poured is the one established in this work.

It may be necessary to modify the viscosity of the film-forming solution; in this case, the volumes of water and ethanol used could be slightly increased or decreased.

Having a large surface area could hinder the transmission of electrons between the two electrodes; in this case the device could be surrounded with copper tape in order to better distribute the applied potential along its entire frame.

Also preparing a solution with a higher concentration of copper nanowires and using it as a grid-like printed circuit on the electrode area, could be a good idea. A 3D printer might be suitable for this purpose.

Starting from this idea, one could try to develop cheaper and more flexible electrodes than ITO/PET in order to increase the potential applications of the device and significantly reduce its cost.

Self-sealing of the film may not be sufficient to keep a large device perfectly sealed; if so, UV cured resins could be used as sealants. Alternatively, one could investigate and evaluate the use of sodium hyaluronate which, as others demonstrate¹⁶⁶, improves the self-sealing and elasticity of chitosan-based films.

Finally, the power supply of our device could derive from green energy, for example from small photovoltaic panels, therefore an adequate circuit must be developed to allow it to work; moreover, it will possible to automate its activation through an input/output system triggered by ambient light sensors and regulated by an Arduino-type board.

5. REFERENCES

- 1 P. M. S. Monk, R. J. Mortimer and D. R. Rosseinsky, *Electrochromism and electrochromic devices*, Cambridge University Press, 2007.
- 2 A. Rouger, D. Rauh and G.-A. Nazri, *Electrochromic Materials and Applications*, The Electrochemical Society, Inc., 2003.
- 3 C.-G. Granqvist, *Nat. Mater.* 2006 52, 2006, **5**, 89–90.
- 4 C. Pozo-Gonzalo, M. Salsamendi, A. Viñuales, J. A. Pomposo and H. J. Grande, *Sol. Energy Mater. Sol. Cells*, 2009, **93**, 2093–2097.
- 5 H. J. Byker, *Electrochim. Acta*, 2001, **46**, 2015–2022.
- 6 Y. Alesanco, A. Viñuales, J. Rodriguez and R. Tena-Zaera, *Materials (Basel)*, 2018, **11**, 1–27.
- 7 A. Way, J. Luke, A. D. Evans, Z. Li, J.-S. Kim, J. R. Durrant, H. K. H. Lee and W. C. Tsoi, *AIP Adv.*, 2019, **9**, 085220.
- 8 M. Girtan, *Sol. Energy Mater. Sol. Cells*, 2012, **100**, 153–161.
- 9 G. Torrisi, E. Cavaliere, F. Banfi, G. Benetti, R. Raciti, L. Gavioli and A. Terrasi, *Sol. Energy Mater. Sol. Cells*, 2019, **199**, 114–121.
- 10 K. hee Pyo and J. W. Kim, *Compos. Sci. Technol.*, 2016, **133**, 7–14.
- 11 W. Huang, J. Li, S. Zhao, F. Han, G. Zhang, R. Sun and C. P. Wong, *Compos. Sci. Technol.*, 2017, **146**, 169–176.
- 12 W. Hu, R. Wang, Y. Lu and Q. Pei, *J. Mater. Chem. C*, 2014, **2**, 1298–1305.
- 13 T. W. Lee and H. H. Park, *Compos. Sci. Technol.*, 2015, **114**, 11–16.
- 14 M. Zu, Q. Li, G. Wang, J.-H. Byun and T.-W. Chou, *Adv. Funct. Mater.*, 2013, **23**, 789–793.
- 15 Z. Chen, W. Ren, L. Gao, B. Liu, S. Pei and H.-M. Cheng, *Nat. Mater.*, 2011, **10**, 424–428.
- 16 J. Y. Oh, S. Kim, H.-K. Baik and U. Jeong, *Adv. Mater.*, 2016, **28**, 4455–4461.
- 17 J. R. Platt, *J. Chem. Phys.*, 1961, **34**, 862–863.
- 18 P. M. S. Monk, R. J. Mortimer and D. R. Rosseinsky, *Electrochromism*, Wiley, 1995.
- 19 I. F. Chang, B. L. Gilbert and T. I. Sun, *J. Electrochem. Soc.*, 1975, **122**, 955–962.
- 20 J. W. Xu, M. H. Chua and K. W. Shah, *Electrochromic Smart Materials*, The Royal Society of Chemistry, 2019.

- 21 F. Carpi and D. De Rossi, *Opt. Laser Technol.*, 2006, **38**, 292–305.
- 22 P. R. Somani and S. Radhakrishnan, *Mater. Chem. Phys.*, 2003, **77**, 117–133.
- 23 G. C. S. Collins and D. J. Schiffrin, *J. Electroanal. Chem. Interfacial Electrochem.*, 1982, **139**, 335–369.
- 24 J. Zhang, F. Lu, H. Huang, J. Wang, H. Yu, J. Jiang, D. Yan and Z. Wang, *Synth. Met.*, 2005, **148**, 123–126.
- 25 S. Wang, X. Li, S. Xun, X. Wan and Z. Y. Wang, *Macromolecules*, 2006, **39**, 7502–7507.
- 26 D. M. De Leeuw, M. M. J. Simenon, A. R. Brown and R. E. F. Einerhand, *Synth. Met.*, 1997, **87**, 53–59.
- 27 R. H. Friend, R. W. Gymer, A. B. Holmes, J. H. Burroughes, R. N. Marks, C. Taliani, D. D. C. Bradley, D. A. Dos Santos, J. L. Brédas, M. Lögdlund and W. R. Salaneck, *Nature*, 1999, 397, 121–128.
- 28 F. P. Byrne, S. Jin, G. Paggiola, T. H. M. Petchey, J. H. Clark, T. J. Farmer, A. J. Hunt, C. R. Mcelroy, J. Sherwood, C. Robert McElroy and J. Sherwood, *Sustain. Chem. Process.*, 2016, **4**, 1–24.
- 29 T. A. Welsh and E. R. Draper, *RSC Adv.*, 2021, **11**, 5245–5264.
- 30 L. Michaelis and E. S. Hill, *J. Gen. Physiol.*, 1933, **16**, 859–873.
- 31 R. J. Mortimer, D. R. Rosseinsky and P. M. S. Monk, *Electrochromic materials and devices*, John Wiley & Sons, 2015.
- 32 D. R. Rosseinsky and P. M. S. Monk, *J. Chem. Soc. Faraday Trans.*, 1994, **90**, 1127–1131.
- 33 J. G. Carey, J. F. Cairns and J. E. Colchester, *J. Chem. Soc. D Chem. Commun.*, 1969, 1280–1281.
- 34 H. T. van Dam and J. J. Ponjeé, *J. Electrochem. Soc.*, 1974, **121**, 1555.
- 35 R. J. Jasinski, *J. Electrochem. Soc.*, 1977, **124**, 637–641.
- 36 R. G. Compton, A. M. Waller, P. M. S. Monk and D. R. Rosseinsky, *J. Chem. Soc. Faraday Trans.*, 1990, **86**, 2583–2586.
- 37 N. S. Sariciftci, M. Mehring and H. Neugebauer, *Synth. Met.*, 1991, **43**, 2971–2974.
- 38 H. Kamogawa and T. Suzuki, *J. Chem. Soc. Chem. Commun.*, 1985, 525–526.
- 39 M. Tagliazucchi, D. B. Tice, C. M. Sweeney, A. J. Morris-Cohen and E. A. Weiss, *ACS Nano*, 2011, **5**, 9907–9917.
- 40 D. Dervishogullari, E. A. Gizzie, G. K. Jennings and D. E. Cliffler, *Langmuir*, 2018, **34**, 15658–15664.

- 41 A. Factor and G. E. Heinsohn, *J Polym Sci Part B Polym Lett*, 1971, **9**, 289–295.
- 42 K. C. Ho, Y. W. Fang, Y. C. Hsu and L. C. Chen, *Solid State Ionics*, 2003, **165**, 279–287.
- 43 P. M. S. Monk, R. D. Fairweather, M. D. Ingram and J. A. Duffy, *J. Chem. Soc. Perkin Trans. 2*, 1992, 2039–2041.
- 44 N. J. Goddard, A. C. Jackson and M. G. Thomas, *J. Electroanal. Chem. Interfacial Electrochem.*, 1983, **159**, 325–335.
- 45 E. M. Kosower, J. L. Cotter Vol, B. M. Edward Kosower, J. L. Cotter, E. M. Kosower and E. J. Poziomek, *J. Am. Chem. Soc.*, 1964, **86**, 5528.
- 46 S. Y. Kao, H. C. Lu, C. W. Kung, H. W. Chen, T. H. Chang and K. C. Ho, *ACS Appl. Mater. Interfaces*, 2016, **8**, 4175–4184.
- 47 K. Ho, T. G. Rukavina and C. B. Greenberg, *J. Electrochem. Soc.*, 1994, **141**, 2061–2067.
- 48 G. Chidichimo, M. De Benedittis, J. Lanzo, B. C. De Simone, D. Imbardelli, B. Gabriele, L. Veltri and G. Salerno, *Chem. Mater.*, 2007, **19**, 353–358.
- 49 J. E. Dubois, A. Desbene-Monvernay and P. C. Lacaze, *J. Electroanal. Chem. Interfacial Electrochem.*, 1982, **132**, 177–190.
- 50 A. Desbène-Monvernay, P. C. Lacaze and A. Cherigui, *J. Electroanal. Chem. Interfacial Electrochem.*, 1989, **260**, 75–90.
- 51 A. Yasuda and J. Seto, *J. Electroanal. Chem. Interfacial Electrochem.*, 1991, **303**, 161–169.
- 52 L. Michaelis, M. P. Schubert and S. Granick, *J. Am. Chem. Soc.*, 1939, **61**, 1981–1992.
- 53 L. L. Wu, J. Luo and Z. H. Lin, *J. Electroanal. Chem.*, 1996, **417**, 53–58.
- 54 S. Y. Kao, Y. Kawahara, S. Nakatsuji and K. C. Ho, *J. Mater. Chem. C*, 2015, **3**, 3266–3272.
- 55 A. Rougier, D. Rauh and G. Nazri, *Electrochromic materials and applications : proceedings of the international symposium*, Electrochemical Society, 2003.
- 56 L. Michaelis, *J. Am. Chem. Soc.*, 1931, **53**, 2953–2962.
- 57 P. Barbosa, L. Rodrigues, M. Silva, M. Smith, A. Gonçalves and E. Fortunato, *J. Mater. Chem.*, 2010, **20**, 723–730.
- 58 K. R. Jeffrey, G. Z. Zukowska and J. R. Stevens, *J. Chem. Phys.*, 2003, **119**, 2422.
- 59 L. Su, H. Wang and Z. Lu, *Supramol. Sci.*, 1998, **5**, 657–659.
- 60 N. Xin, Y. Sun, M. He, C. J. Radke and J. M. Prausnitz, *Fluid Phase Equilib.*,

- 2018, **461**, 1–7.
- 61 X. Z. Yuan, S. Zhang, J. C. Sun and H. Wang, *J. Power Sources*, 2011, **196**, 9097–9106.
- 62 P. Y. Pennarun, P. Jannasch, S. Papaefthimiou, N. Skarpenzoz and P. Yianoulis, *Thin Solid Films*, 2006, **514**, 258–266.
- 63 N. A. Choudhury, S. Sampath and A. K. Shukla, *Energy Environ. Sci.*, 2008, **2**, 55–67.
- 64 R. C. Agrawal and G. P. Pandey, *J. Phys. D. Appl. Phys.*, 2008, **41**, 223001.
- 65 R. Meziane, J. P. Bonnet, M. Courty, K. Djellab and M. Armand, *Electrochim. Acta*, 2011, **57**, 14–19.
- 66 A. M. Stephan and K. S. Nahm, *Polymer (Guildf.)*, 2006, **47**, 5952–5964.
- 67 A. Gonçalves, C. Costa, S. Pereira, N. Correia, M. M. Silva, P. C. Barbosa, L. C. Rodrigues, I. Henriques, R. Martins and E. Fortunato, *Polym. Adv. Technol.*, 2012, **23**, 791–795.
- 68 T. Winie, A. K. Arof and S. Thomas, *Polymer electrolytes: Characterization techniques and energy applications*, Wiley, 2019.
- 69 D. E. Fenton, J. M. Parker and P. V. Wright, *Polymer (Guildf.)*, 1973, **14**, 589.
- 70 S. Ramesh and S.-C. Lu, *J. Appl. Polym. Sci.*, 2012, **126**, E484–E492.
- 71 H. J. Rhoo, H. T. Kim, J. K. Park and T. S. Hwang, *Electrochim. Acta*, 1997, **42**, 1571–1579.
- 72 F. Croce, L. L. Persi, B. Scrosati, F. Serraino-Fiory, E. Plichta and M. A. Hendrickson, *Electrochim. Acta*, 2001, **46**, 2457–2461.
- 73 C. O. Dasenbrock, T. H. Ridgway, C. J. Seliskar and W. R. Heineman, *Electrochim. Acta*, 1998, **43**, 3497–3502.
- 74 Y. Lu, D. Wang, T. Li, X. Zhao, Y. Cao, H. Yang and Y. Y. Duan, *Biomaterials*, 2009, **30**, 4143–4151.
- 75 S. Y. Lin, C. M. Wang, P. T. Hsieh, Y. C. Chen, C. C. Liu and S. C. Shih, *Colloid Polym. Sci.*, 2009, **287**, 1355–1358.
- 76 Z. Osman and A. K. Arof, *Electrochim. Acta*, 2003, **48**, 993–999.
- 77 K. H. Teoh, S. Ramesh and A. K. Arof, *J. Solid State Electrochem.*, 2012, **16**, 3165–3170.
- 78 M. H. Khanmirzaei and S. Ramesh, *Int. J. Electrochem. Sci.*, 2013, **8**, 9977–9991.
- 79 V. Thangadurai and W. Weppner, *J. Power Sources*, 2005, **142**, 339–344.

- 80 V. K. Thakur, G. Ding, J. Ma, P. S. Lee and X. Lu, *Adv. Mater.*, 2012, **24**, 4071–4096.
- 81 A. J. C. Da Silva, F. A. Ribeiro Nogueira, J. Tonholo and A. S. Ribeiro, *Sol. Energy Mater. Sol. Cells*, 2011, **95**, 2255–2259.
- 82 M. Pan, S. Zhao, L. Ma, N. Wu and D. Xiao, *Sol. Energy Mater. Sol. Cells*, 2019, **189**, 27–32.
- 83 H. El Knidri, R. Belaabed, A. Addaou, A. Laajeb and A. Lahsini, *Int. J. Biol. Macromol.*, 2018, **120**, 1181–1189.
- 84 J. Kumirska, M. Czerwicka, Z. Kaczyński, A. Bychowska, K. Brzozowski, J. Thöming and P. Stepnowski, *Mar. Drugs* 2010, Vol. 8, Pages 1567-1636, 2010, **8**, 1567–1636.
- 85 S. Gopi, S. Thomas and A. Pius, *Handbook of Chitin and Chitosan: Composites and Nanocomposites from Chitin and Chitosan, Manufacturing and Characterizations*, Elsevier, 2020, vol. 2.
- 86 W. G. Birolli, J. A. D. M. Delezuk and S. P. Campana-Filho, *Appl. Acoust.*, 2016, **103**, 239–242.
- 87 H. Hattori, H. Tsujimoto, K. Hase and M. Ishihara, *Carbohydr. Polym.*, 2017, **175**, 592–600.
- 88 A. Sabir, F. Altaf and M. Shafiq, in *Sustainable Polymer Composites and Nanocomposites*, Springer International Publishing, Cham, 2019, pp. 1365–1405.
- 89 D. Golodnitsky, E. Strauss, E. Peled and S. Greenbaum, *J. Electrochem. Soc.*, 2015, **162**, A2551.
- 90 Z. Osman, Z. A. Ibrahim and A. K. Arof, *Carbohydr. Polym.*, 2001, **44**, 167–173.
- 91 W. H. Meyer, *Adv. Mater.*, 1998, **10**, 439–448.
- 92 P. V. Wright, *Electrochim. Acta*, 1998, **43**, 1137–1143.
- 93 R. Alves, F. Sentanin, R. C. Sabadini, A. Pawlicka and M. M. Silva, *Electrochim. Acta*, 2016, **217**, 108–116.
- 94 J. Cho, M. C. Heuzey, A. Bégin and P. J. Carreau, *J. Food Eng.*, 2006, **74**, 500–515.
- 95 C. N. Costa, V. G. Teixeira, M. C. Delpech, J. V. S. Souza and M. A. S. Costa, *Carbohydr. Polym.*, 2015, **133**, 245–250.
- 96 J. F. Fundo, A. C. Galvis-Sanchez, I. Delgadillo, C. L. M. Silva and M. A. C. Quintas, *Food Biophys.*, 2015, **10**, 324–333.
- 97 N. E. Suyatma, L. Tighzert, A. Copinet and V. Coma, *J. Agric. Food Chem.*, 2005, **53**, 3950–3957.

- 98 M. Z. A. Yahya and A. K. Arof, *Eur. Polym. J.*, 2003, **39**, 897–902.
- 99 V. Epure, M. Griffon, E. Pollet and L. Avérous, *Carbohydr. Polym.*, 2011, **83**, 947–952.
- 100 M. E. Castelló, P. S. Anbinder, J. I. Amalvy and P. J. Peruzzo, *MRS Adv.*, 2018, **3**, 3601–3610.
- 101 J. F. Fundo, R. Fernandes, P. M. Almeida, A. Carvalho, G. Feio, C. L. M. Silva and M. A. C. Quintas, *Food Chem.*, 2014, **144**, 2–8.
- 102 M. V. Debandi, C. Bernal and N. J. Francois, *J. Tissue Sci. Eng.*, 2016, **7**, 1–9.
- 103 Y. N. Sudhakar and M. Selvakumar, *Electrochim. Acta*, 2012, **78**, 398–405.
- 104 M. Vlachá, A. Giannakas, P. Katapodis, H. Stamatis, A. Ladavos and N. M. Barkoula, *Food Hydrocoll.*, 2016, **57**, 10–19.
- 105 M. Chen, T. Runge, L. Wang, R. Li, J. Feng, X. L. Shu and Q. S. Shi, *Carbohydr. Polym.*, 2018, **200**, 115–121.
- 106 X. Ma, M. Lv, D. P. Anderson and P. R. Chang, *Food Hydrocoll.*, 2017, **66**, 276–285.
- 107 K. Lei, X. Wang, X. Li and L. Wang, *Colloids Surfaces B Biointerfaces*, 2019, **175**, 688–696.
- 108 S. Prateepchanachai, W. Thakhiew, S. Devahastin and S. Soponronnarit, *Carbohydr. Polym.*, 2017, **174**, 253–261.
- 109 M. J. Hostetler, J. E. Wingate, C. J. Zhong, J. E. Harris, R. W. Vachet, M. R. Clark, J. D. Londono, S. J. Green, J. J. Stokes, G. D. Wignall, G. L. Glish, M. D. Porter, N. D. Evans and R. W. Murray, *Langmuir*, 1998, **14**, 17–30.
- 110 J. Deng, M. Gu and J. Di, *Appl. Surf. Sci.*, 2011, **257**, 5903–5907.
- 111 T. He, Y. Ma, Y. Cao, W. Yang and J. Yao, *J. Electroanal. Chem.*, 2001, **514**, 129–132.
- 112 M. A. G. Namboothiry, T. Zimmerman, F. M. Coldren, J. Liu, K. Kim and D. L. Carroll, *Synth. Met.*, 2007, **157**, 580–584.
- 113 *Mineral Commodity Summaries*, U.S. Geological Survey, Reston, VA, 2014.
- 114 M. B. Gawande, A. Goswami, F. X. Felpin, T. Asefa, X. Huang, R. Silva, X. Zou, R. Zboril and R. S. Varma, *Chem. Rev.*, 2016, **116**, 3722–3811.
- 115 P. K. Khanna, S. Gaikwad, P. V. Adhyapak, N. Singh and R. Marimuthu, *Mater. Lett.*, 2007, **61**, 4711–4714.
- 116 P. Liu, H. Wang, X. Li, M. Rui and H. Zeng, *RSC Adv.*, 2015, **5**, 79738–79745.
- 117 A. Umer, S. Naveed, N. Ramzan, M. S. Rafique and M. Imran, *Rev. Mater.*, 2014, **19**, 197–203.

- 118 M. S. Usman, N. A. Ibrahim, K. Shameli, N. Zainuddin and W. M. Z. W. Yunus, *Molecules*, 2012, **17**, 14928–14936.
- 119 K. Jiang, D. Zhao, S. Guo, X. Zhang, X. Zhu, J. Guo, G. Lu and X. Huang, *Sci. Adv.*, 2017, **3**, 1–8.
- 120 N. Zhang, L. Bu, S. Guo, J. Guo and X. Huang, *Nano Lett.*, 2016, **16**, 5037–5043.
- 121 M. J. Kim, M. A. Cruz, F. Yang and B. J. Wiley, *Curr. Opin. Electrochem.*, 2019, **16**, 19–27.
- 122 S. I. Park, Y. J. Quan, S. H. Kim, H. Kim, S. Kim, D. M. Chun, C. S. Lee, M. Taya, W. S. Chu and S. H. Ahn, *Int. J. Precis. Eng. Manuf. - Green Technol.*, 2016, **3**, 397–421.
- 123 L. L. Hench and J. K. West, *Chem. Rev.*, 1990, **90**, 33–72.
- 124 C. J. Brinker and A. J. Hurd, *J. Phys. III*, 1994, **4**, 1231–1242.
- 125 N. Sahu, B. Parija and S. Panigrahi, *Indian J. Phys.* 2009 834, 2009, **83**, 493–502.
- 126 A. Moridi, S. M. Hassani-Gangaraj, M. Guagliano and M. Dao, *Surf. Eng.*, 2014, **30**, 369–395.
- 127 U. Siemann, *Prog. Colloid Polym. Sci.*, 2005, **130**, 1–14.
- 128 H. Yang and P. Jiang, *Langmuir*, 2010, **26**, 13173–13182.
- 129 J. M. Abboud, R. Notario, J. Bertrán and M. Solà, in *Progress in Physical Organic Chemistry*, 1990, vol. 19, pp. 1–182.
- 130 T. Škorjanc, D. Shetty, M. A. Olson and A. Trabolsi, *ACS Appl. Mater. Interfaces*, 2019, **11**, 6705–6716.
- 131 M. Y. Jo, Y. E. Ha and J. H. Kim, *Sol. Energy Mater. Sol. Cells*, 2012, **107**, 1–8.
- 132 S. M. Beladi-Mousavi, S. Sadaf, A. M. Mahmood and L. Walder, *ACS Nano*, 2017, **11**, 8730–8740.
- 133 H. Y. Zhang, A. J. Miao and M. Jiang, *Mater. Chem. Phys.*, 2013, **141**, 482–487.
- 134 T. Saika, T. Iyoda and T. Shimidzu, *Bull. Chem. Soc. Jpn.*, 1993, **66**, 2054–2060.
- 135 P. K. Bhowmik, H. Han, J. J. Cebe, R. A. Burchett and A. M. Sarker, *J. Polym. Sci. Part A Polym. Chem.*, 2002, **40**, 659–674.
- 136 D. Zhang, S. Yang, K. Zhang, G. Zhou, Z. Jiang and J. Gu, *J. Appl. Polym. Sci.*, 2019, **136**, 1–7.
- 137 E. Raphael, C. O. Avellaneda, M. A. Aegerter, M. M. Silva and A. Pawlicka, *Mol. Cryst. Liq. Cryst.*, 2012, **554**, 264–272.

- 138 B. Q. Y. Chan, Z. W. K. Low, S. J. W. Heng, S. Y. Chan, C. Owh and X. J. Loh, *ACS Appl. Mater. Interfaces*, 2016, **8**, 10070–10087.
- 139 X. Ma, C. Qiao, J. Zhang and J. Xu, *Int. J. Biol. Macromol.*, 2018, **119**, 1294–1297.
- 140 K. W. Shah, S. X. Wang, D. X. Y. Soo and J. Xu, *Polymers (Basel)*, 2019, **11**, 1839.
- 141 S. Ding and Y. Tian, *RSC Adv.*, 2019, **9**, 26961–26980.
- 142 V. Nam and D. Lee, *Nanomaterials*, 2016, **6**, 47.
- 143 W. Huang, J. Li, F. Han, G. Zhang, R. Sun and C. P. Wong, *J. Chinese Chem. Soc.*, 2017, **64**, 1354–1359.
- 144 Z. Yin, S. K. Song, D. J. You, Y. Ko, S. Cho, J. Yoo, S. Y. Park, Y. Piao, S. T. Chang and Y. S. Kim, *Small*, 2015, **11**, 4576–4583.
- 145 A. R. Rathmell, S. M. Bergin, Y. L. Hua, Z. Y. Li and B. J. Wiley, *Adv. Mater.*, 2010, **22**, 3558–3563.
- 146 S. Zhao, F. Han, J. Li, X. Meng, W. Huang, D. Cao, G. Zhang, R. Sun and C. P. Wong, *Small*, 2018, **14**, 1–30.
- 147 H. Yoon, D. S. Shin, B. Babu, T. G. Kim, K. M. Song and J. Park, *Mater. Des.*, 2017, **132**, 66–71.
- 148 H. G. Im, S. H. Jung, J. Jin, D. Lee, J. Lee, D. Lee, J. Y. Lee, I. D. Kim and B. S. Bae, *ACS Nano*, 2014, **8**, 10973–10979.
- 149 M. Jin, G. He, H. Zhang, J. Zeng, Z. Xie and Y. Xia, *Angew. Chemie Int. Ed.*, 2011, **50**, 10560–10564.
- 150 S. Li, Y. Chen, L. Huang and D. Pan, *Inorg. Chem.*, 2014, **53**, 4440–4444.
- 151 D. M. Grant and R. Kollrack, *J. Inorg. Nucl. Chem.*, 1961, **23**, 25–29.
- 152 D. V. Ravi Kumar, I. Kim, Z. Zhong, K. Kim, D. Lee and J. Moon, *Phys. Chem. Chem. Phys.*, 2014, **16**, 22107–22115.
- 153 H. J. Yang, S. Y. He and H. Y. Tuan, *Langmuir*, 2014, **30**, 602–610.
- 154 C. J. Murphy, T. K. Sau, A. M. Gole, C. J. Orendorff, J. Gao, L. Gou, S. E. Hunyadi and T. Li, *J. Phys. Chem. B*, 2005, **109**, 13857–13870.
- 155 M. Grzelczak, J. Pérez-Juste, P. Mulvaney and L. M. Liz-Marzán, *Chem. Soc. Rev.*, 2008, **37**, 1783–1791.
- 156 K. C. Pradel, K. Sohn and J. Huang, *Angew. Chemie - Int. Ed.*, 2011, **50**, 3412–3416.
- 157 F. Qian, P. C. Lan, T. Olson, C. Zhu, E. B. Duoss, C. M. Spadaccini and T. Y. J. Han, *Chem. Commun.*, 2016, **52**, 11627–11630.

- 158 A. Glaria, J. Cure, K. Piettre, Y. Coppel, C. O. Turrin, B. Chaudret and P. Fau, *Chem. - A Eur. J.*, 2015, **21**, 1169–1178.
- 159 M. Rycenga, C. M. Cobley, J. Zeng, W. Li, C. H. Moran, Q. Zhang, D. Qin and Y. Xia, *Chem. Rev.*, 2011, **111**, 3669–3712.
- 160 Y. Li, Z. Fan, X. Yuan, H. Yang, Y. Li and C. Wang, *Mater. Lett.*, 2020, **274**, 128029.
- 161 H. Guo, N. Lin, Y. Chen, Z. Wang, Q. Xie, T. Zheng, N. Gao, S. Li, J. Kang, D. Cai and D. L. Peng, *Sci. Rep.*, , DOI:10.1038/srep02323.
- 162 L. Xu, Y. Yang, Z. W. Hu and S. H. Yu, *ACS Nano*, 2016, **10**, 3823–3834.
- 163 H. W. Heuer, R. Wehrmann and S. Kirchmeyer, *Adv. Funct. Mater.*, 2002, **12**, 89–94.
- 164 S. Y. Lin, Y. C. Chen, C. M. Wang, C. Y. Wen and T. Y. Shih, *Solid State Ionics*, 2012, **212**, 81–87.
- 165 H. C. Moon, C. H. Kim, T. P. Lodge and C. D. Frisbie, *ACS Appl. Mater. Interfaces*, 2016, **8**, 6252–6260.
- 166 R. Shi, T. L. Sun, F. Luo, T. Nakajima, T. Kurokawa, Y. Z. Bin, M. Rubinstein and J. P. Gong, *Macromolecules*, 2018, **51**, 8887–8898.

La borsa di dottorato è stata cofinanziata con risorse del
Programma Operativo Nazionale Ricerca e Innovazione 2014-2020 (CCI 2014IT16M2OP005)
Fondo Sociale Europeo, Azione I.1 “Dottorati Innovativi con caratterizzazione Industriale”



UNIONE EUROPEA
Fondo Sociale Europeo



*Ministero dell'Università
e della Ricerca*

